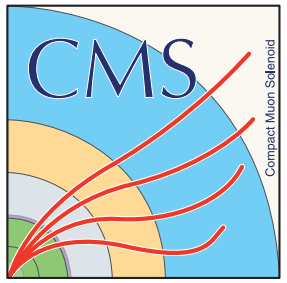

Development of Large-Area GEM Detectors for the Forward Muon Endcap Upgrade of the CMS Experiment and Search for the SM Higgs Boson Decay in the $H \rightarrow \tau^{-}\tau^{+} \rightarrow \mu^{-}\mu^{+}\bar{\nu}_{\mu}\nu_{\mu}\nu_{\tau}\bar{\nu}_{\tau}$ Channel

---

Ph.D. Dissertation Defense: Vallary Bhopatkar

Thesis Advisor: Prof. Marcus Hohlmann

29 Nov 2017

Outline

- The Compact Muon Solenoid (CMS) Experiment at the LHC, CERN

Part I

- GEMs Technology for the CMS Phase II Muon Endcap Upgrade
  - Gaseous Electron Multiplier (GEM) Detector
  - Fermilab Beam Test Results
  - Upgrade Status

Part II

- Physics Analyses with CMS Run II Data (2015, 2016)
  - Standard Model (SM) Higgs Boson
  - $Z \rightarrow \tau\tau$ Cross Section Measurements
  - $H \rightarrow \tau\tau \rightarrow \mu\mu$ Analysis
- Summary

Large Hadron Collider (LHC)

- Largest and most powerful circular particle collider
- Built at CERN (European Center for Nuclear Research), Geneva, Switzerland
- Consist of 7 detectors-

  ATLAS: A Toroidal LHC ApparatuS

  ALICE: A Large Ion Collider Experiment

  CMS: Compact Muon Solenoid

  LHCb: Large Hadron Collider beauty

  LHCf: Large Hadron Collider forward

  TOTEM: Total Elastic and diffractive cross section Measurements

  MoeDAL: Monopole and Exotic Detector At the LHC

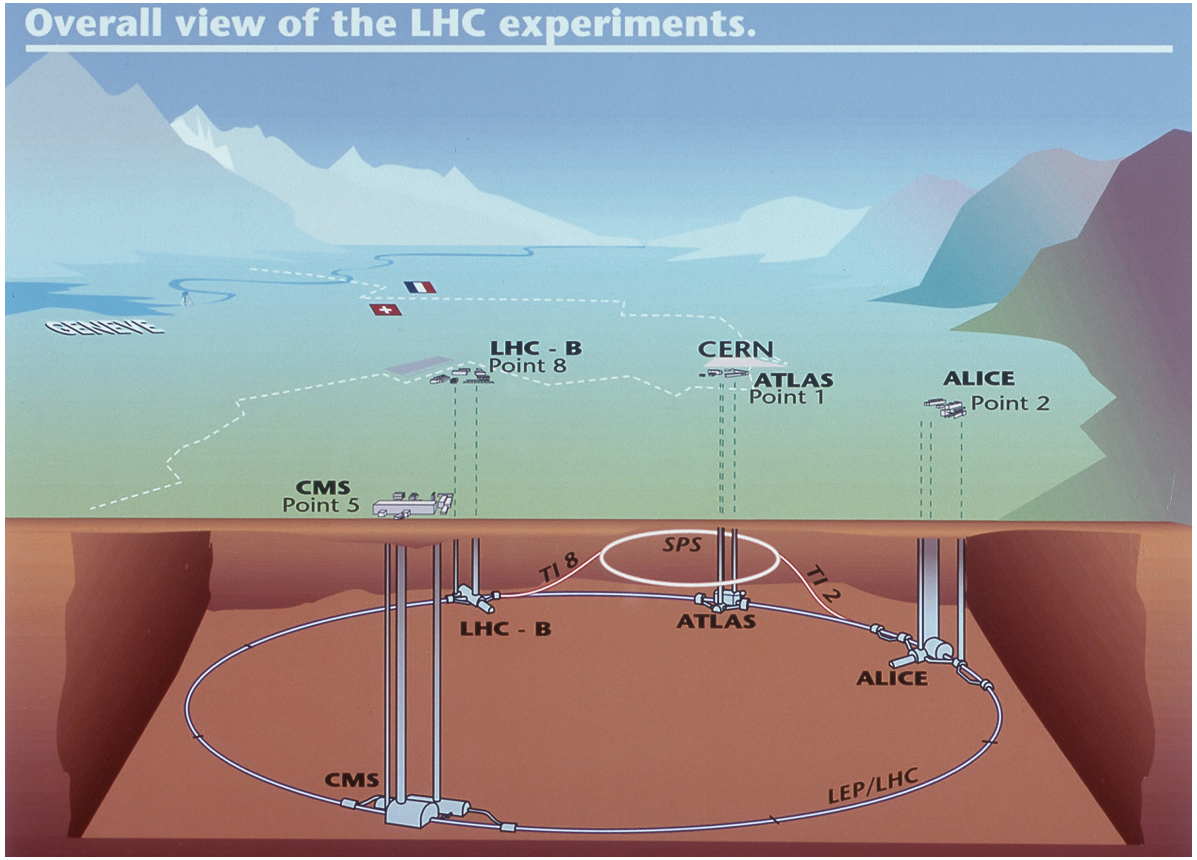

Compact Muon Solenoid (CMS) Experiment

CMS DETECTOR

Total weight 14,000 tonnes
Overall diameter 15m
Overall length 28.7 m
Magnetic field 3.8T

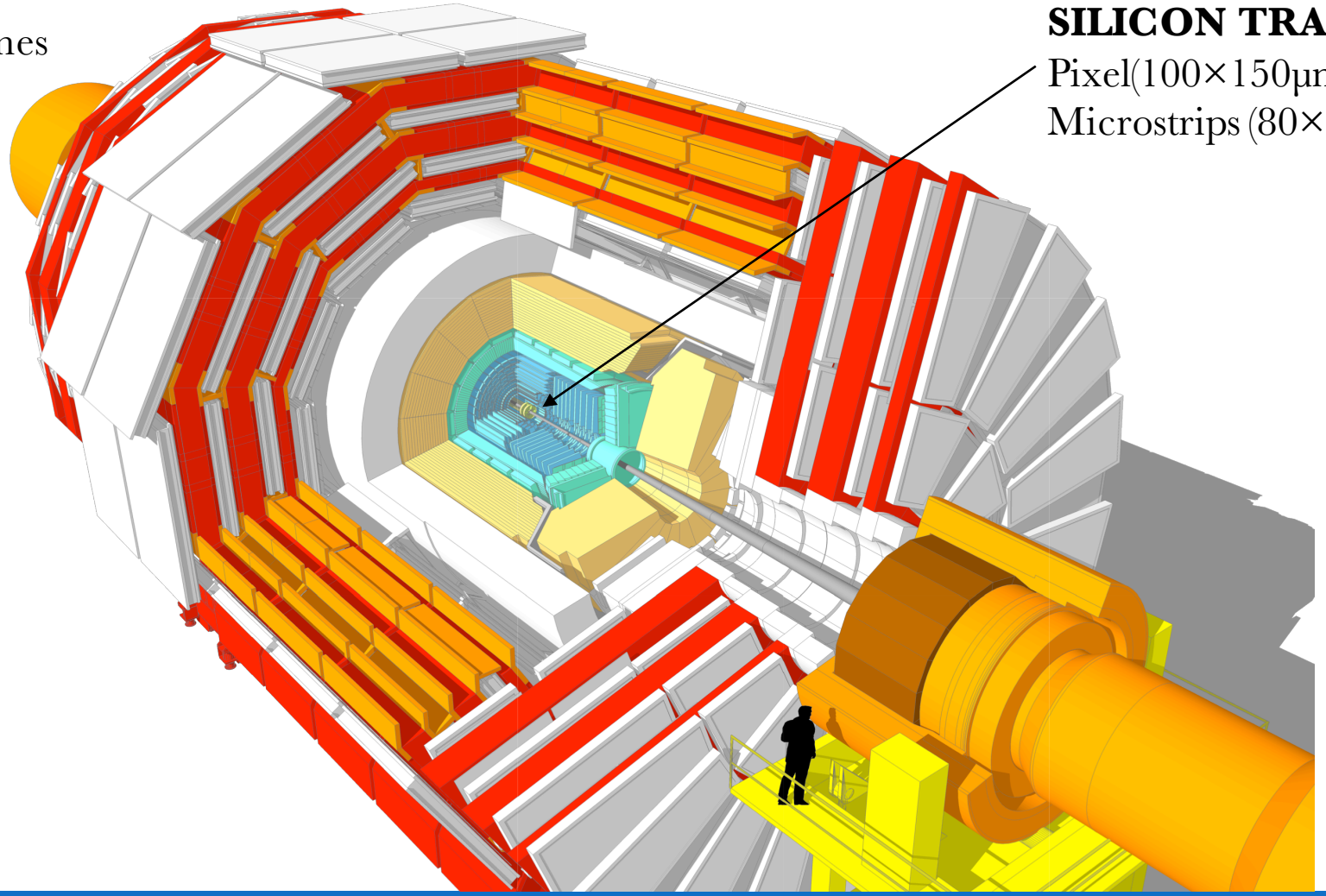

SILICON TRACKER

Pixel(100×150μm) ~66M Channels
Microstrips (80×180μm) ~9.6M Channels

Compact Muon Solenoid (CMS) Experiment

CMS DETECTOR

Total weight 14,000 tonnes
Overall diameter 15m
Overall length 28.7 m
Magnetic field 3.8T

PRESHOWER

Silicon Strips ~137,000 channels

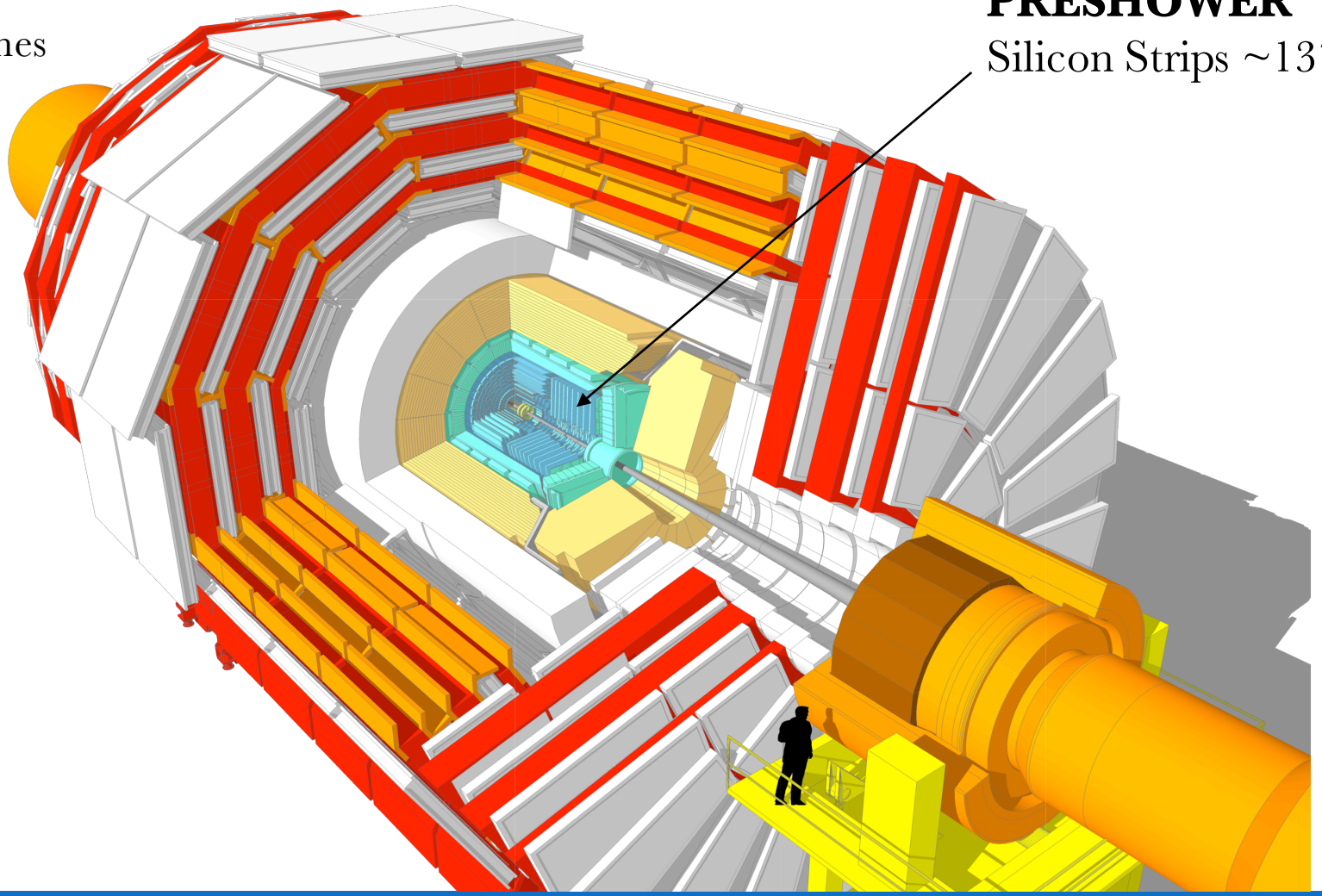

Compact Muon Solenoid (CMS) Experiment

CMS DETECTOR

Total weight 14,000 tonnes
Overall diameter 15m
Overall length 28.7 m
Magnetic field 3.8T

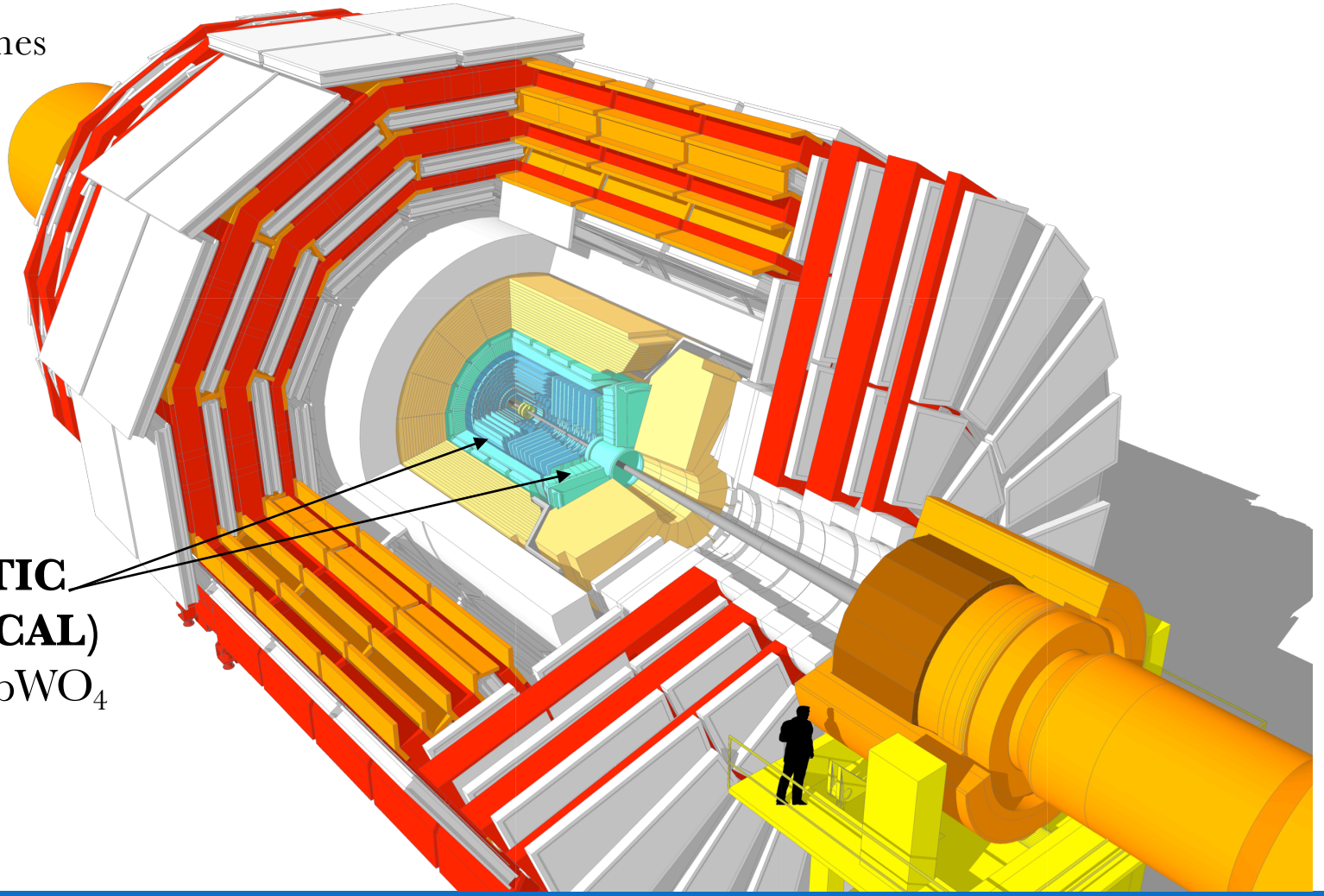

CRYSTAL ELECTROMAGNETIC CALORIMETER (ECAL)

~76,000 scintillating $PbWO_4$ crystals

Compact Muon Solenoid (CMS) Experiment

CMS DETECTOR

Total weight 14,000 tonnes
Overall diameter 15m
Overall length 28.7 m
Magnetic field 3.8T

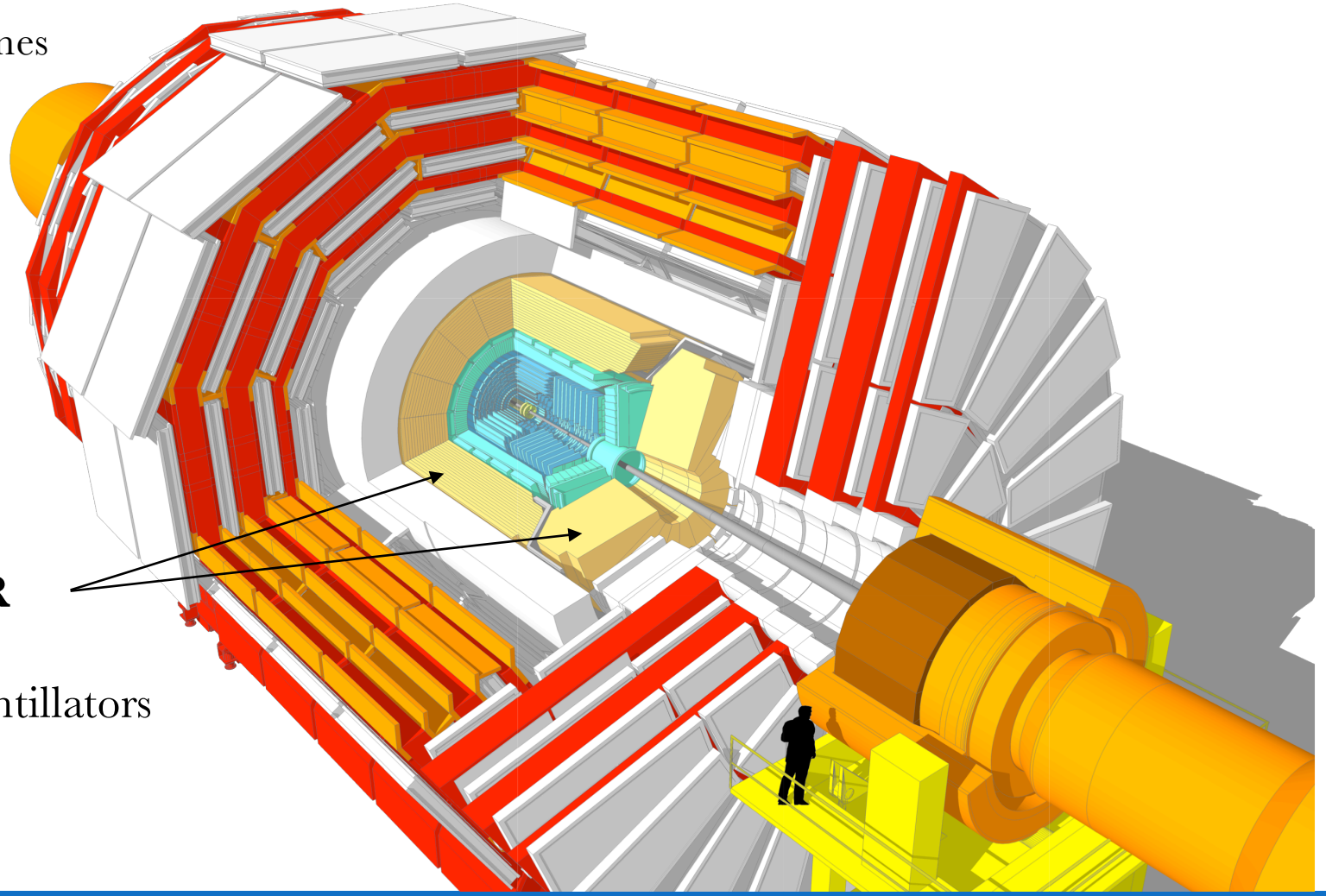

HADRON CALORIMETER (HCAL)

Brass + Plastic Scintillators
~7,000 Channels

Compact Muon Solenoid (CMS) Experiment

CMS DETECTOR

Total weight 14,000 tonnes
Overall diameter 15m
Overall length 28.7 m
Magnetic field 3.8T

SUPER CONDUCTING SOLENOID

Niobium Titanium coil carrying ~18,000A

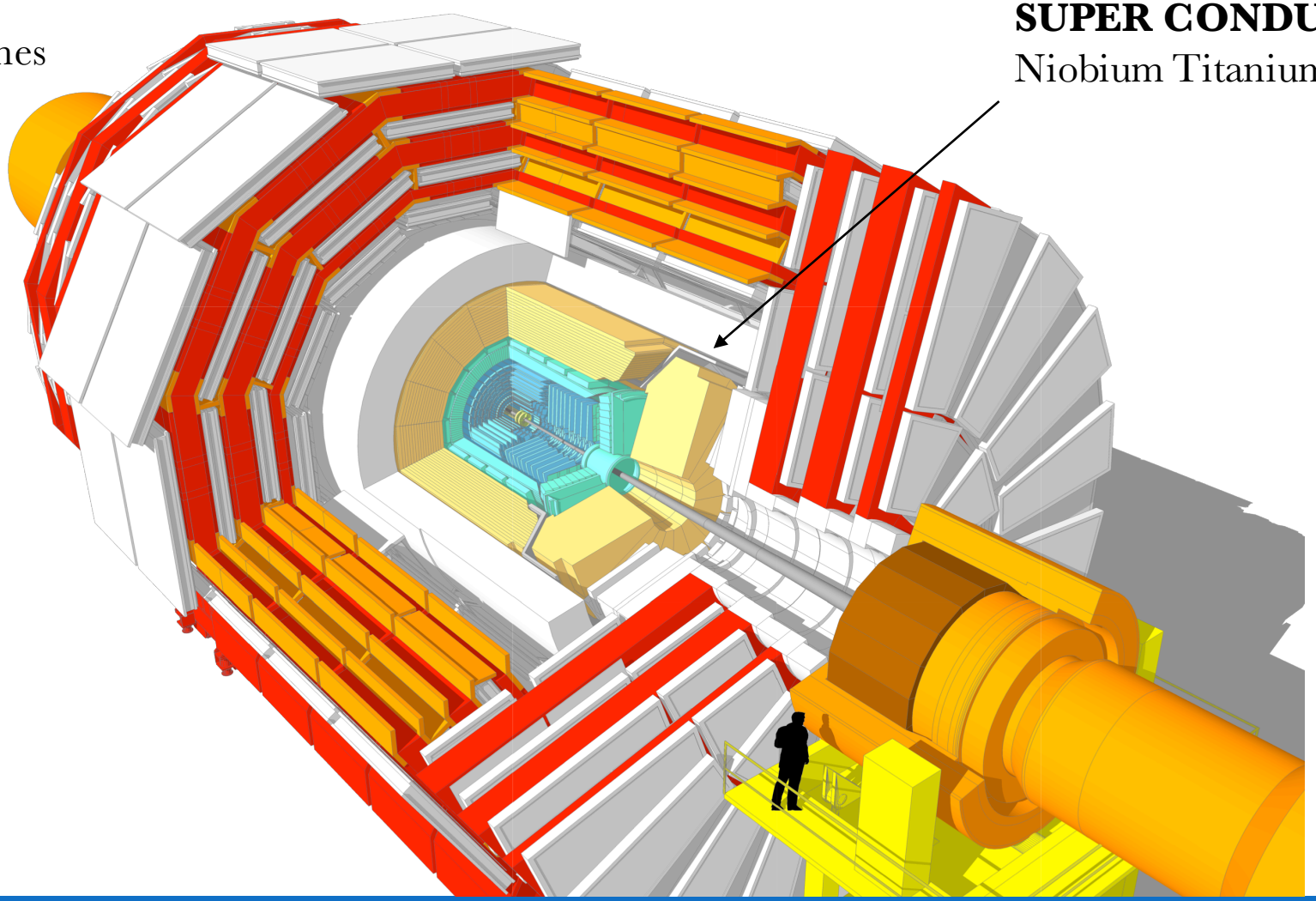

Compact Muon Solenoid (CMS) Experiment

CMS DETECTOR

Total weight 14,000 tonnes
Overall diameter 15m
Overall length 28.7 m
Magnetic field 3.8T

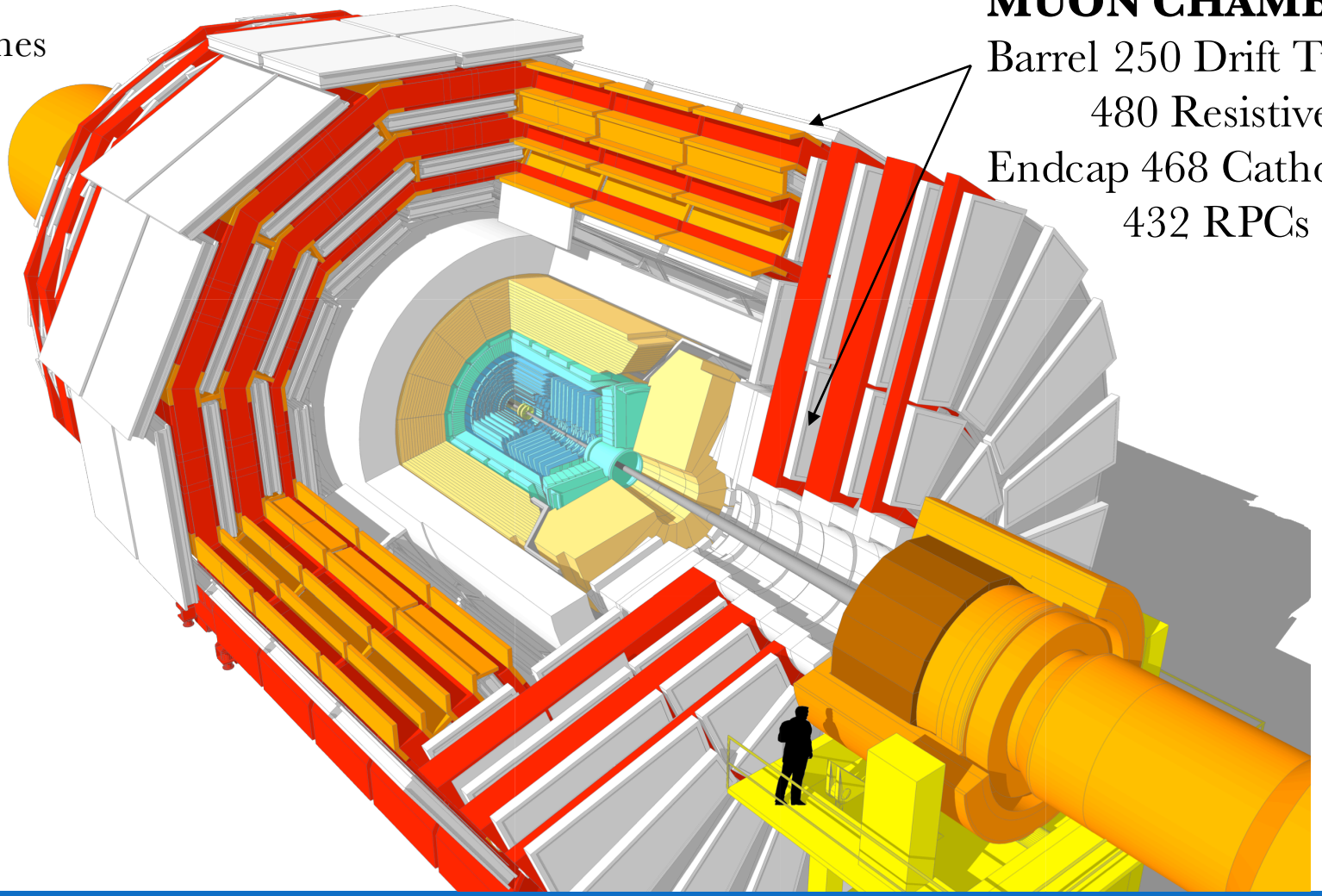

MUON CHAMBERS

Barrel 250 Drift Tube (DT),
480 Resistive Plate Chambers (RPC)
Endcap 468 Cathode strips (CSC),
432 RPCs

Compact Muon Solenoid (CMS) Experiment

CMS DETECTOR

Total weight 14,000 tonnes
Overall diameter 15m
Overall length 28.7 m
Magnetic field 3.8T

FORWARD CALORIMETER

Steel + Quartz Fiber ~2,000 Channels

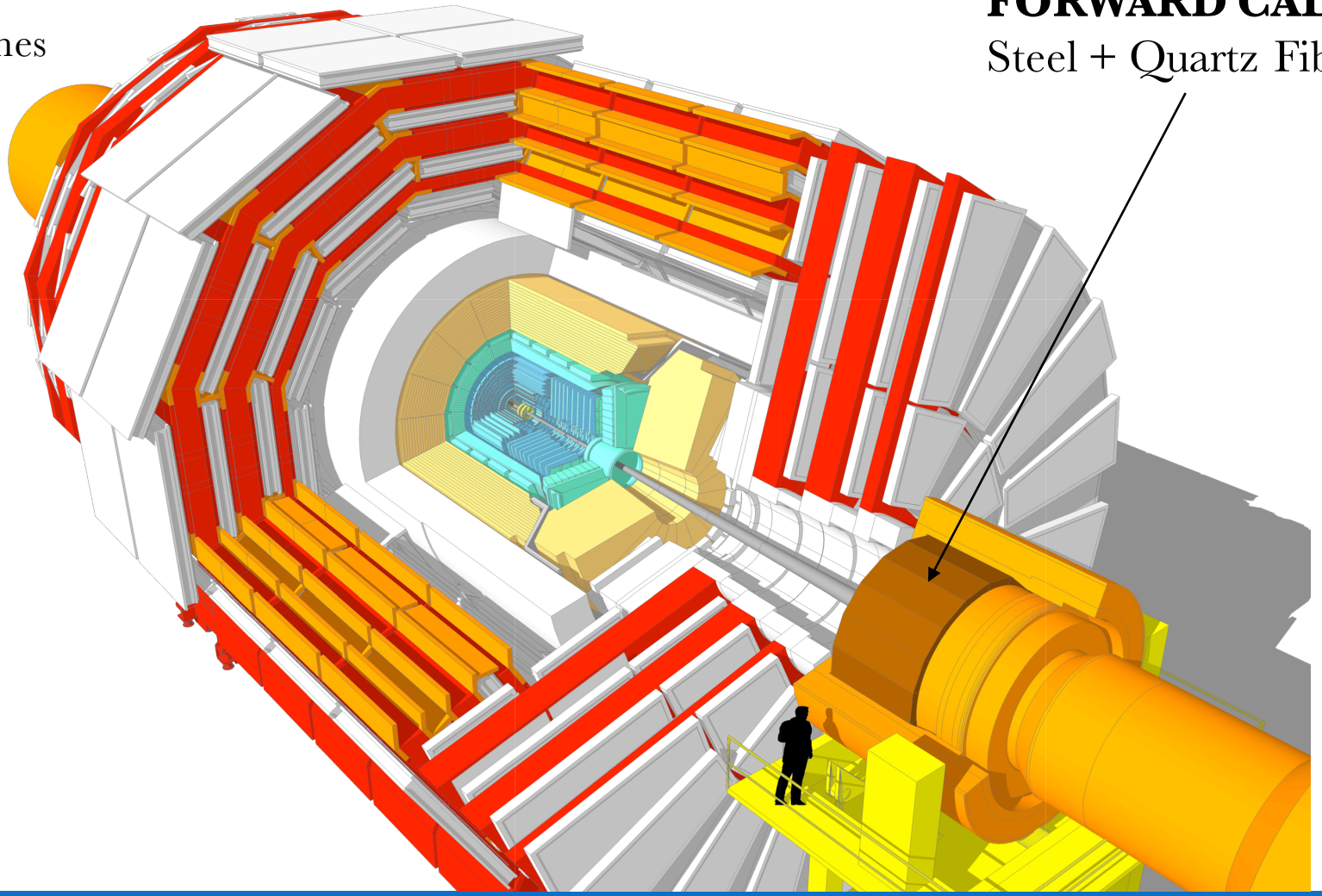

Compact Muon Solenoid (CMS) Experiment

CMS DETECTOR

Total weight 14,000 tonnes
Overall diameter 15m
Overall length 28.7 m
Magnetic field 3.8T

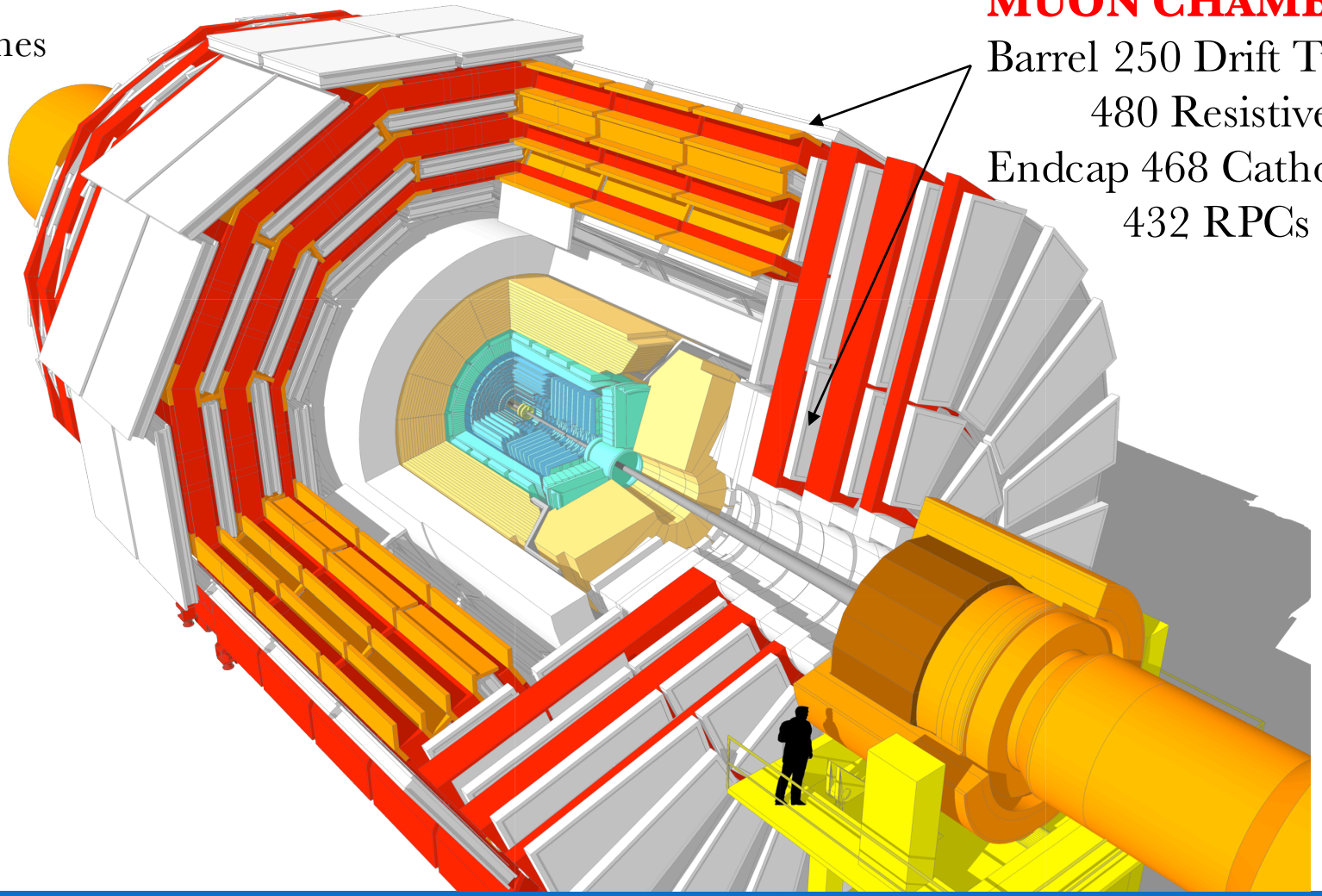

MUON CHAMBERS

Barrel 250 Drift Tube (DT),
480 Resistive Plate Chambers (RPC)
Endcap 468 Cathode strips (CSC),
432 RPCs

Coordinate Systems

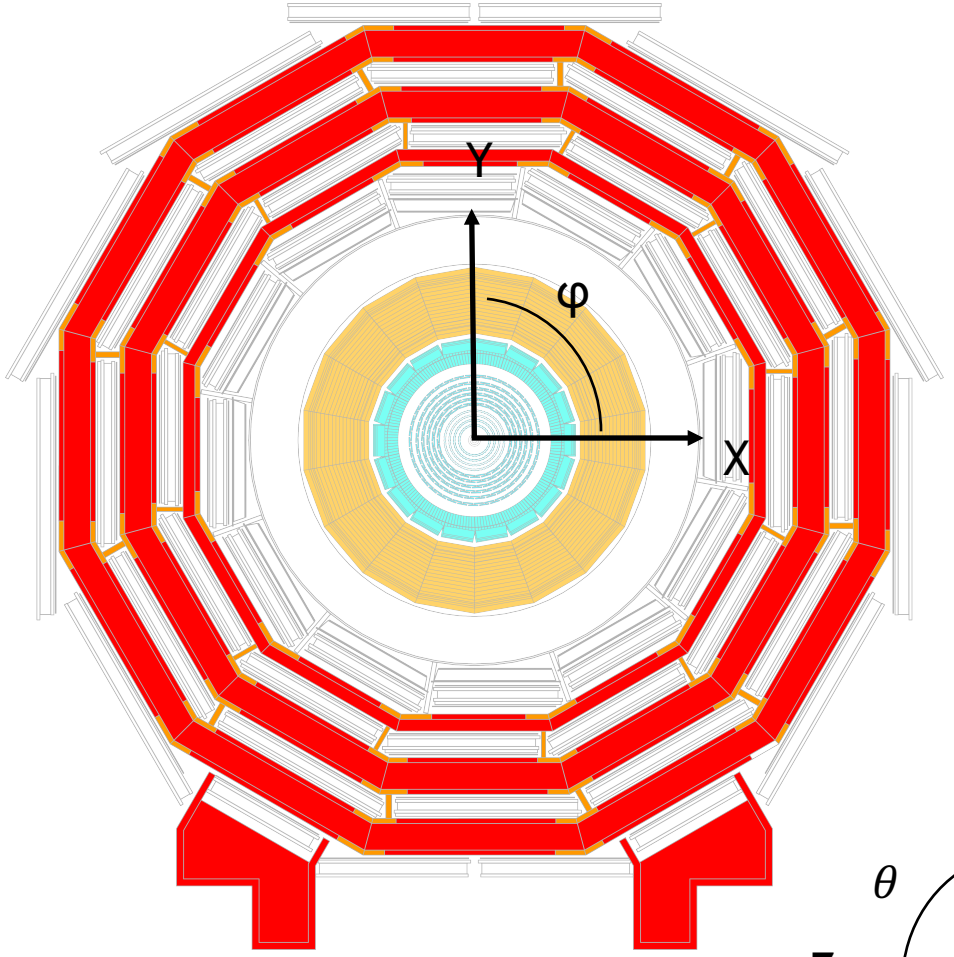

- X directed towards the center of LHC
- Y is in the upwards direction
- Z is along the beam line
- Φ is in the X-Y plane starting from X –axis
- θ is in the plane of Y-Z
- In CMS preferred coordinates are Φ-η, where η is pseudorapidity and defined with in terms of θ as

$$\eta = -ln\left[tan\left(\frac{\theta}{2}\right)\right]$$

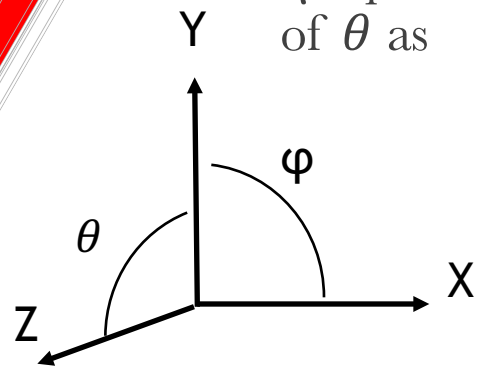

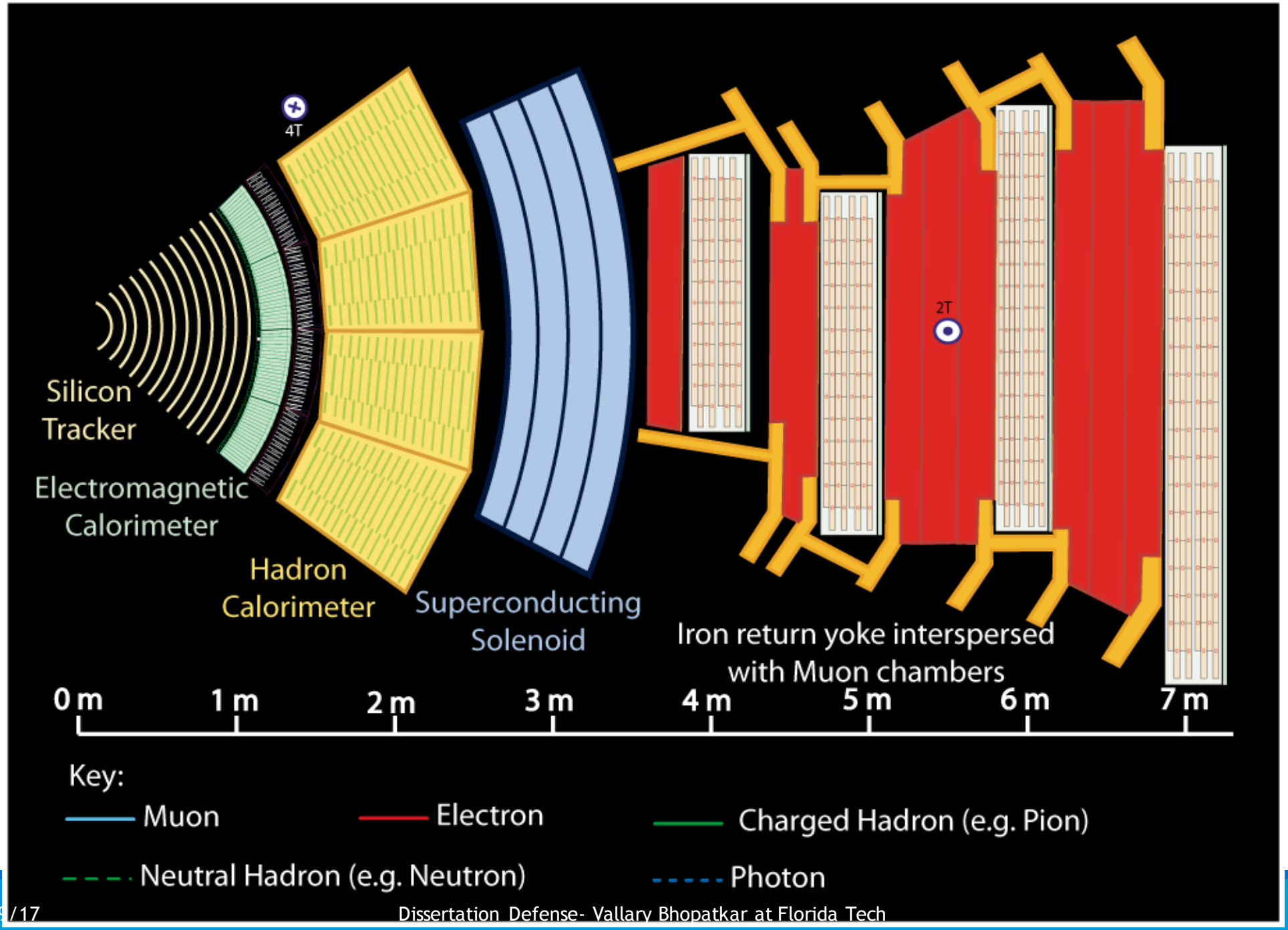
4T
2T
Silicon Tracker
Electromagnetic Calorimeter
Hadron Calorimeter
Superconducting Solenoid
Iron return yoke interspersed with Muon chambers
0 m
1 m
2 m
3 m
4 m
5 m
6 m
7 m
Key:
Muon
Electron
Charged Hadron (e.g. Pion)
Neutral Hadron (e.g. Neutron)
Photon

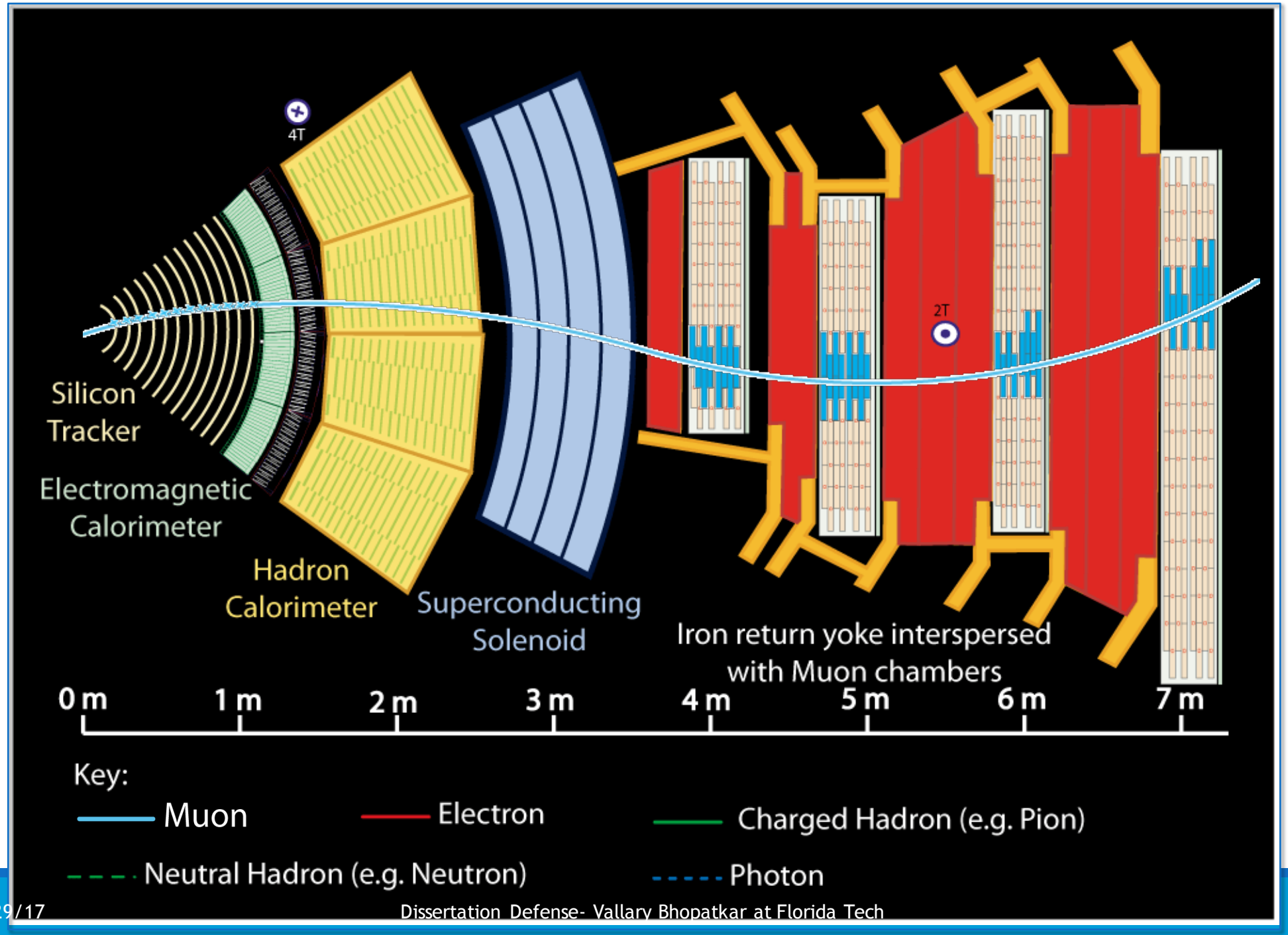
4T
2T
Silicon Tracker
Electromagnetic Calorimeter
Hadron Calorimeter
Superconducting Solenoid
Iron return yoke interspersed with Muon chambers
0 m
1 m
2 m
3 m
4 m
5 m
6 m
7 m
Key:
Muon
Electron
Charged Hadron (e.g. Pion)
Neutral Hadron (e.g. Neutron)
Photon

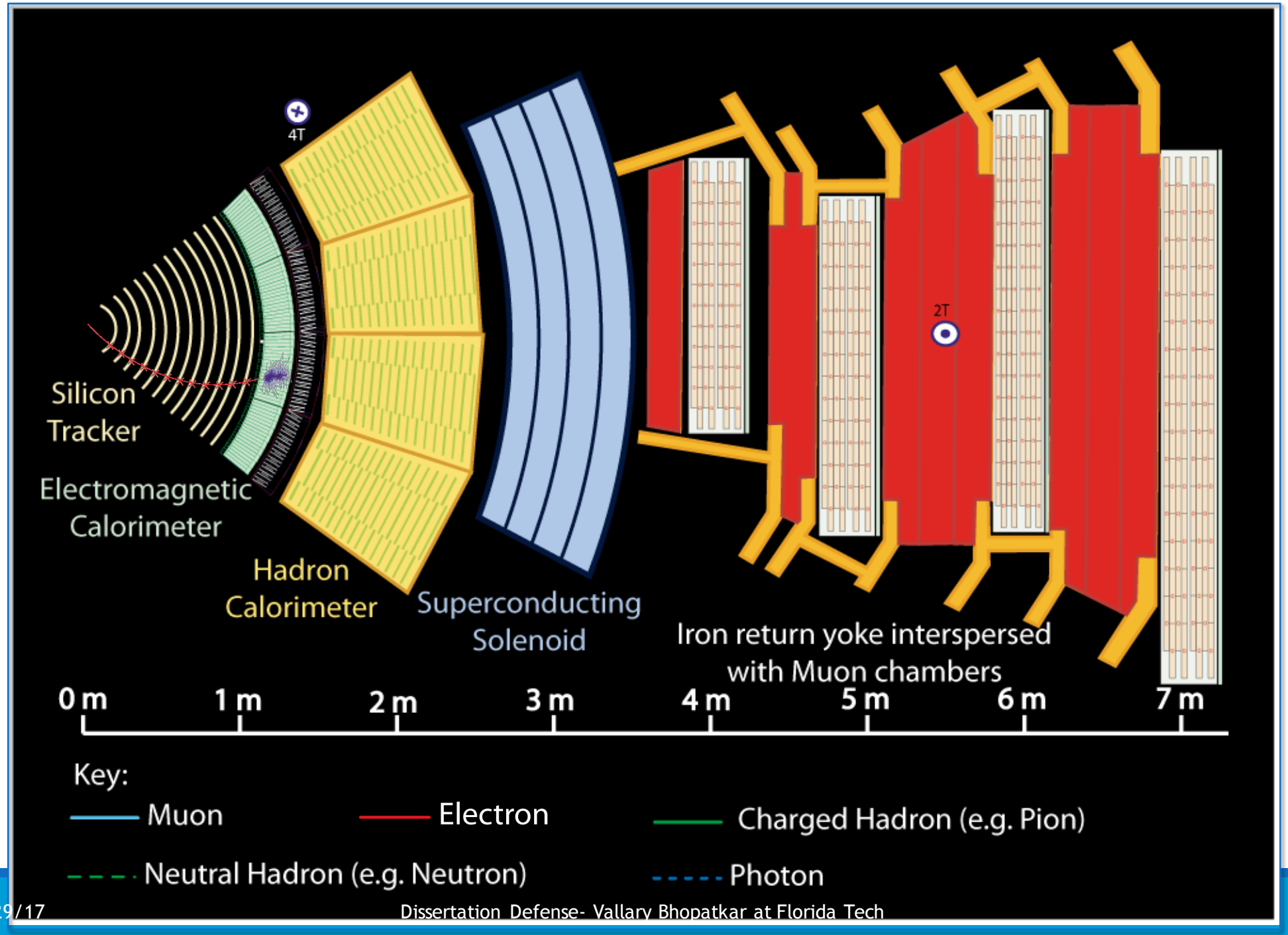
4T
2T
Silicon Tracker
Electromagnetic Calorimeter
Hadron Calorimeter
Superconducting Solenoid
Iron return yoke interspersed with Muon chambers
0 m
1 m
2 m
3 m
4 m
5 m
6 m
7 m
Key:
Muon
Electron
Charged Hadron (e.g. Pion)
Neutral Hadron (e.g. Neutron)
Photon

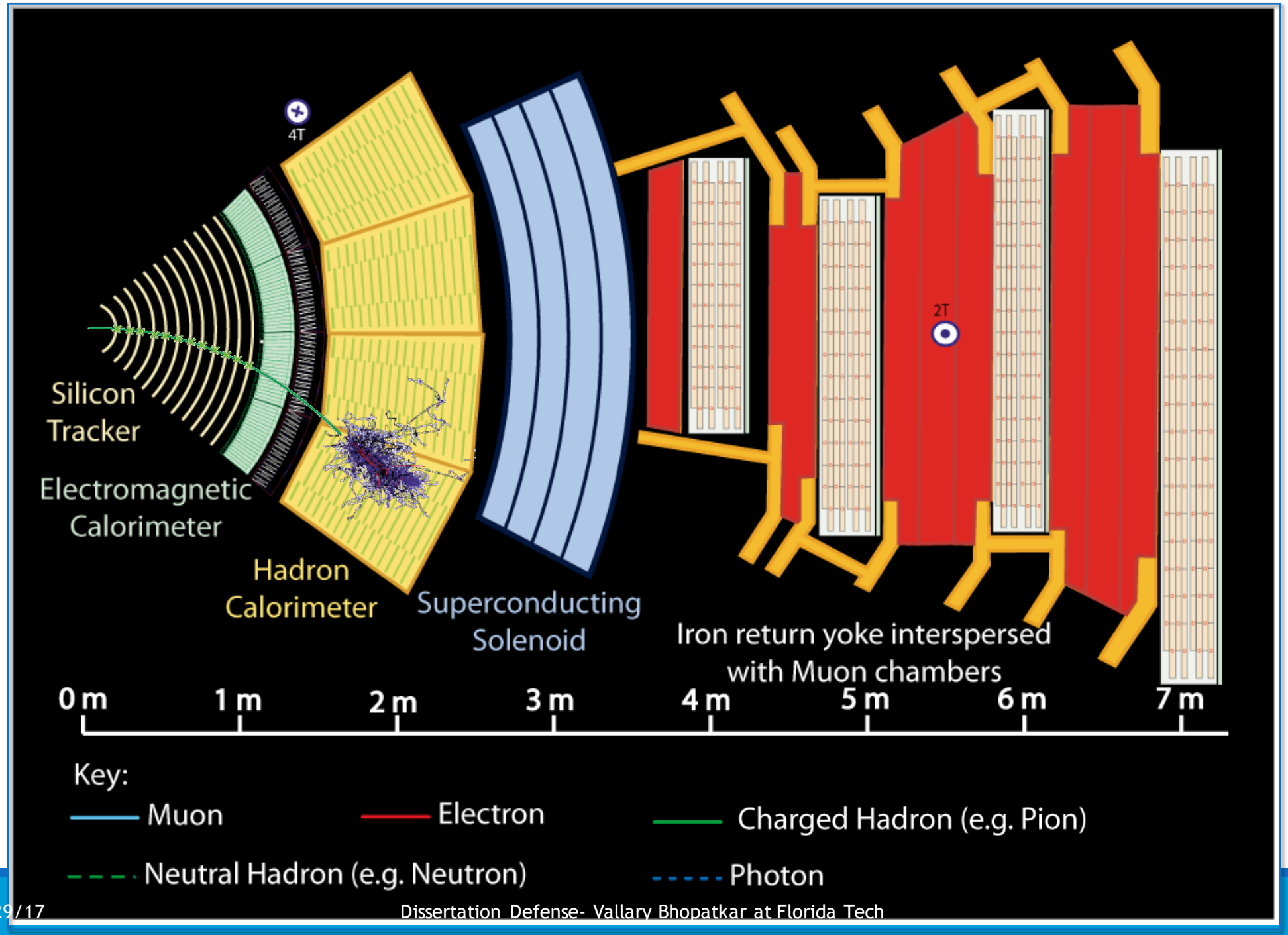
4T
2T
Silicon Tracker
Electromagnetic Calorimeter
Hadron Calorimeter
Superconducting Solenoid
Iron return yoke interspersed with Muon chambers
0 m
1 m
2 m
3 m
4 m
5 m
6 m
7 m
Key:
Muon
Electron
Charged Hadron (e.g. Pion)
Neutral Hadron (e.g. Neutron)
Photon

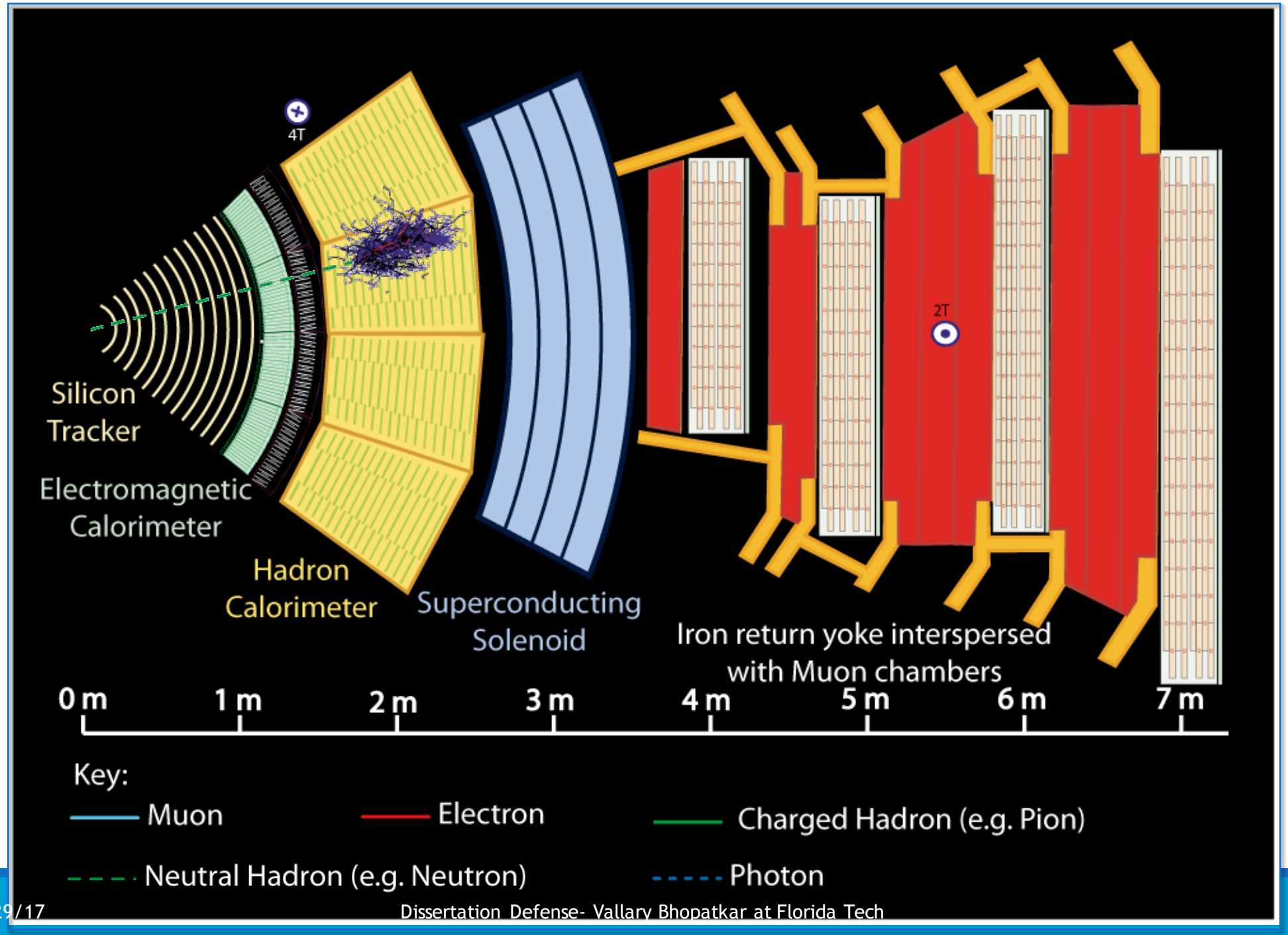
4T
2T
Silicon Tracker
Electromagnetic Calorimeter
Hadron Calorimeter
Superconducting Solenoid
Iron return yoke interspersed with Muon chambers
0 m
1 m
2 m
3 m
4 m
5 m
6 m
7 m
Key:
Muon
Electron
Charged Hadron (e.g. Pion)
Neutral Hadron (e.g. Neutron)
Photon

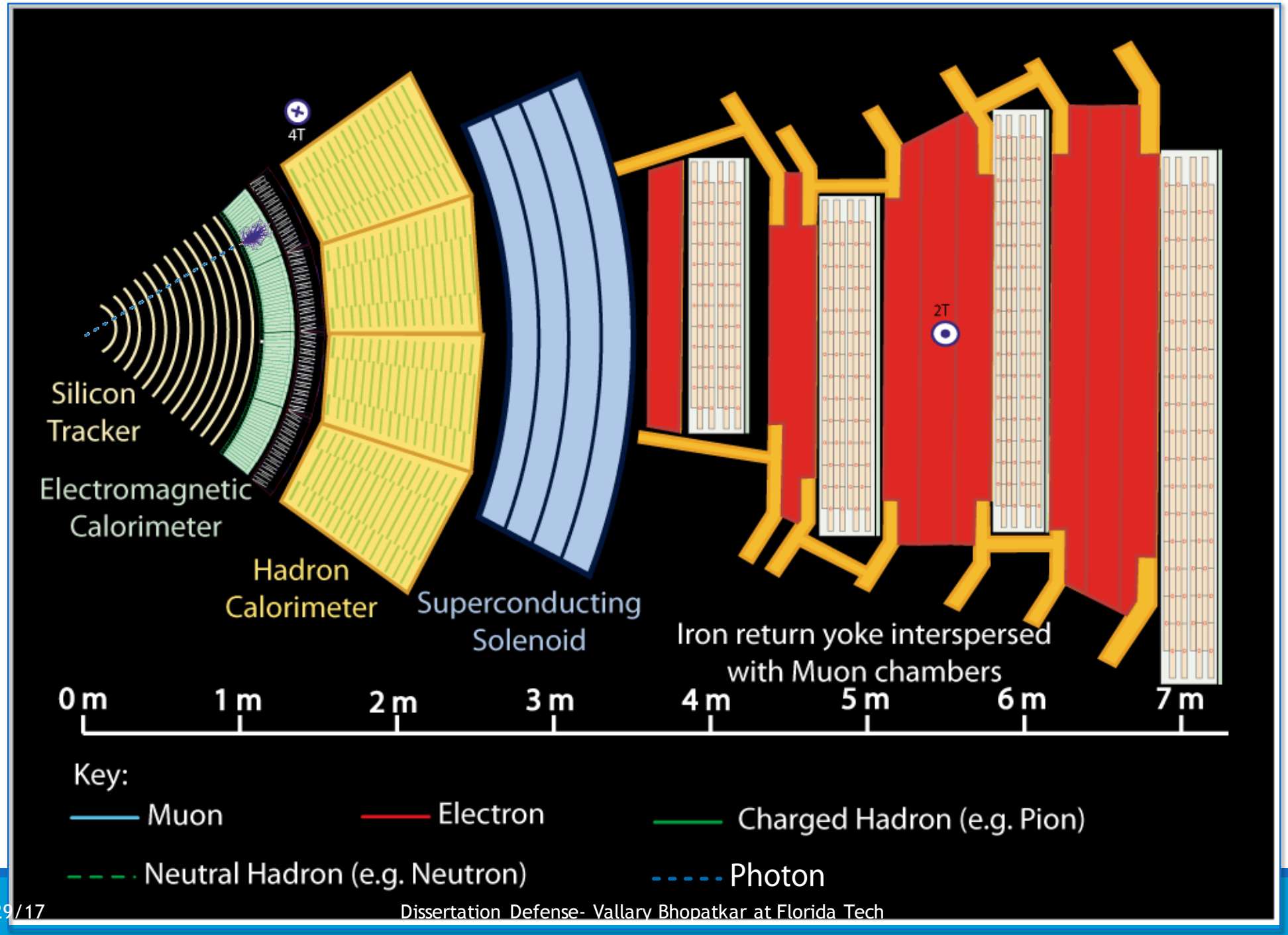
4T
2T
Silicon Tracker
Electromagnetic Calorimeter
Hadron Calorimeter
Superconducting Solenoid
Iron return yoke interspersed with Muon chambers
0 m
1 m
2 m
3 m
4 m
5 m
6 m
7 m
Key:
Muon
Electron
Charged Hadron (e.g. Pion)
Neutral Hadron (e.g. Neutron)
Photon

Part I
CMS Hardware Upgrade

GEMs for the Future CMS Muon Endcap Upgrade

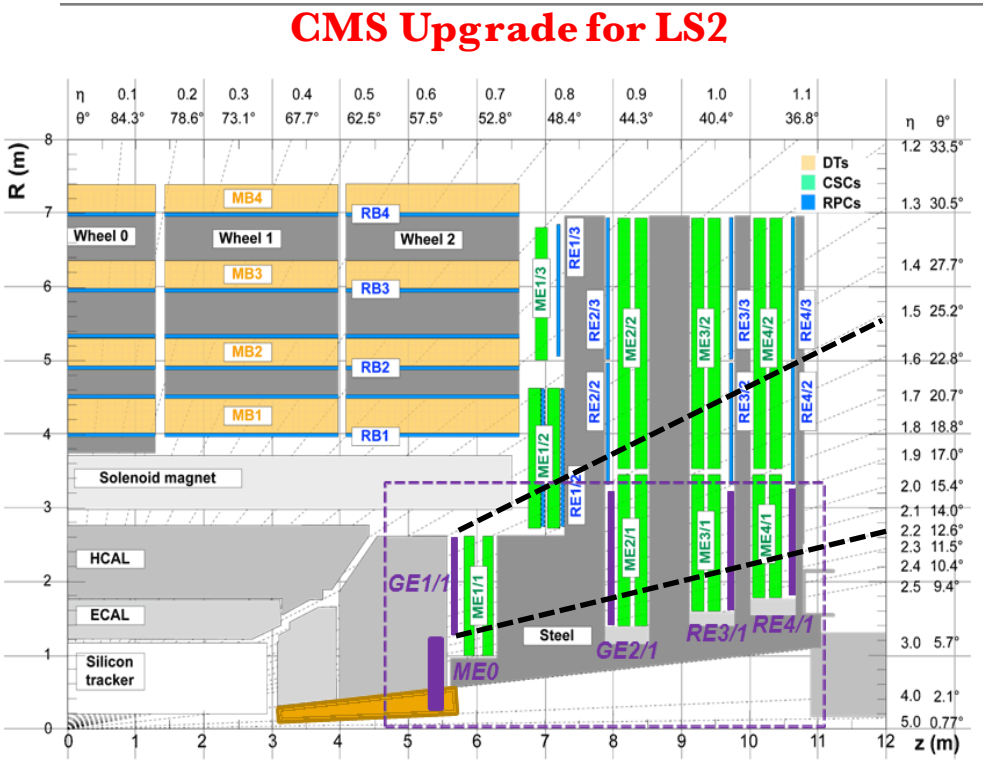

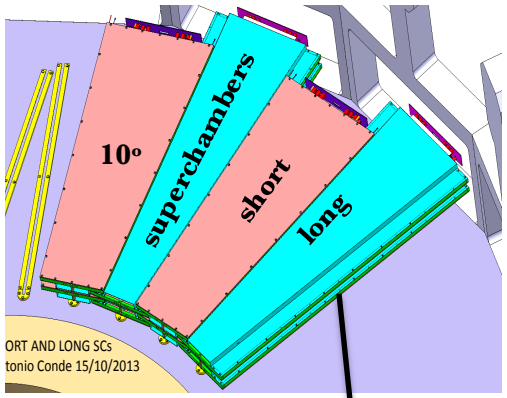

Super-chamber = 2 triple GEM detector (Short + Long)

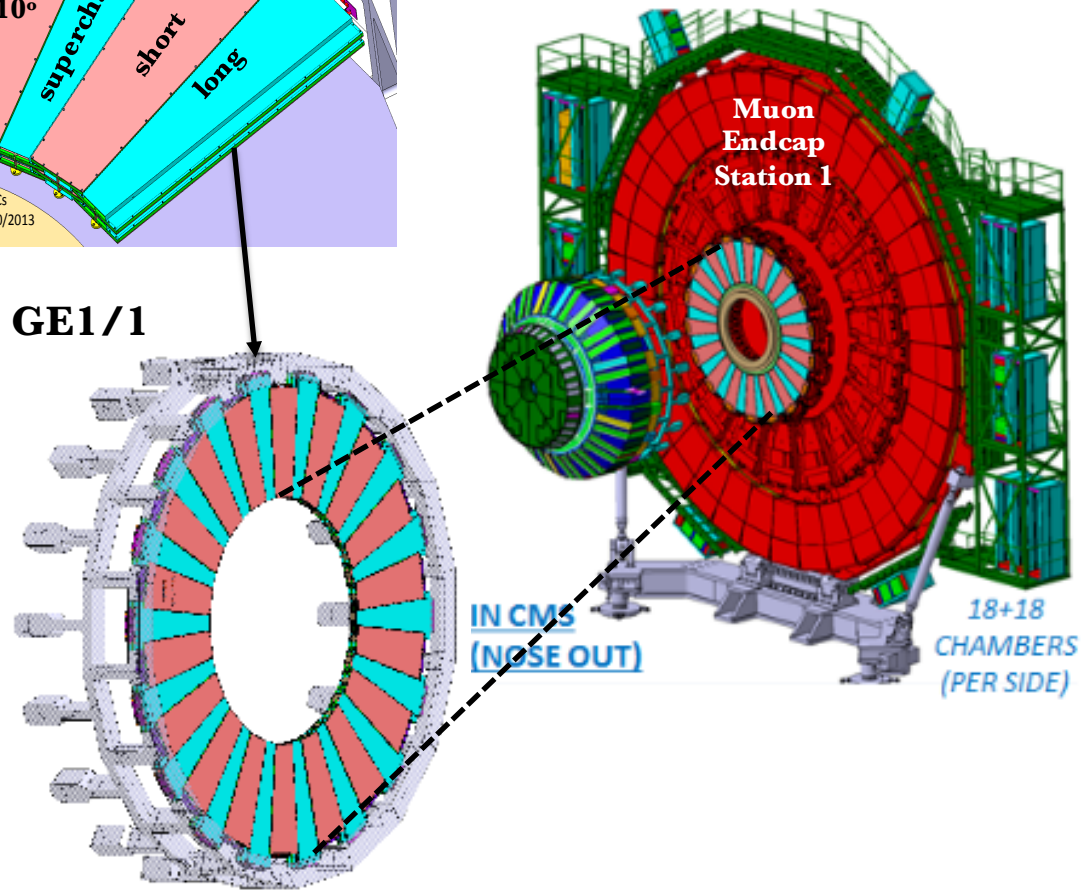

- Introducing **GE1/1** station **in high-η region1.5<|η|<2.2**
- **10^0 super-chambers** (trapezoidal triple-GEM detectors) with long (1.5<|η|<2.2) and short (1.6<|η|<2.2) version
- 36 super-chambers in each endcap

Why GEMs?

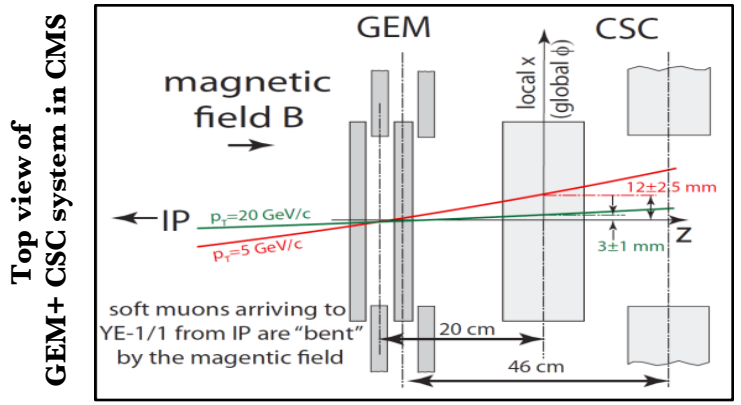

- High gain (~10^4)
- Sustains a high rate (~MHz/cm^2)
- Precise tracking and time resolution
- High spatial resolution
- In High-Luminosity (HL) LHC, pile will increase
- CSC + GEM ⟹ accurate muon bending angle by reducing the multiple scattering
- Discriminates lower p_T muon from higher p_T
- Lowers the global muon trigger rate

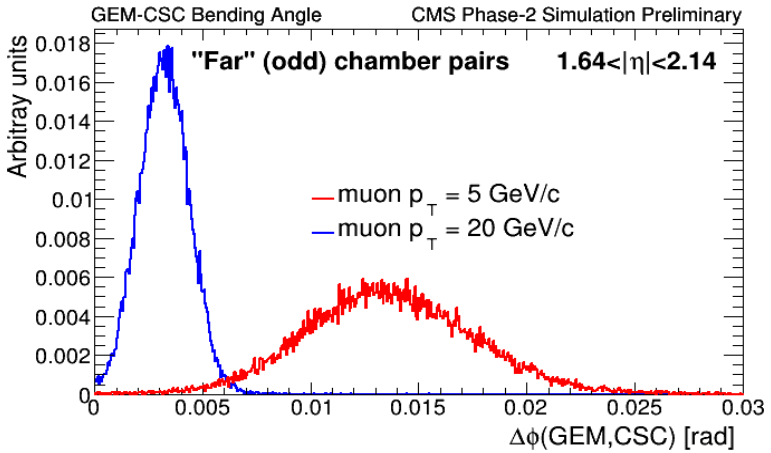

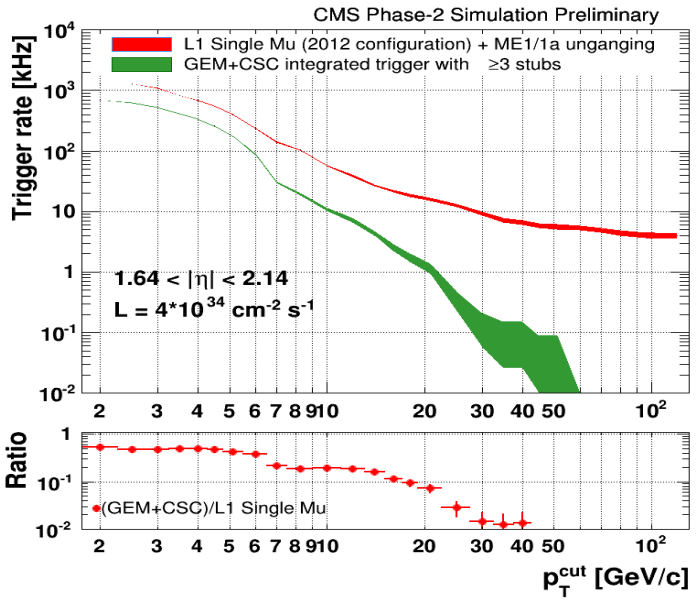

GEM Detectors

- Micro Pattern Gas Detectors (MPGD)
- Gem foil is a kapton foil coated with copper on both sides that has an array of holes (typically 140 µm pitch
- Triple-GEM, most popular and reliable configuration
- Typical gas gain 10^4 with gas mixture Ar/CO_2 in 70:30 proportional
- When applied high voltage across the foils, creates avalanche of electrons through holes
- Provides good detection efficiency and spatial resolution

Triple-GEM configuration

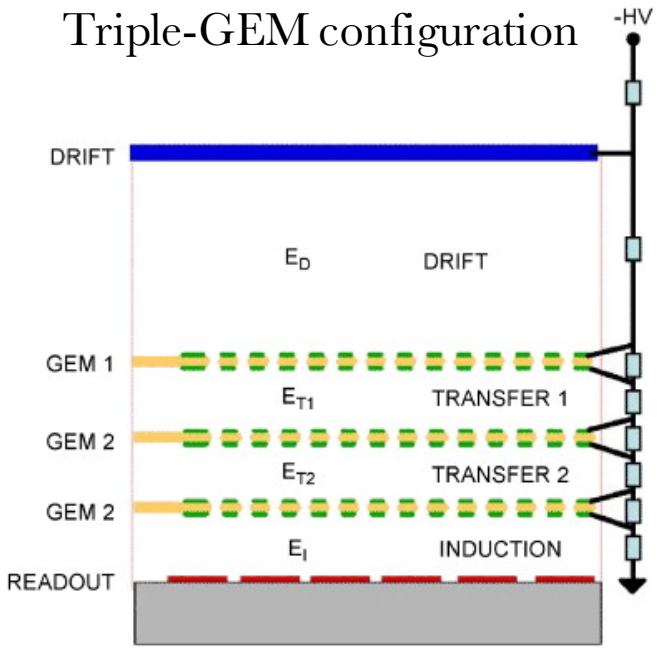

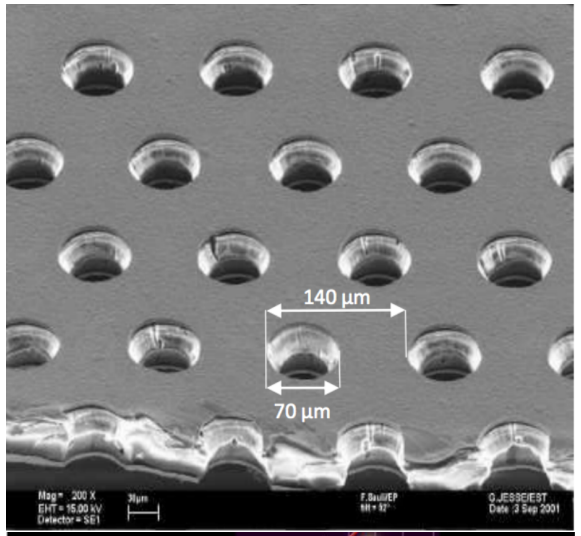

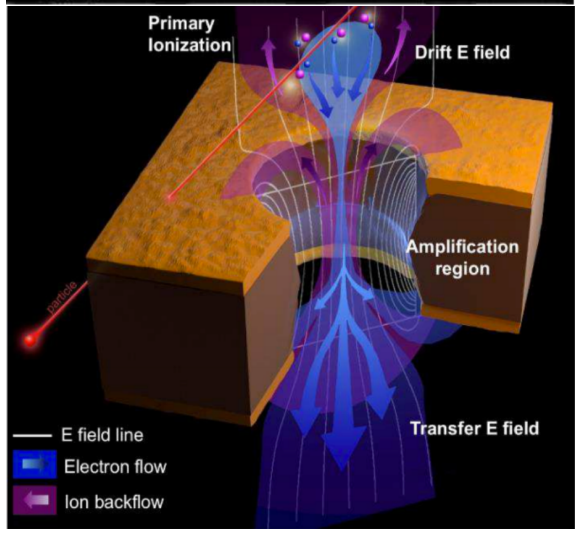

Construction of a Large-Area GEM Detector GE1/1-III Prototype at Florida Tech

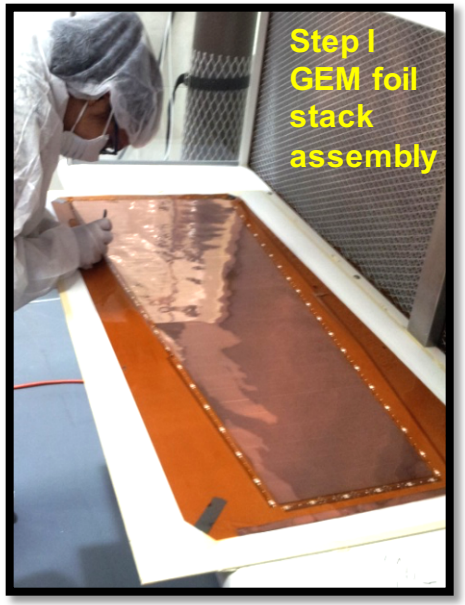

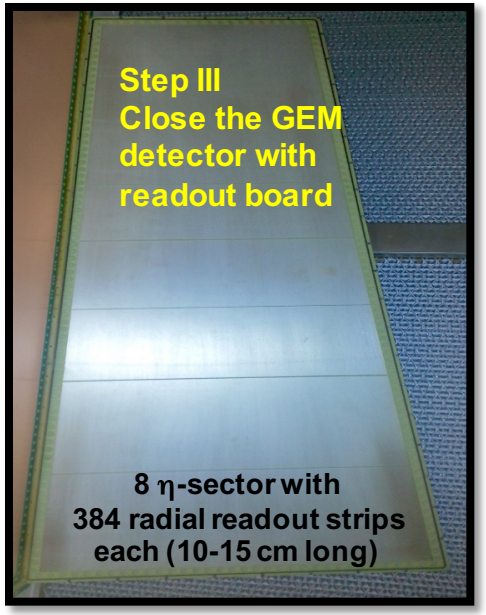

Total assembly time 3 Hrs 40 mins with 2 people

- Active area: ~ 99 × (28 -45) cm^2
- Internal gap configuration 3/1/2/1 mm
- GEM foils are produced by single-mask etching techniques at CERN
- Strip pitch = 455 μrad (384 radial strip per η-sector)

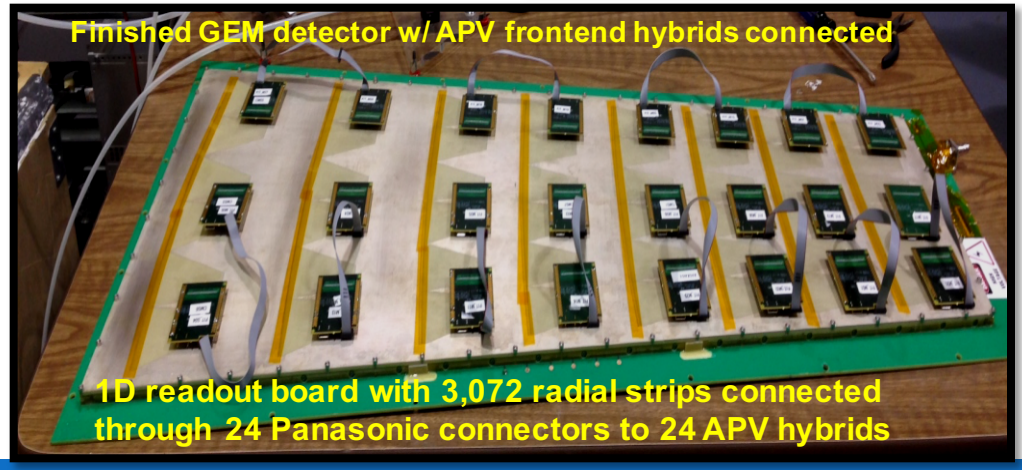

FNAL Test Beam Setup and Measurements

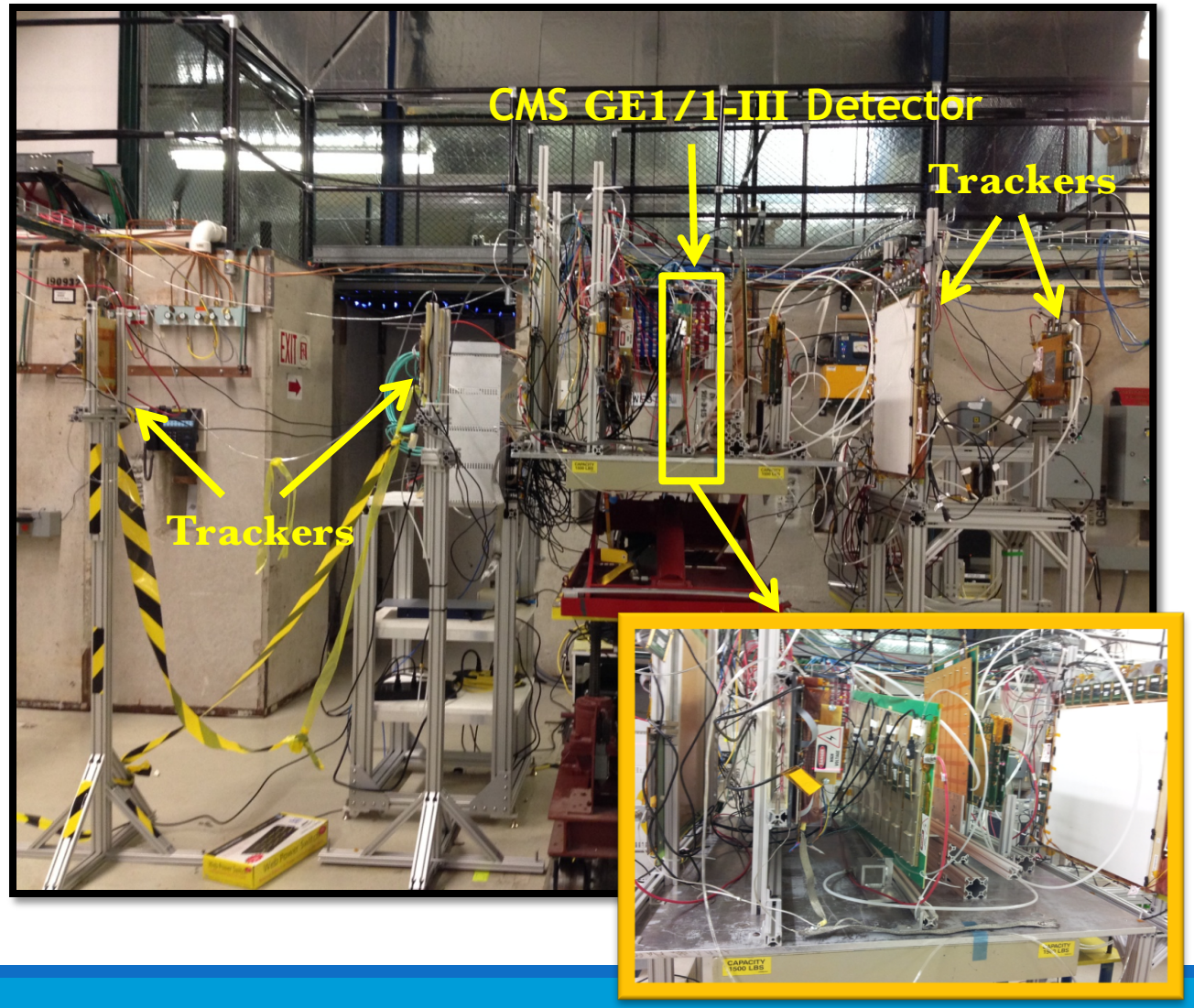

- Gas Mixture used in all detectors Ar/CO_2 70:30
- Beam Energies: 32 GeV mixed hadrons and 120 GeV proton
- Four GEM trackers with 2D readout operated at 4200V
  - three 10 cm × 10 cm
  - one 50 cm × 50 cm (10 cm × 10 cm active area)
- DAQ with RD51 Scalable Readout System
- GE1/1-III detectors measurements
  - High voltage scan (2900 V – 3350 V)
  - Position scan at 3250 V operating voltage
    - Upper, Middle, Lower APV rows

Performance Characteristics from FNAL Beam Test Data

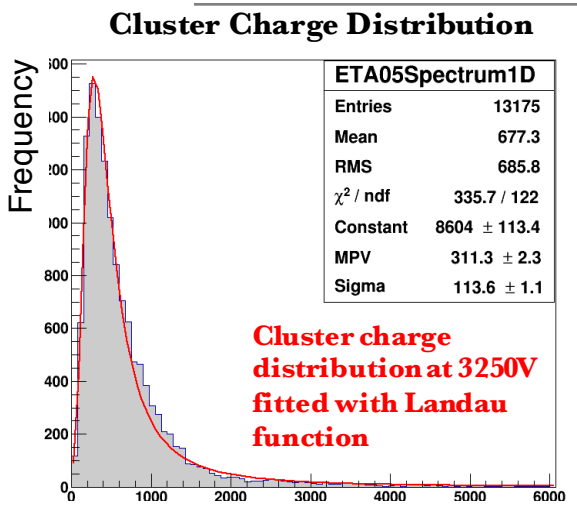

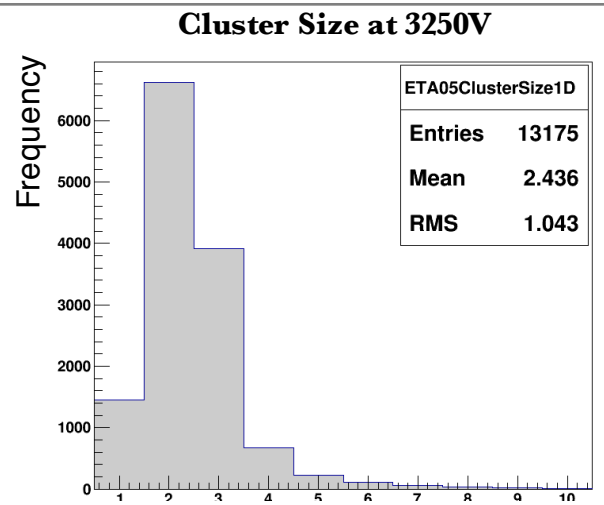

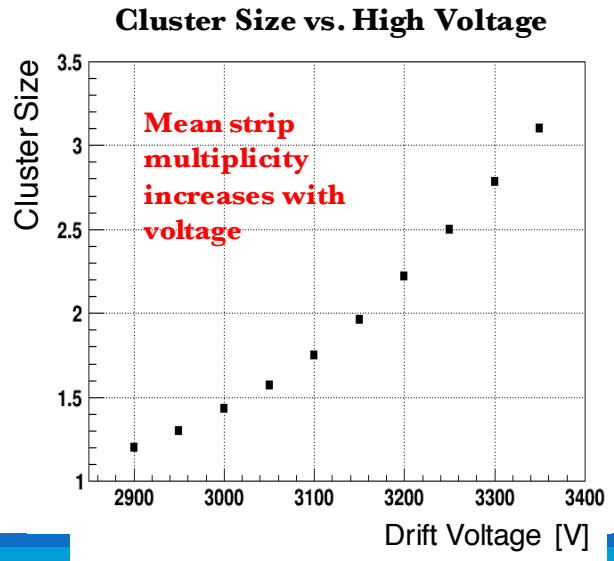

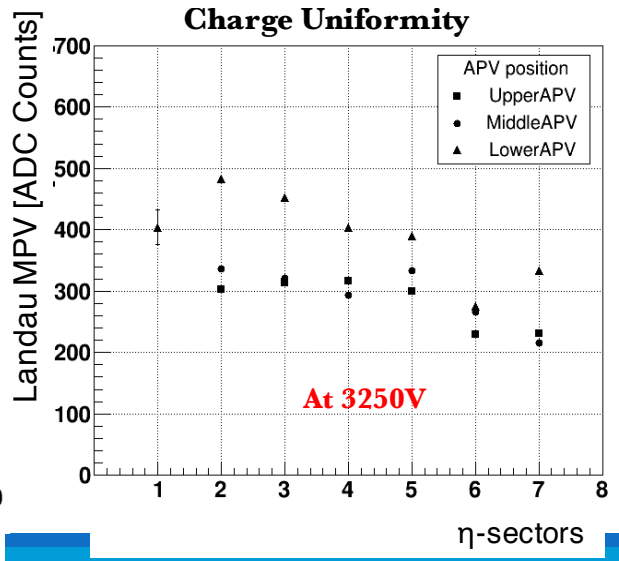

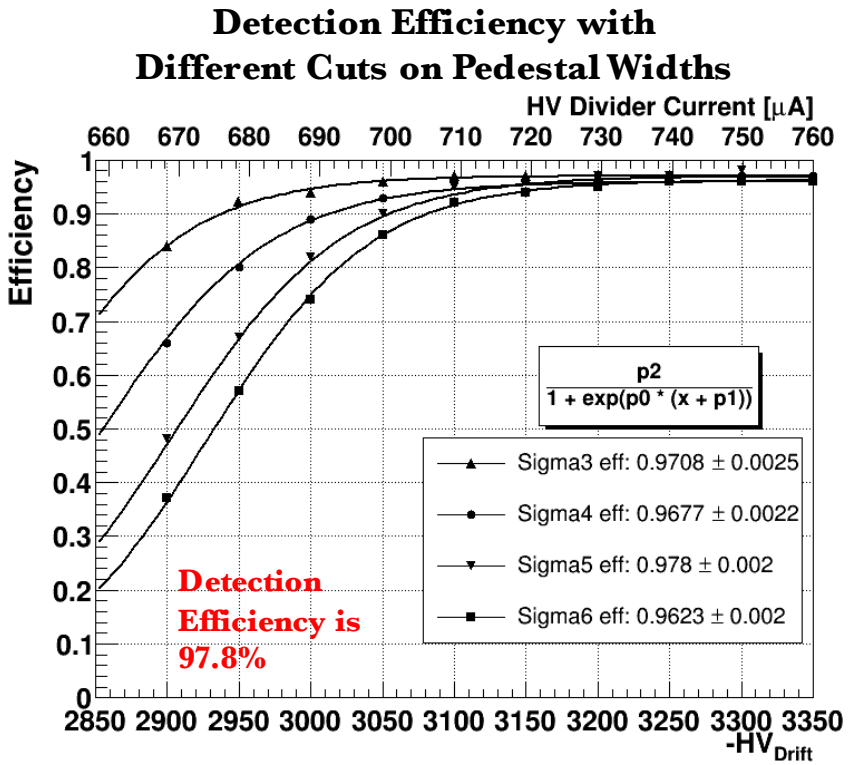

- Average strip multiplicity at operating voltage is 2.4 strips
- At 3250 V, most probable values for three APV positions are used to determine the charge uniformity across detector
- Detection efficiency 97.8% (measured) with 5-sigma cut on the pedestal width

Tracking Results
Resolution of the GE1/1-III Detector in η-sector 5

Inclusive Residual

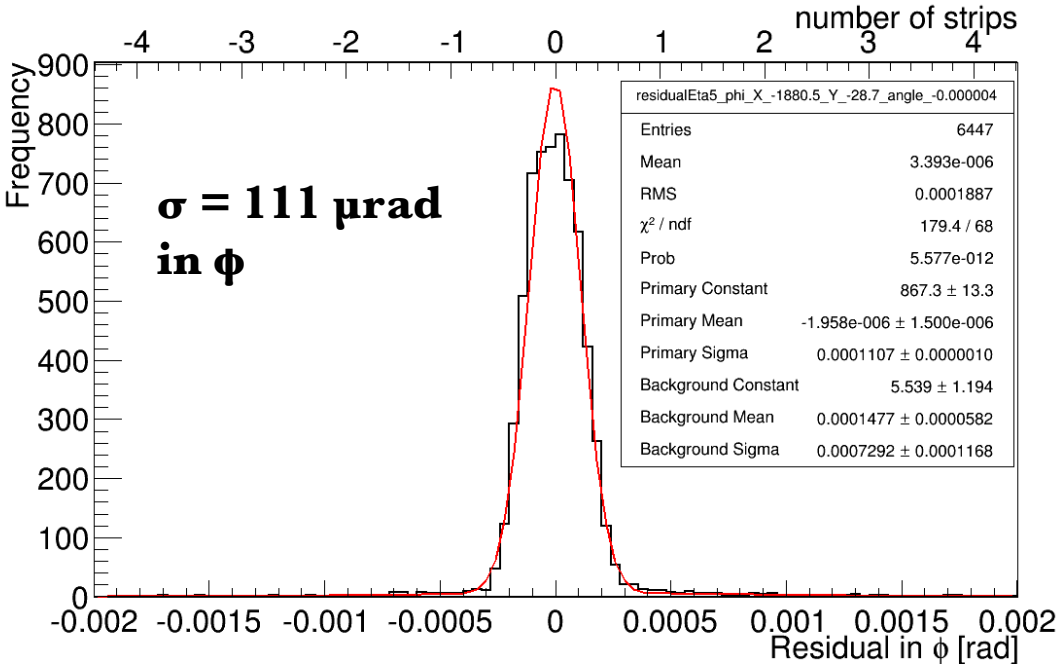

Exclusive Residual

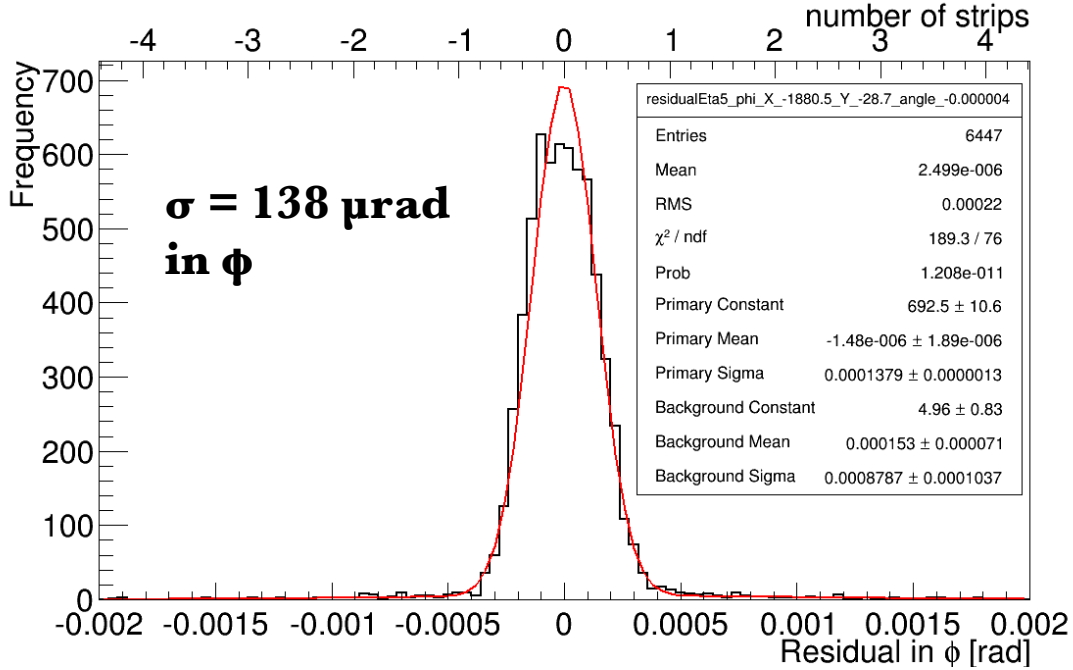

The resolution of the GE1/1-III detector is obtained from the geometric mean of inclusive and exclusive resolution

$$\sigma = \sqrt{\sigma_{inc} \times \sigma_{exc}} = \mathbf{124\ \mu rad}\ (27\%\ \text{of the strip pitch})$$

(corresponding to σ = 233 μm in azimuthal direction)

Charge Measurements with Binary Hit Method

- VFAT3 front-end chip (provides binary hit output) is being designed to read the output from GE1/1
- Charge induced on the GE1/1 readout strip is used as an input for amplifier-shaper of the VFAT3 chip
- For retaining good quality of signal, it is important to match the dynamic range of the induced charge to the dynamic range of the chip input
- Dynamic charge range for the GE1/1 detector is measured using the pulse height sensitive APV-25 chip.
- Estimated the charge range for VFAT3 using the data collected by APV-25 chip

CMS-IN-2017-001 ; CERN-CMS-IN-2017-001

After ADC to fC conversion 99 percentile charge for various strip clusters calculated

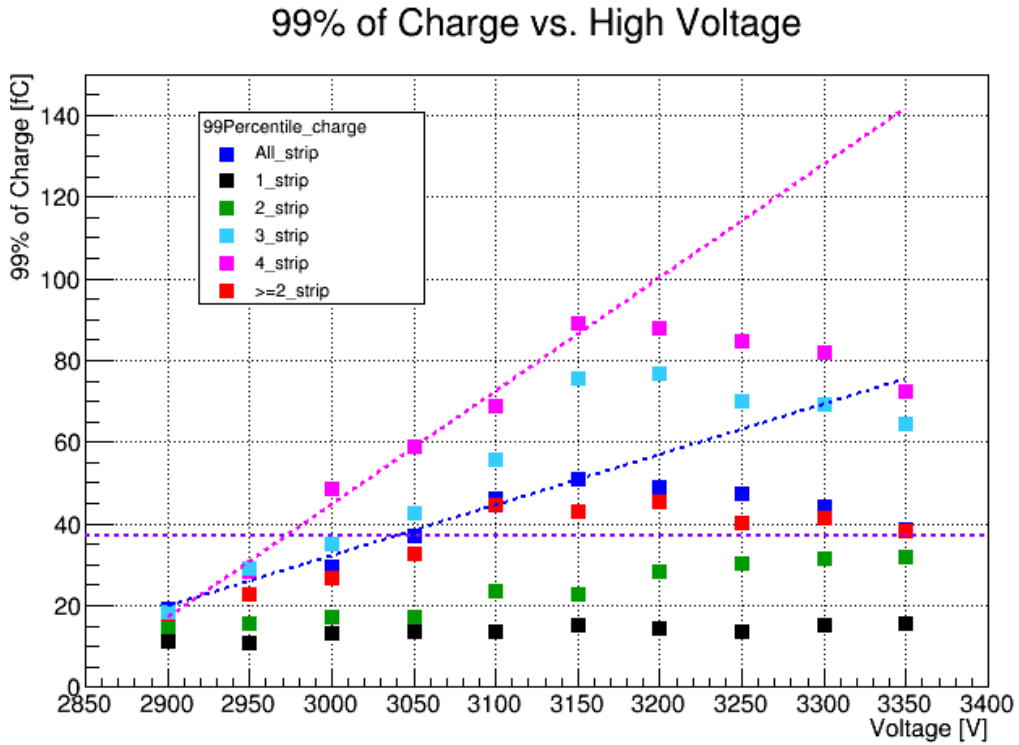

99% (operating voltage) = ~115fC
99% (Max HV) = ~140fC

Available on CMS information server

CMS IN -2017/001

CMS Internal Note

The content of this note is intended for CMS internal use and distribution only

05 April 2017

Measurement of the Charge Induced on the Readout Strips of a GE1/1 Detector Prototype for the CMS Muon Endcap GEM Upgrade

Vallary Bhopatkar, Marcus Hohlmann, Aiwu Zhang

Abstract

Early in the second phase of the LHC program, Gas Electron Multiplier (GEM) technology will be implemented in the GE1/1 muon chambers for the region $1.6 < |\eta| < 2.2$ of the CMS muon endcap. A VFAT3 front-end chip is being designed to read out the GE1/1 detector that will provide binary hit output. The charge that is induced on the GE1/1 readout strips by minimum-ionizing particles is an important parameter that informs the design of the amplifier-shaper input stage of the VFAT3 chip. We have measured this charge distribution directly with a GE1/1-III prototype chamber read out with the pulse-height-sensitive APV25 chip and exposed to a mixed-hadron beam at Fermilab. When operating 50 V above the start of the efficiency plateau in an Ar/CO_2 70:30 gas mixture, i.e. with 3250 V applied to the drift electrode, the most probable value, mean value, and 99^{th} percentile value of the Landau distribution of the charge induced on a single strip are found to be 4 fC, 11 fC, and 115 fC, respectively. Measurements with a more economical readout structure with 128 zigzag strips per η-sector instead of the 384 strips per η-sector in the GE1/1 are also analyzed. When equipping the same GE1/1 chamber with a readout board that features such zigzag strips and operating the chamber in the same way as before, the corresponding measured values for most probable and mean values are 7 fC and 16 fC, respectively.

Emulated VFAT Binary Readout Results using APV Analog Readout

- VFAT threshold reconstructed using the following conversion factors

1ADC count = 0.03172 fC

1VFAT unit = 0.08 fC

- Efficiency is plotted for three VFAT thresholds 10VFAT, 12VFAT, 15VFAT units

Detection Efficiency is 97%

Detection efficiency using different VFAT thresholds

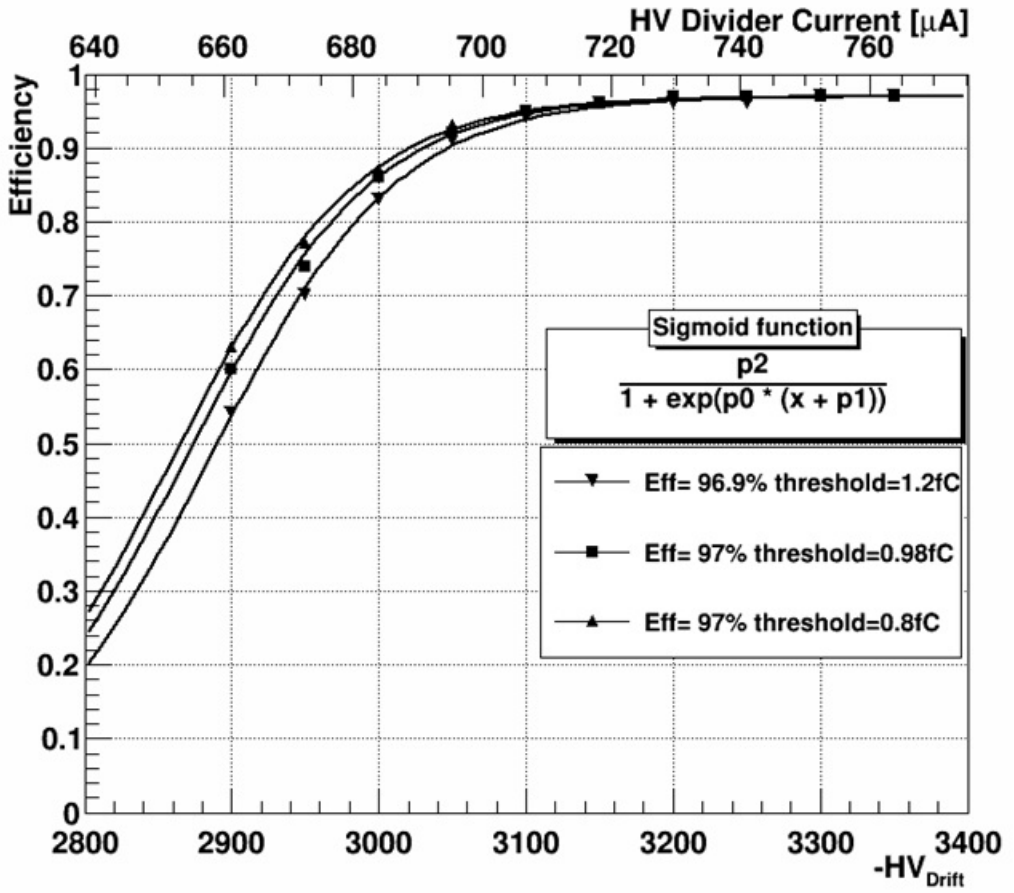

Resolution of the GE1/1-III Detector in η-sector 5 with Emulated VFAT Binary Readout

Inclusive Residual

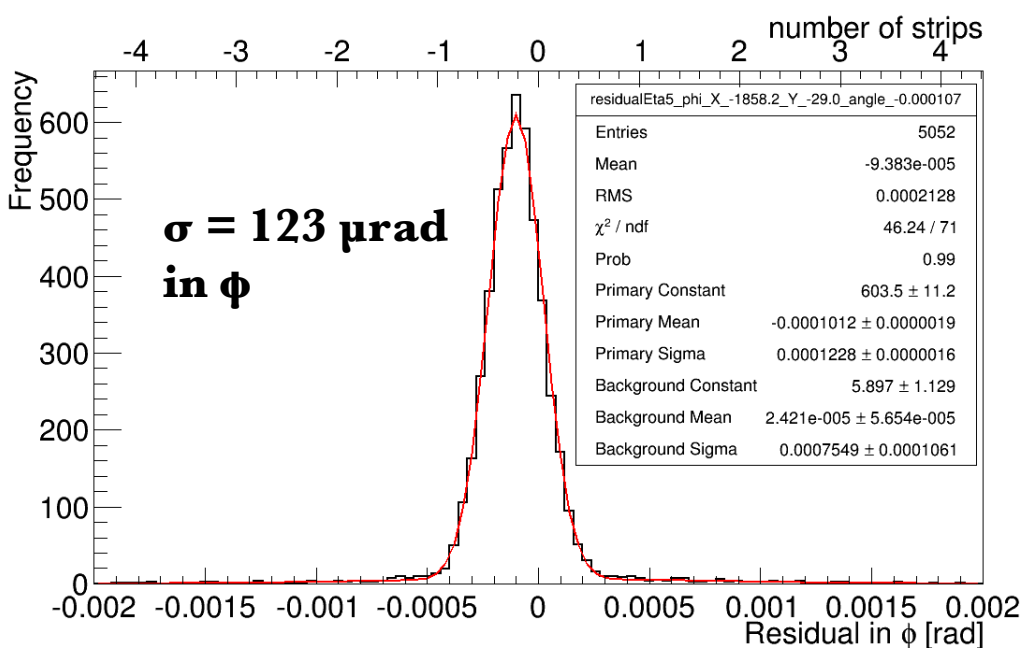

Exclusive Residual

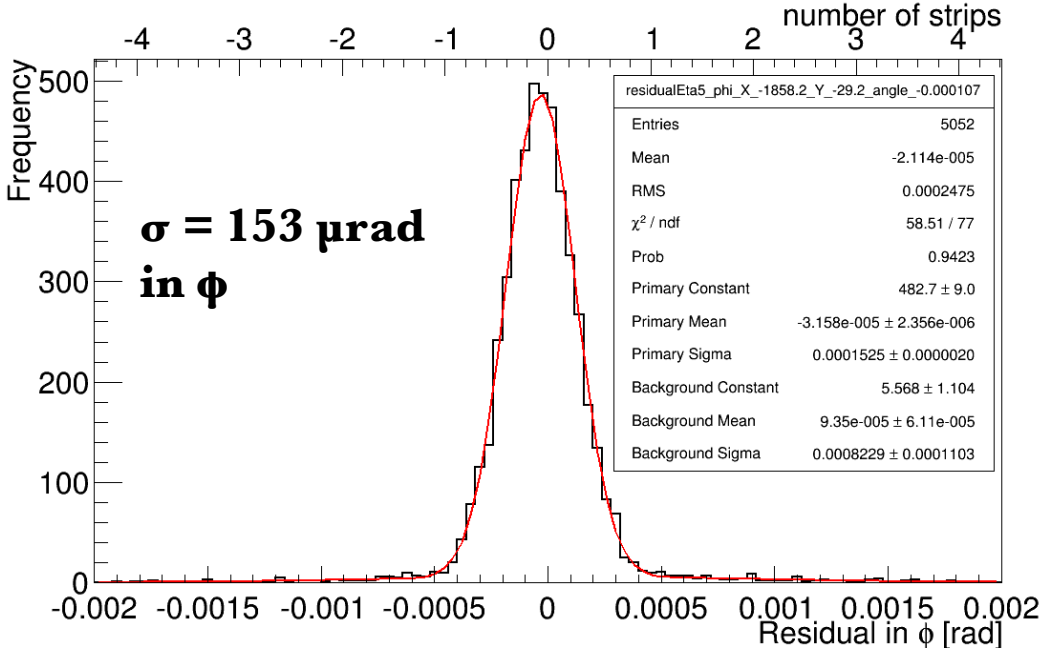

$$\sigma = \sqrt{\sigma_{inc} \times \sigma_{exc}} = \mathbf{137\ \mu rad}$$

(corresponding to σ = 233 μm in azimuthal direction)

Expected resolution from the strip pitch: **pitch/√12 = 131 μrad**

Performance of a Large-Area GEM Detector Prototype for the Upgrade of the CMS Muon Endcap System

D. Abbaneo[15], M. Abbas[15], M. Abbrescia[2], A.A. Abdelalim[8], M. Abi Akl[13], W. Ahmed[8], W. Ahmed[17], P. Altieri[2], R. Aly[8], C. Asawatangtrakuldee[3], A. Ashfaq[17], P. Aspell[15], Y. Assran[7], I. Awan[17], S. Bally[15], Y. Ban[3], S. Banerjee[19], P. Barria[5], L. Benussi[14], V. Bhopatkar[22]*, *Member, IEEE,* S. Bianco[14], J. Bos[15], O. Bouhali[13], S. Braibant[4], S. Buontempo[24], C. Calabria[2], M. Caponero[14], C. Caputo[2], F. Cassese[24], A. Castaneda[13], S. Cauwenbergh[16], F.R. Cavallo[4], A. Celik[9], M. Choi[31], K. Choi[31], S. Choi[29], J. Christiansen[15], A. Cimmino[16], S. Colafranceschi[15], A. Colaleo[2], A. Conde Garcia[15], M.M. Dabrowski[15], G. De Lentdecker[5], R. De Oliveira[15], G. de Robertis[2], S. Dildick[9,16], B. Dorney[15], W. Elmetenawee[8], G. Fabrice[27], M. Ferrini[14], S. Ferry[15], P. Giacomelli[4], J. Gilmore[9], L. Guiducci[4], A. Gutierrez[12], R.M. Hadjiiska[28], A. Hassan[8], J. Hauser[21], K. Hoepfner[1], M. Hohlmann[22]*, *Member, IEEE,* H. Hoorani[17], Y.G. Jeng[18], T. Kamon[9], P.E. Karchin[12], H.S. Kim[18], S. Krutelyov[9], A. Kumar[11], J. Lee[31], T. Lenzi[5], L. Litov[28], F. Loddo[2], T. Maerschalk[5], G. Magazzu[26], M. Maggi[2], Y. Maghrbi[13], A. Magnani[25], N. Majumdar[19], P.K. Mal[6], K. Mandal[6], A. Marchioro[15], A. Marinov[15], J.A. Merlin[15], A.K. Mohanty[23], A. Mohapatra[22], S. Muhammad[17], S. Mukhopadhyay[19], M. Naimuddin[11], S. Nuzzo[2], E. Oliveri[15], L.M. Pant[23], P. Paolucci[24], I. Park[31], G. Passeggio[24], B. Pavlov[28], B. Philipps[1], M. Phipps[22], D. Piccolo[14], H. Postema[15], G. Pugliese[2], A. Puig Baranac[15], A. Radi[7], R. Radogna[2], G. Raffone[14], S. Ramkrishna[11], A. Ranieri[2], C. Riccardi[25], A. Rodrigues[15], L. Ropelewski[15], S. RoyChowdhury[19], M.S. Ryu[18], G. Ryu[31], A. Safonov[9], A. Sakharov[10], S. Salva[16], G. Saviano[14], A. Sharma[15], *Senior Member, IEEE,* S.K. Swain[6], J.P. Talvitie[15,20], C. Tamma[2], A. Tatarinov[9], N. Turini[26], T. Tuuva[20], J. Twigger[22], M. Tytgat[16], *Member, IEEE,* I. Vai[25], M. van Stenis[15], R. Venditi[2], E. Verhagen[5], P. Verwilligen[2], P. Vitulo[25], D. Wang[3], M. Wang[3], U. Yang[30], Y. Yang[5], R. Yonamine[5], N. Zaganidis[16], F. Zenoni[5], A. Zhang[22]

Manuscript received November 30, 2014.

[1]RWTH Aachen University, III Physikalisches Institut A, Aachen, Germany
[2]Politecnico di Bari, Università di Bari and INFN Sezione di Bari, Bari, Italy
[3]Peking University, Beijing, China
[4]University and INFN Bologna, Bologna, Italy
[5]Université Libre de Bruxelles, Brussels, Belgium
[6]National Institute of Science Education and Research, Bhubaneswar, India
[7]Academy of Scientific Research and Technology, ENHEP, Cairo, Egypt
[8]Helwan University & CTP, Cairo, Egypt
[9]Texas A&M University, College Station, USA
[10]Kyungpook National University, Daegu, Korea
[11]University of Delhi, Delhi, India
[12]Wayne State University, Detroit, USA
[13]Texas A&M University at Qatar, Doha, Qatar
[14]Laboratori Nazionali di Frascati - INFN, Frascati, Italy
[15]CERN, Geneva, Switzerland
[16]Ghent University, Dept. of Physics and Astronomy, Ghent, Belgium
[17]National Center for Physics, Quaid-i-Azam University Campus, Islamabad, Pakistan
[18]Chonbuk National University, Jeonju, Korea
[19]Saha Institute of Nuclear Physics, Kolkata, India
[20]Lappeenranta University of Technology, Lappeenranta, Finland
[21]University of California, Los Angeles, USA
[22]Florida Institute of Technology, Melbourne, USA
[23]Bhabha Atomic Research Centre, Mumbai, India
[24]INFN Napoli, Napoli, Italy
[25]INFN Pavia and University of Pavia, Pavia, Italy
[26]INFN Sezione di Pisa, Pisa, Italy
[27]IRFU CEA-Saclay, Saclay, France

***Abstract*—Gas Electron Multiplier (GEM) technology is being considered for the forward muon upgrade of the CMS experiment in Phase 2 of the CERN LHC. Its first implementation is planned for the GE1/1 system in the $1.5 < |\eta| < 2.2$ region of the muon endcap mainly to control muon level-1 trigger rates after the second long LHC shutdown. A GE1/1 triple-GEM detector is read out by 3,072 radial strips with 455 μrad pitch arranged in eight η-sectors. We assembled a full-size GE1/1 prototype of 1m length at Florida Tech and tested it in 20-120 GeV hadron beams at Fermilab using Ar/CO_2 70:30 and the RD51 scalable readout system. Four small GEM detectors with 2-D readout and an average measured azimuthal resolution of 36 μrad provided precise reference tracks. Construction of this largest GEM detector built to-date is described. Strip cluster parameters, detection efficiency, and spatial resolution are studied with position and high voltage scans. The plateau detection efficiency is [97.1 $\pm$ 0.2 (stat)]%. The azimuthal resolution is found to be [123.5 $\pm$ 1.6 (stat)] μrad when operating in the center of the efficiency plateau and using full pulse height information. The resolution can be slightly improved by $\sim$ 10 μrad when correcting for the bias due to discrete readout strips. The CMS upgrade design calls for readout electronics with binary hit output. When strip clusters are formed correspondingly without charge-**

[28]Sofia University, Sofia, Bulgaria
[29]Korea University, Seoul, Korea
[30]Seoul National University, Seoul, Korea
[31]University of Seoul, Seoul, Korea
*Corresponding authors: vbhopatkar2010@my.fit.edu, hohlmann@fit.edu

978-1-4799-6097-2/14/$31.00 ©2014 IEEE

CERN-LHCC-2015-012
CMS-TDR-013
30 September 2015

CMS TECHNICAL DESIGN REPORT FOR THE MUON ENDCAP GEM UPGRADE

CERN-LHCC-2015-012 / CMS-TDR-013
03/11/2015

This report describes both the technical design and the expected performance of the Phase-II upgrade, using Gas Electron Multiplier (GEM) detectors, of the first endcap station of the CMS muon system. The upgrade is targeted for the second long shutdown of the CERN LHC and is designed to improve the muon trigger and tracking performance at high luminosity. The GEM detectors will add redundancy to the muon system in the $1.6 < |\eta| < 2.2$ pseudorapidity region, where the amount of detection layers is lowest while the background rates are highest and the bending of the muon trajectories due to the CMS magnetic field is small. GEM detectors have been identified as a suitable technology to operate in the high radiation environment present in that region. The first muon endcap station will be instrumented with a double layer of triple-GEM chambers in the $1.6 < |\eta| < 2.2$ region. The detector front-end electronics uses the custom designed VFAT3 chip to provide both fast input for the level-1 muon trigger and full granularity information for offline muon reconstruction. This document describes the design of detectors, electronics, and services. The expected performance of the upgraded muon system is discussed in the context of several benchmark physics channels. The document also presents the plan - including the project schedule, cost, and organization - for the detector construction, testing, and integration into the CMS detector.

ISBN 978-92-9083-396-3

Contributors

M. A. Akl, M. Abbrescia, O. Aboamer, N. Amapane, P. Aspell, S. Banerjee, S. Bally, A. Puig-Barnac, P. Barria, G. Bencze, N. Beni, L. Benussi, V. Bhopatkar, S. Bianco, O. Bouhali, C. Calabria, A. Castaneda, F. Cavallo, A. Cimmino, S. Colafranceschi, A. Colaleo, A. Conde Garcia, I. Crotty, M. Dabrowski, G. De Lentdecker, R. De Oliveira, G. De Robertis, S. Dildick, B. Dorney, A. Gaddi, P. Giacomelli, J. Gilmore, M. Hadjiiska, J. Hauser, K. Hoepfner, M. Hohlmann, T. Huang, A.K. Kalsi, T. Kamon, P. Karchin, V. Krutelyov, A. Lanaro, J. Lee, T. Lenzi, F. Loddo, A. Madorsky, T. Maerschalk, M. Maggi, A. Magnani, A. Marinov, J. Merlin, G. Mitselmakher, A. Mohapatra, P. Paolucci, R. Radogna, A. Ranieri, C. Riccardi, A. Safonov, M. Saleh, G. Saviano, A. Sharma, J. Sturdy, Z. Szillasi, J. Talvitie, S. Teruki, M. Tytgat, R. Venditti, E. Verhagen, P. Verwilligen, Y. Yang, F. Zenoni, A. Zhang

Current Updates on the GEM Upgrade Project

- The beam test at FNAL was successful as the performance of the GE1/1 detector meets the expectation for this upgrade
- These results are contributed towards the GEM Technical Design Report **https://cds.cern.ch/record/2021453/**
- With extensive R & D, GEM endcap has been approved and will be install in the forward muon endcap region in 2019
- Total 160 1-m long detectors are being constructed and commissioned at CERN and five external sites. Florida Tech is one of them
- Standard and stringent quality control protocols are created to ensure the successful production run at all commissioning sites
- At Florida Tech, we have implemented all quality control steps and successful built the first GE1/1 mass production module GE1/1-X-S-FIT001

Part II
CMS Physics Analyses

Cross Section Measurement of Z Boson
and
Search for the SM Higgs Boson Decay in
$H \rightarrow \tau\tau \rightarrow \mu\mu$ Channel

Standard Model (SM) and Higgs Boson

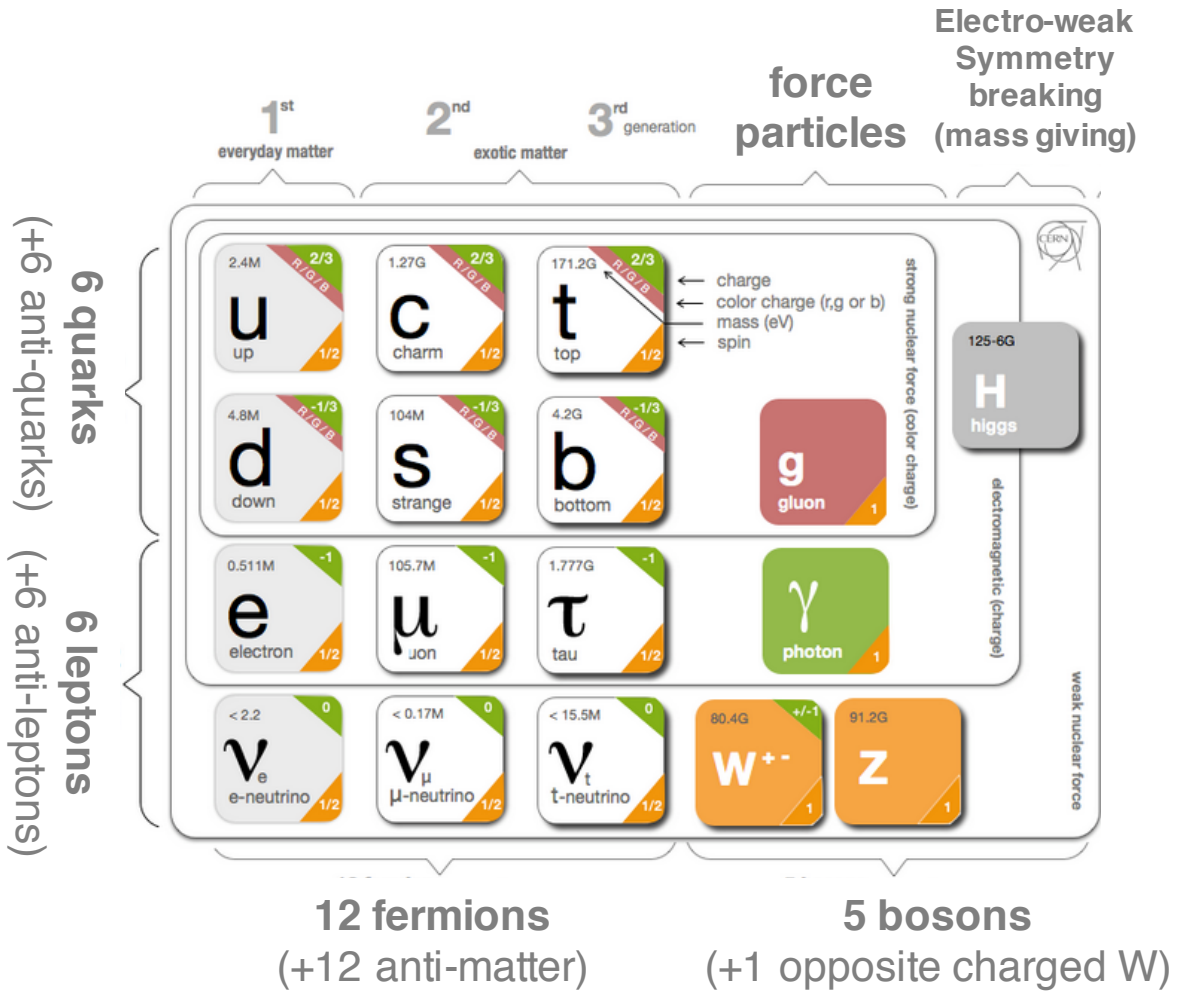

- Higgs Boson predicted by standard model
  Scalar Particle, m_H = 125 GeV, Spin =0
- In SM, particle acquire masses through their interaction with Higgs field
- W and Z Boson acquire masses through electroweak symmetry breaking in gauge theory
- All fermions gain the mass through Yukawa coupling

Higgs: Production and Decay Modes

Production Modes

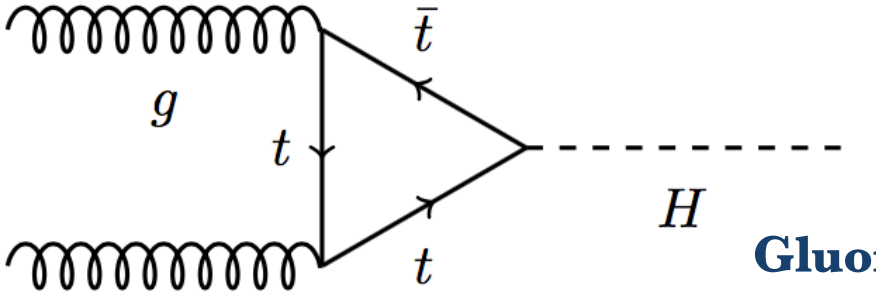

Gluon-Gluon Fusion (GGF, ggH)

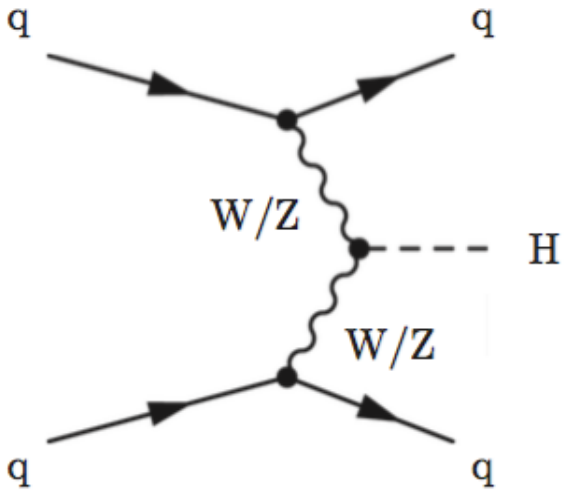

Vector Boson Fusion (VBF, qqH)

Decay Modes

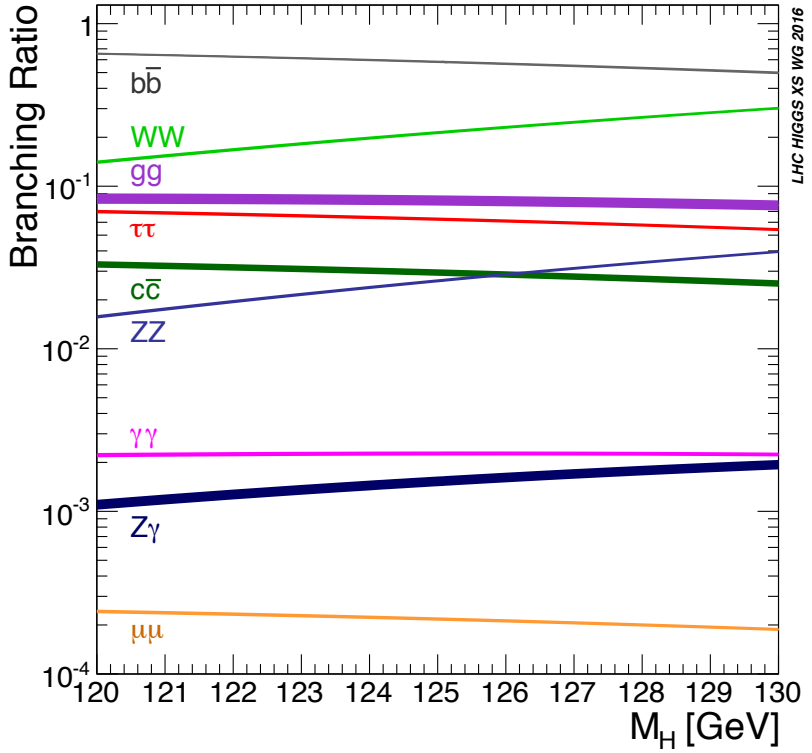

Higgs: Production and Decay Modes

Production Modes

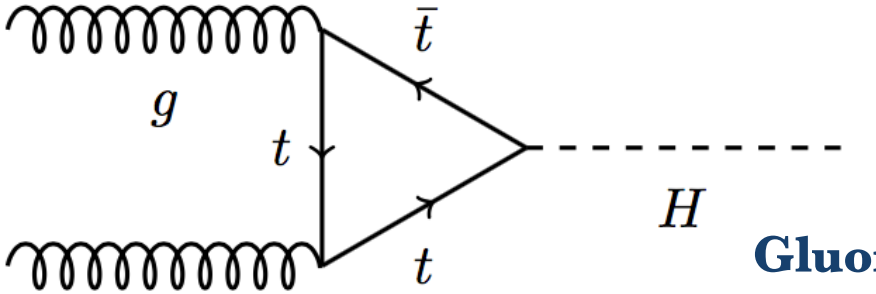

Gluon-Gluon Fusion (GGF, ggH)

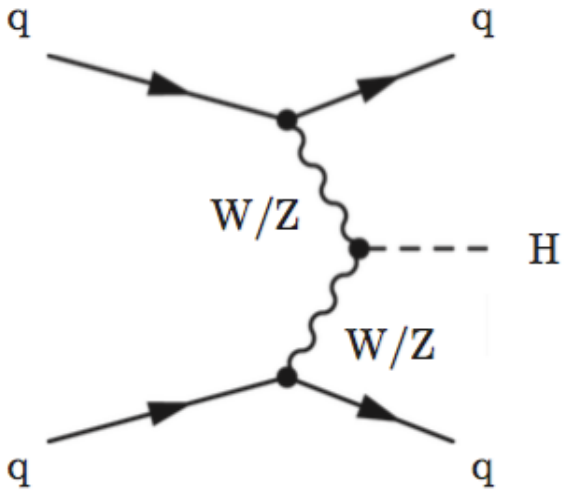

Vector Boson Fusion (VBF, qqH)

Decay Modes

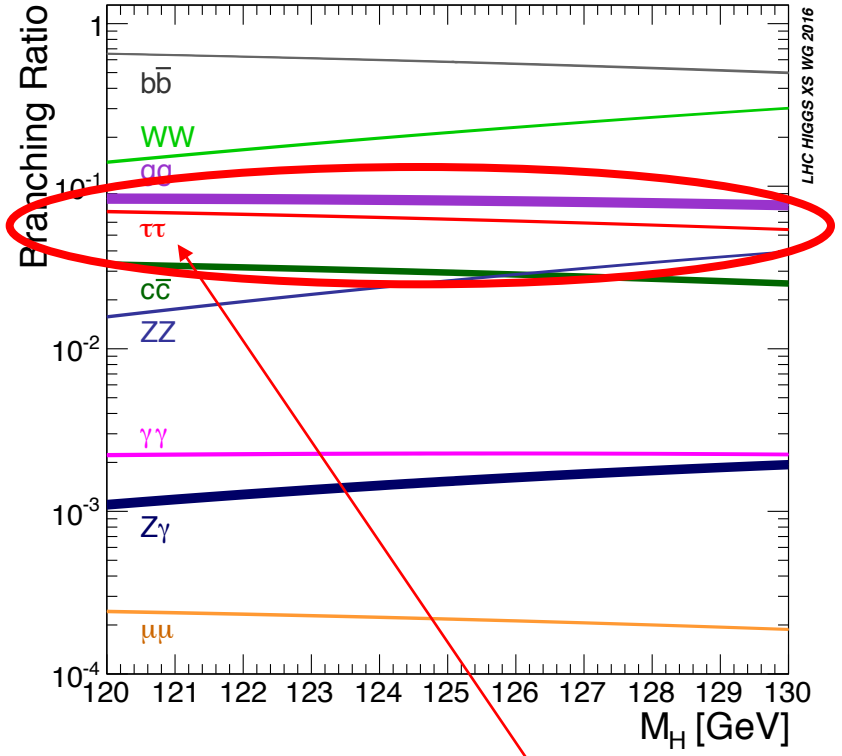

Will be focusing on the **ττ** decay mode

Overview: $H \rightarrow \tau\tau$ Decay Mode

- τ leptons decay hadronically and leptonically
- Promising channel to study Yukawa couplings to leptons
  - Highest event yield among the leptonic channels
  - Lower background compared to $b\bar{b}$ decays
- This dissertation focuses on the leptonic channel where a pair of tau leptons decays into a pair of muons

- Tau decay modes with BR

Decay Mode	BR in [%]
$\tau_{had}\tau_{had}$	42
$\tau_{\mu}\tau_{had}$	23
$\tau_{e}\tau_{had}$	23
$\tau_{e}\tau_{\mu}$	6
$\tau_{e}\tau_{e}$	3
$\tau_{\mu}\tau_{\mu}$	**3**

- **Challenges**:

Small BR + $Z \rightarrow \mu\mu$ background

Cross Section Measurement of $Z \rightarrow \tau\tau$ using CMS Run II 2015 Data

Motivation

- $Z \rightarrow \tau\tau$ is a standard candle for tau physics and dominating background in $H \rightarrow \tau\tau$ analysis
- Main focus is to validate the analysis techniques used in $H \rightarrow \tau\tau$ analysis
- Also these both analyses have similar background model
- $Z\ /\ \gamma^{*} \rightarrow \mu\mu$ is dominating and challenging background for $Z \rightarrow \tau\tau \rightarrow \mu\mu$ channel. Hence, its very crucial to reduce this background to increase the sensitivity of the signal
- Boosted Decision Tree (BDT), a multivariate method is used for the background reduction
- For final cross section measurements, di-tau mass variable is used to extract the signal by performing the likelihood method

Cross Section Measurements

Overview

- $\sqrt{s} = 13$ TeV, $\int \mathcal{L}\, dt = 2.3$ fb^{-1}, 25ns bunch crossing
- Single Muon Dataset is used (2015 RunD) with single muon trigger HLT_IsoMu18_v2
- QCD multijet events derived using data
- Simulated MC samples:
  - Signal: Drell-Yan samples with forced $Z \rightarrow \tau\tau \rightarrow \mu\mu$ events
  - Background, Drell-Yan $Z / \gamma^* \rightarrow \mu\mu$
  - Electroweak background: diboson, single top and W+jets
  - $t\bar{t}$

Base Selection

- Two muons with opposite charges
- $p_T > 10$ GeV and $|\eta| < 2.4$ with leading muon $p_T > 19$ GeV
- Medium Muon Identification criteria with corrected relative isolation < 0.15
- m_{vis} (invariant mass of the dimuon system) < 80 GeV
- BDT (trained to separate $Z \rightarrow \tau\tau \rightarrow \mu\mu$ from $Z/\gamma^* \rightarrow \mu\mu$) > 0.5

Signal Extraction Method

- Di-tau mass ($m_{\tau\tau}$) is reconstructed using **S**econdary **V**ertex **Fit** (SVFit)
  - It is a likelihood-based estimation of the parent boson mass
  - Inputs used for the calculations are: MET, MET uncertainties and four-vectors of the muon candidate
- Signal is extracted using 1-dimensional distribution of reconstructed SVFit mass $m_{\tau\tau}$
- Maximum likelihood fit is performed to obtain event yield for cross section measurements

Signal Extraction

Post Fit inclusive SVFit Mass Plot

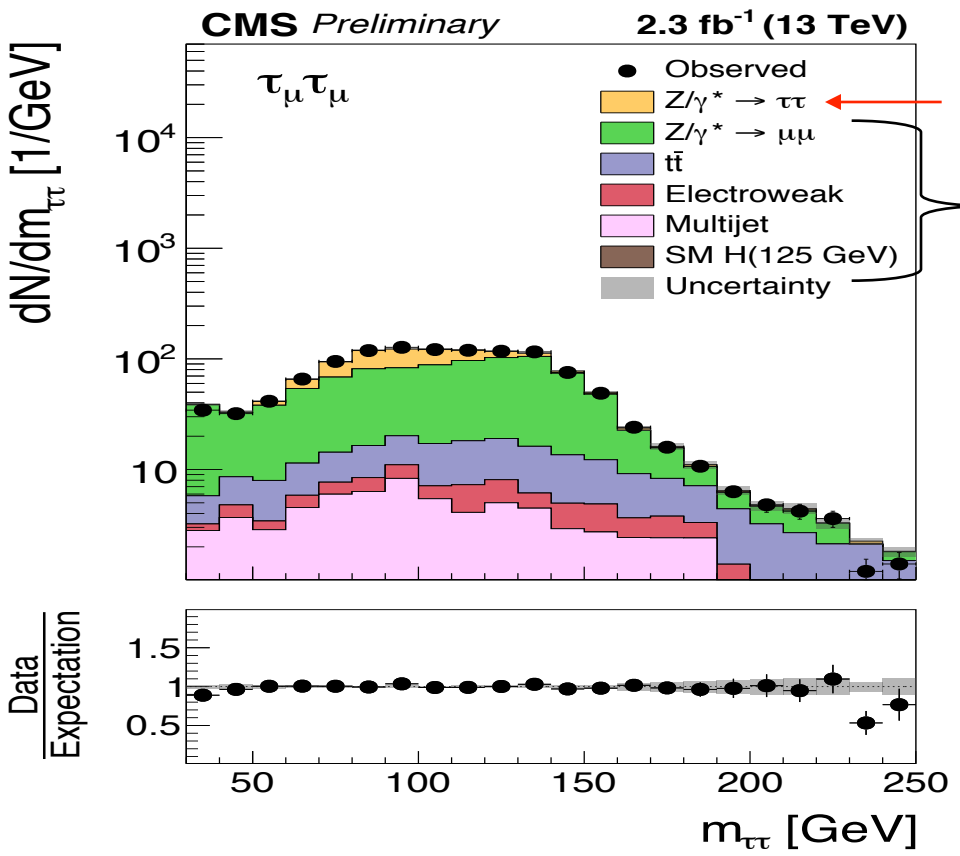

With maximum likelihood fit

Corrections applied to MC

- PileUp reweighting
- Lepton ID/isolation scale factors
- Trigger scale factors
- Top quark pT reweighting
- B-tag scale factors
- Z- recoil correction
- DY pT, mass reweighting

PostFit event yields

Process	$\tau_\mu\tau_\mu$
$Z/\gamma^* \to \tau\tau$	2 067 ± 34
Multijet	710 ± 110
$Z/\gamma^* \to \mu\mu$	8 010 ± 170
$t\bar{t}$	1 239 ± 79
Electroweak	293 ± 30
SM H	18 ± 4
Total expected background	10 270 ± 120
Total SM expectation	12 340 ± 120
Observed data	12 327

Cross Section Extraction

$$\sigma(\mathrm{pp} \to Z/\gamma^* + jets) \times B(Z/\gamma^* \to \tau\tau) = \frac{1}{B_\tau} \cdot \frac{N_{sig}^{fig}(1-f_{out})}{A \cdot \varepsilon \cdot \mathcal{L}}$$

- N_{sig}^{fig} Number of signal events passing selection criteria post fit
- $\mathcal{L}$ Integrated luminosity
- f_{out} Mass window correction for events outside $60 < m_{\tau\tau}^{gen} < 120$ GeV
- $B\tau$ Branching fraction
- A Acceptance
- ε Efficiency

$\tau_\mu\tau_\mu$ Channel

1.967 ± 0.121 (stat.) ± 0.092 (syst.) ± 0.037 (lumi)nb

CMS PAPER HIG-15-007

DRAFT

CMS Paper

The content of this note is intended for CMS internal use and distribution only

2017/11/21
Head Id: 435478
Archive Id: 435480P
Archive Date: 2017/11/21
Archive Tag: trunk

Measurement of the $Z/\gamma^* \to \tau\tau$ cross section in proton-proton collisions at $\sqrt{s} = 13$ TeV and validation of analysis techniques relevant for studies of τ lepton production

The CMS Collaboration

Abstract

We present a measurement of the $Z/\gamma^* \to \tau\tau$ cross section in proton-proton collisions at $\sqrt{s} = 13$ TeV, using data recorded by the CMS experiment at the LHC, corresponding to an integrated luminosity of 2.3 fb^{-1}. The product of the cross section and branching fraction is measured to be $\sigma(pp \to Z/\gamma^*+X) \times \mathcal{B}(Z/\gamma^* \to \tau\tau) = 1848 \pm 12$ (stat.) $\pm$ 67 (syst.+lumi.) pb, in agreement with the standard model expectation, computed at next-to-next-to-leading order accuracy in perturbative quantum chromodynamics. The measurement is used to validate new analysis techniques, relevant for future analyses of τ lepton production. As a byproduct of the measurement, the reconstruction efficiency and energy scale for τ decays to hadron+ν_τ final states are determined with respective relative uncertainties of 2.2% and 0.9%.

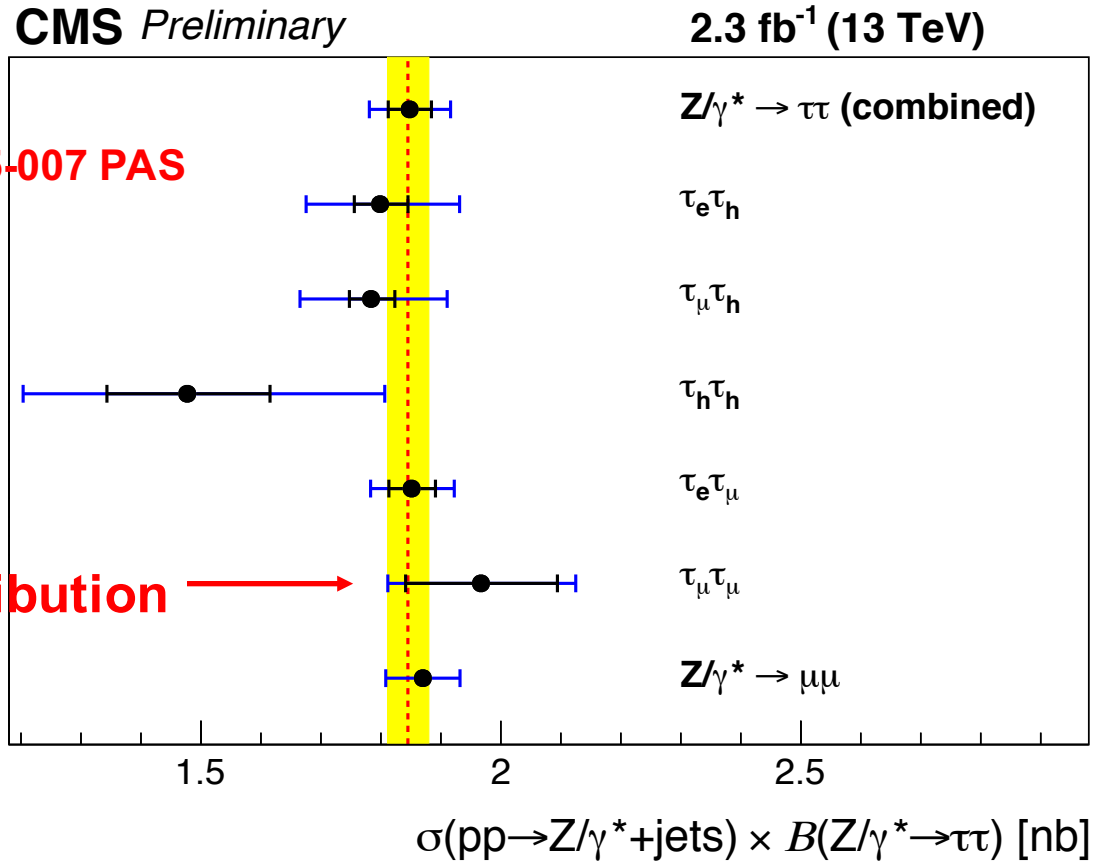

Combined: $1.848 \pm 0.012(\text{Stat.}) \pm 0.057(\text{syst.}) \pm 0.034(\text{lumi.})$nb

NNLO theory prediction: $1.845^{+0.012}_{-0.006}(\text{scale}) \pm 0.033(\text{PDF})$nb

$pp \to Z/\gamma^* \to ee/\mu\mu$**:** $1.870 \pm 0.002\ (\text{stat.}) \pm 0.035\ (\text{syst.}) \pm 0.051\ (\text{lumi})$nb

Combined value shows good agreement with NNLO theory prediction and $Z/\gamma^* \to ee/\mu\mu$ measurement (based on the same data set)

- **Final paper reading in Collaboration is scheduled on December 12**
- **After reading will be submitted to EPJC**

Search for SM Higgs Boson decay in $H \rightarrow \tau\tau \rightarrow \mu\mu$ using CMS Run II 2016 Data

Run I and Run II Overview

Run I (Results with all six decay modes)

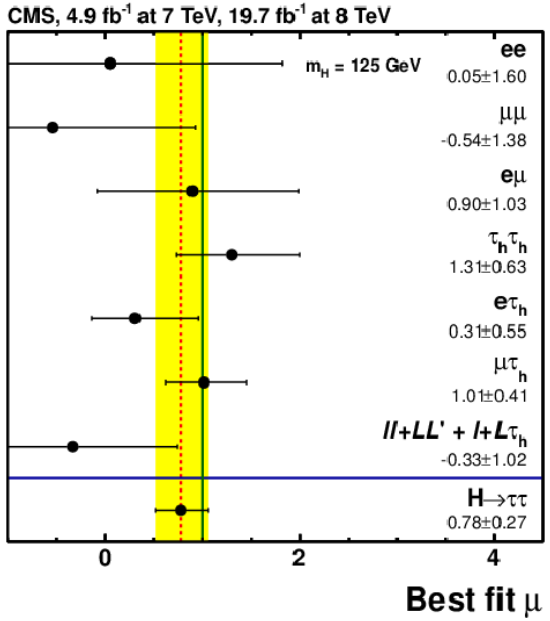

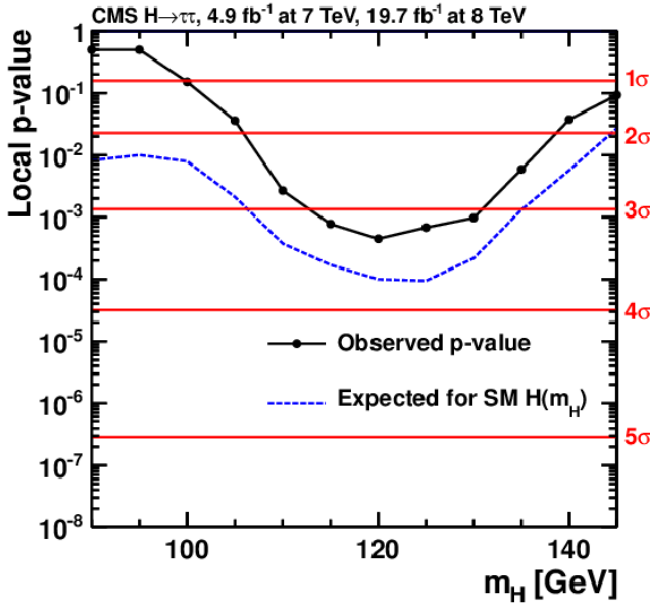

- CMS obtained evidence at 3.2σ with signal strength $\hat{\mu} = 0.78 \pm 0.27$ [JHEP 05 (2014) 104]
- CMS + ATLAS combined results shows evidence at 5.5σ [JHEP 08 (2016) 045]

Run II (Results with $\tau_h\tau_h, \tau_\mu\tau_h, \tau_e\tau_h, \tau_e\tau_\mu$)

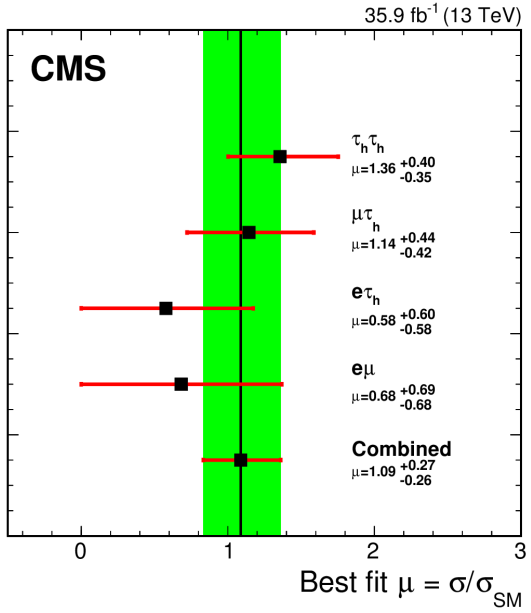

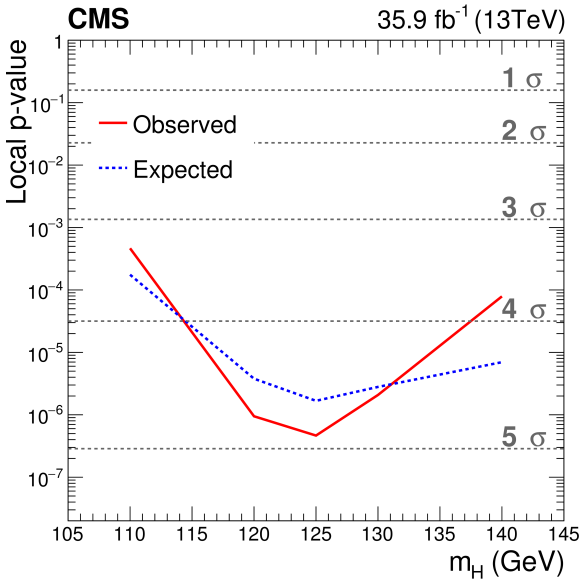

- CMS observed evidence at 4.7σ, with signal strength relative to SM $\hat{\mu} = 1.09^{+0.27}_{-0.26}$
- Submitted to Phys. Lett. B (CMS-HIG-16-043 ; CERN-EP-2017-181)

SM $\boldsymbol{H \rightarrow \tau\tau \rightarrow \mu\mu}$ Analysis With Run II 2016 Data

Event Selection

- Run II full 2016 dataset RunB-H
- $\sqrt{s} = 13$ TeV, $\int \mathcal{L}\, dt = 35.9$ fb^{-1}
- Bunch crossing 25ns
- Single Muon Data used with HLT single muon trigger *HLT_IsoMu24_V*
- $d_{xy} < 0.045$cm
- $d_Z < 0.2$cm
- $\triangle R(\mu^+,\mu^-) \geq 0.5$
- $\triangle\beta$ relIso < 0.15

Channel Specific Selection

- Two muons with opposite charges
- $p_T > 10$ GeV and $|\eta| < 2.4$
- Leading muon $p_T > 25$ GeV and match HLT muon objects with $\triangle R < 0.5$
- Must satisfy medium Particle Flow (PF) muon identification criteria for simulated events and for data from Run G-H
- Special 2016 (ICHEP) medium PF criteria for data from Run B-F
- Visible mass m_{vis}>20 GeV

Event Categorization

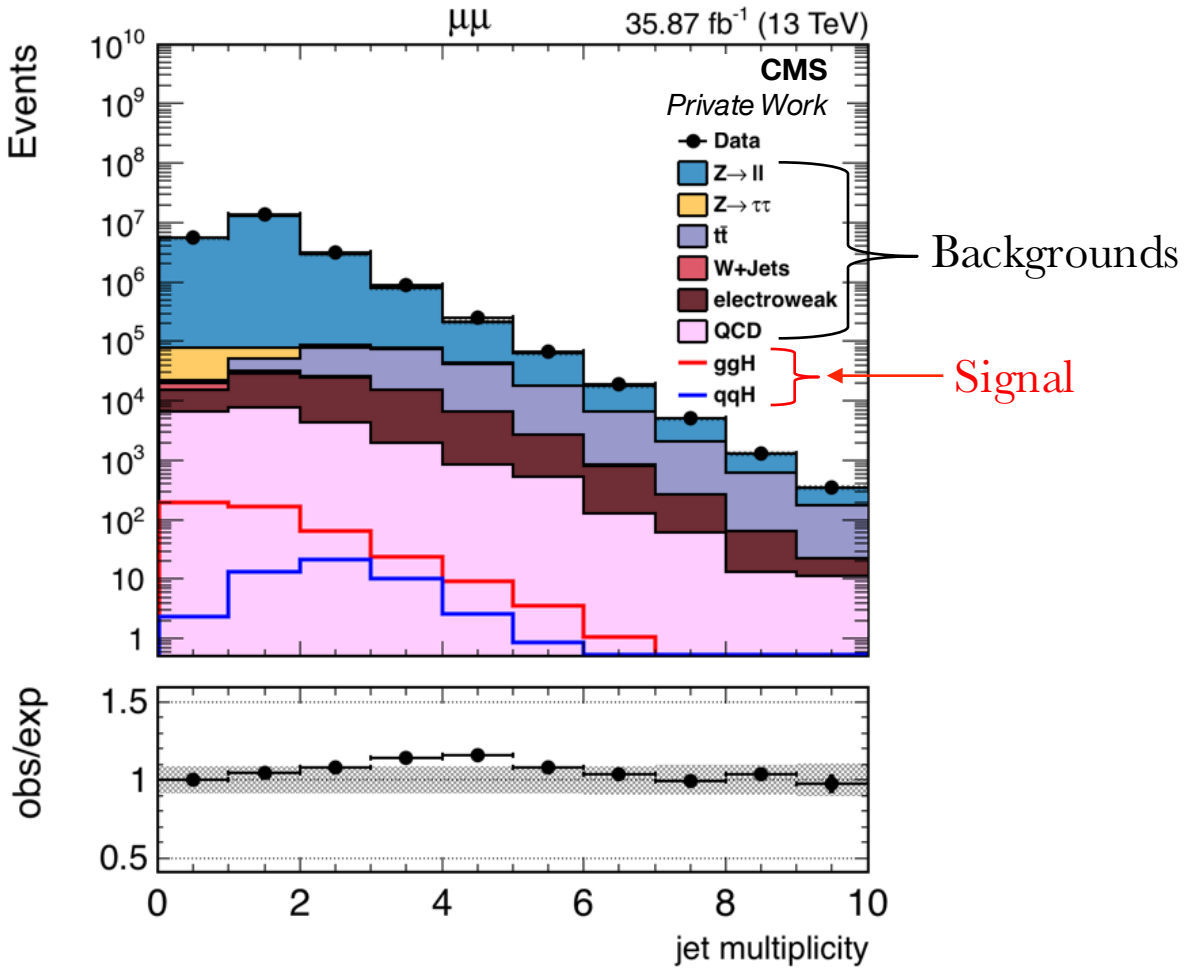

Three event categories based on the jet multiplicity are considered for signal extraction:

- **0-jet** Targets the gluon-gluon fusion production (ggH) (0 jet multiplicity)
- **Boosted** Targeting ggH events with the Higgs recoiling against an additional jet and qqH events that fail the di-jet cut (jet multiplicity is 1 or ≥2 with di-jet mass m_{jj}<300 GeV)
- **VBF** Targets the vector boson fusion (qqH) via di-jet cut (jet multiplicity is exactly 2 with di-jet mass m_{jj}>300 GeV)

Data/MC Corrections and Event Weights

- **Generator event weights** applied to all MC samples on the event-by-event basis.
- **Pile-Up (PU)** reweighting applied to all MC samples (minimum bias xsec 69.2 mb).
- **Lepton ID/Iso scale factors** obtained using "Tag and Probe" method using $Z \rightarrow \mu\mu$ MC samples and applied to all simulated events.
- **Trigger Efficiency** applied to all MC events.
- **DY reweighting** evaluated separately for each jet category in bins of dimuon p_T, η, and mass and applied only to the DY events with mass > 50 GeV.
- **Recoil corrections** applied to DY, W+jets, and Higgs MC samples
- **Top p_T reweighting** applied to $t\bar{t}$ events.

Kinematic Plots for VBF Category

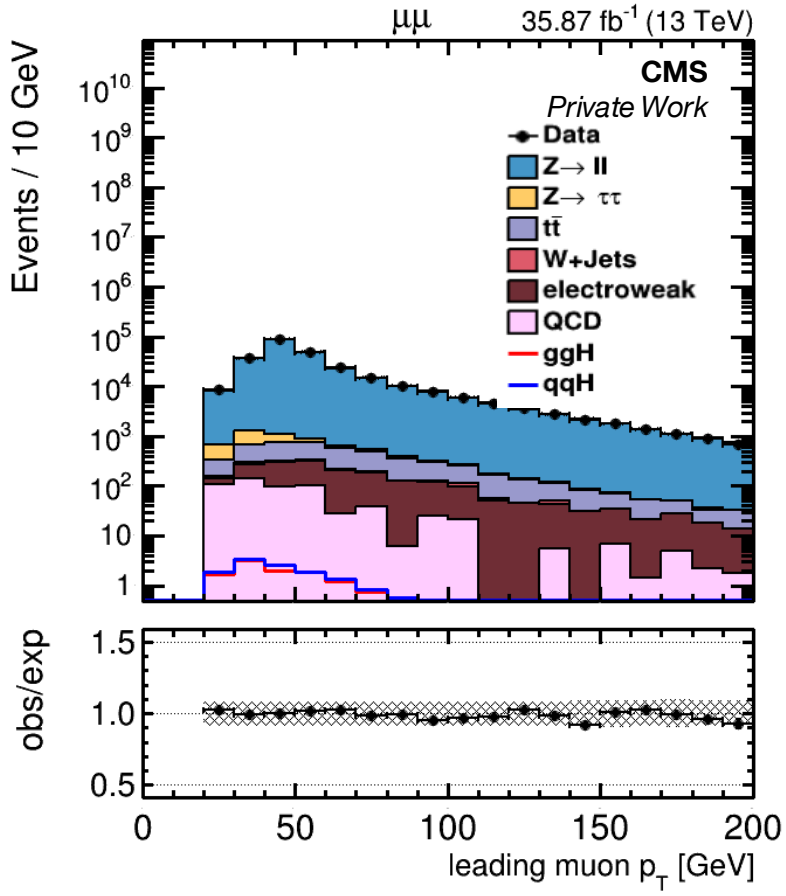

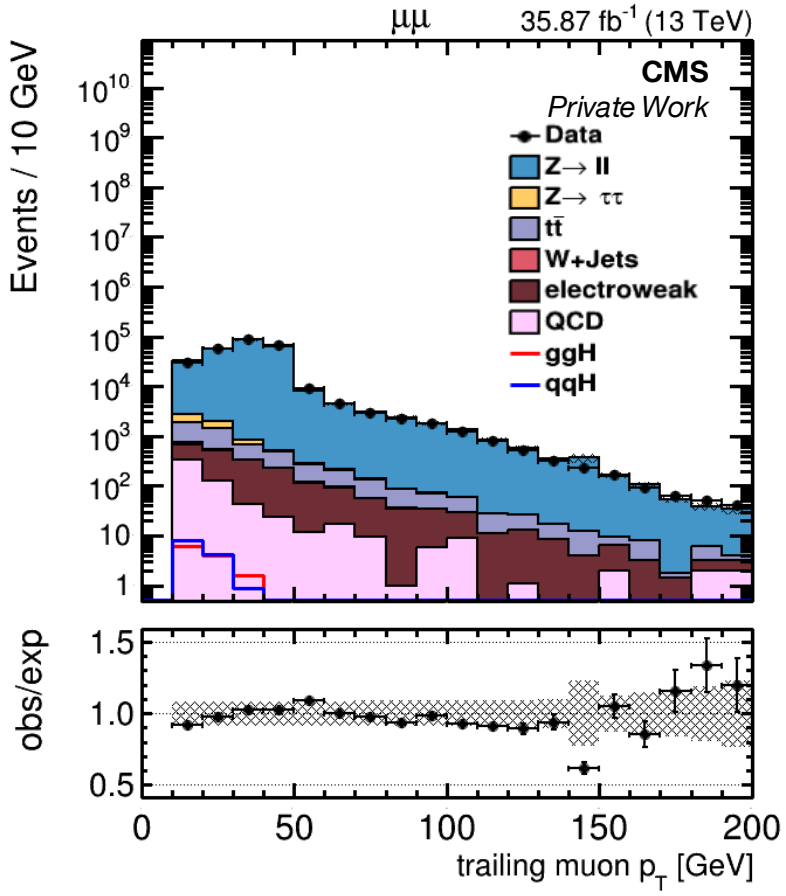

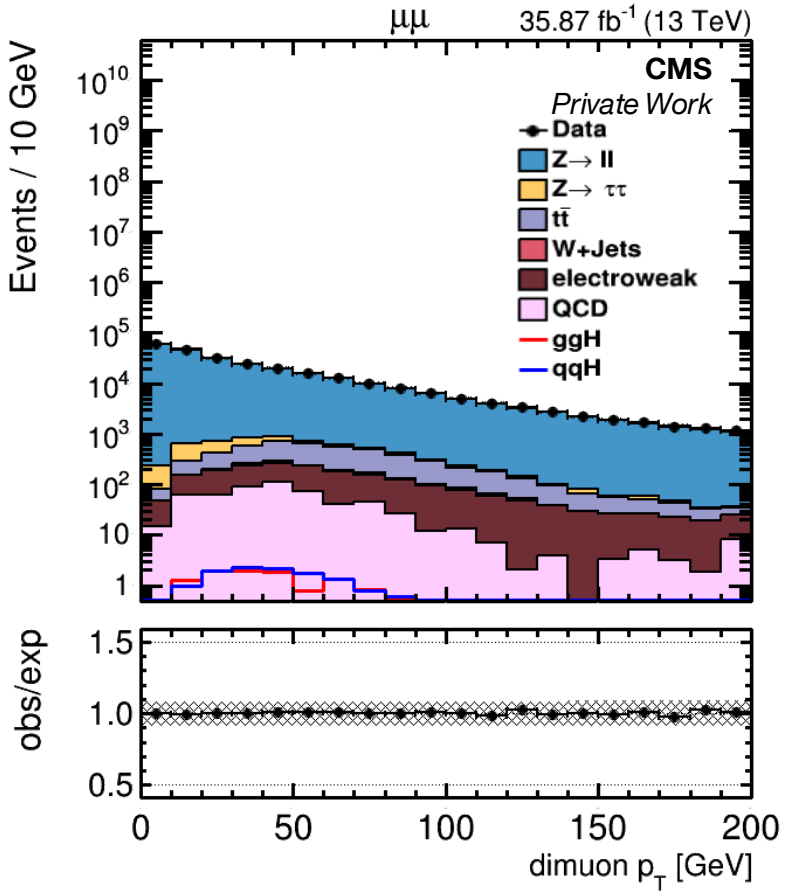

Kinematic Plots for VBF Category

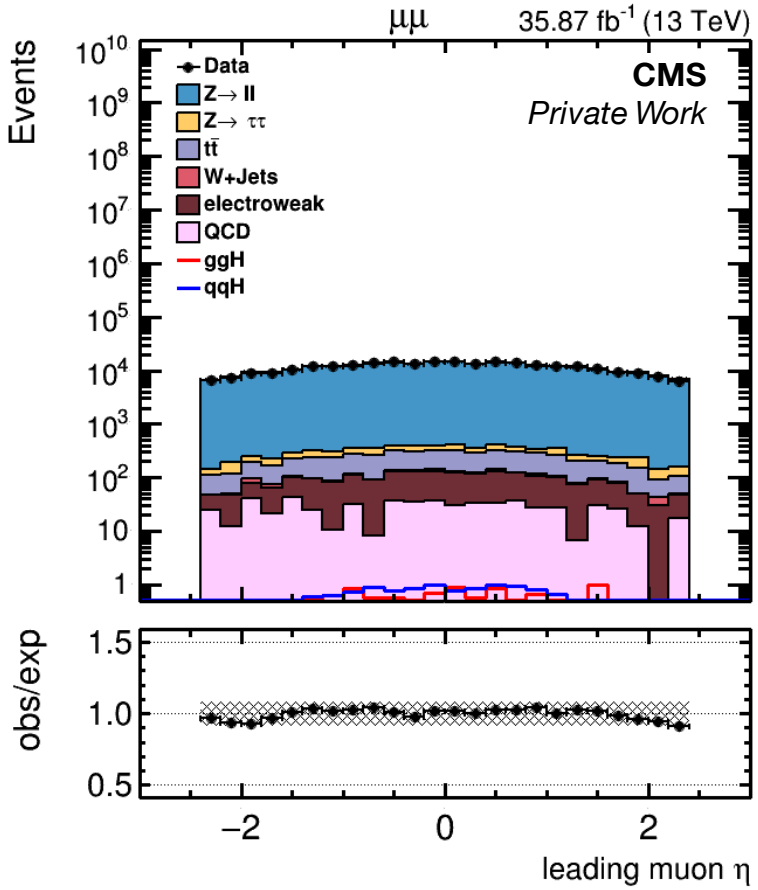

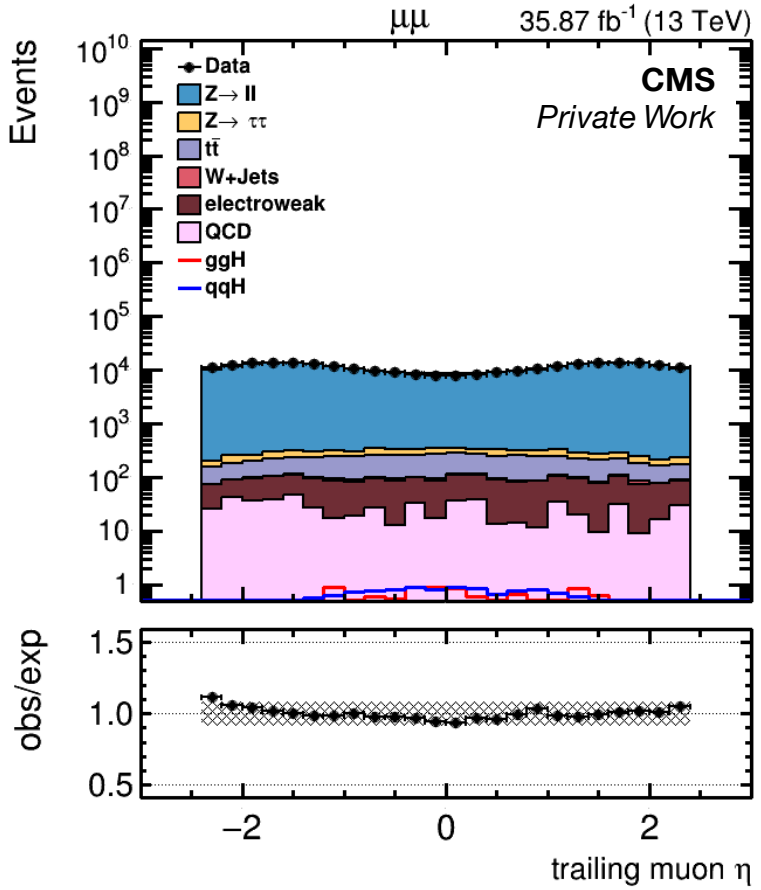

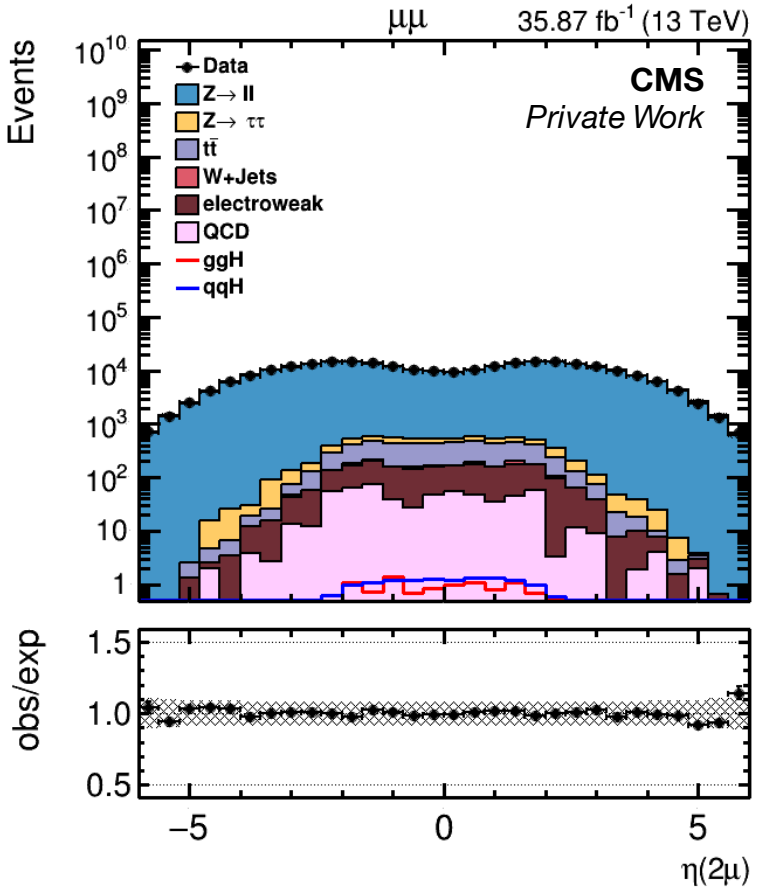

Discriminating Variable Plots for VBF Category

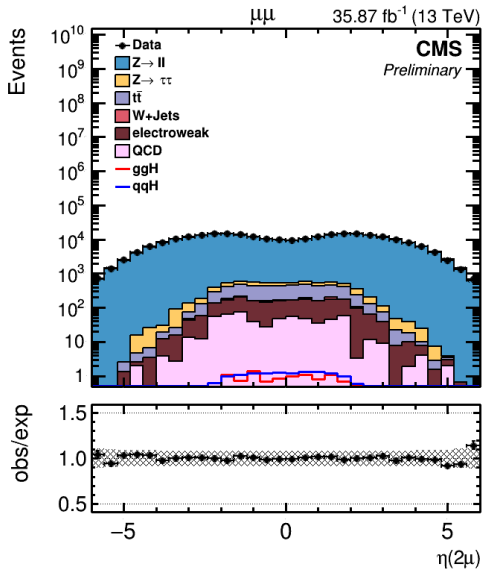

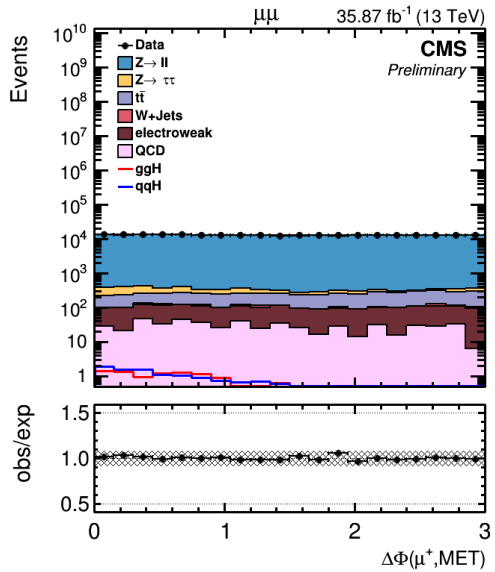

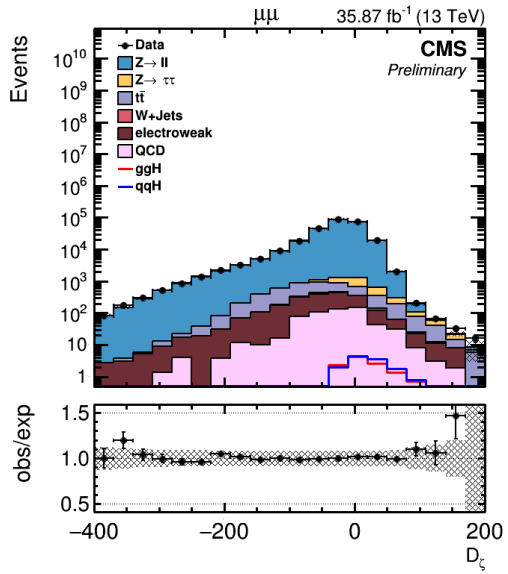

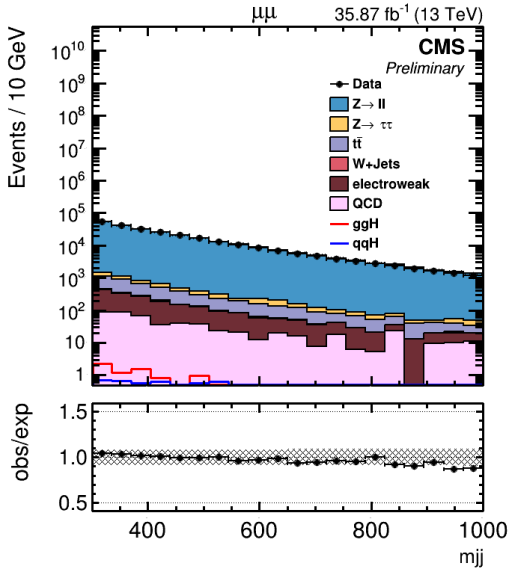

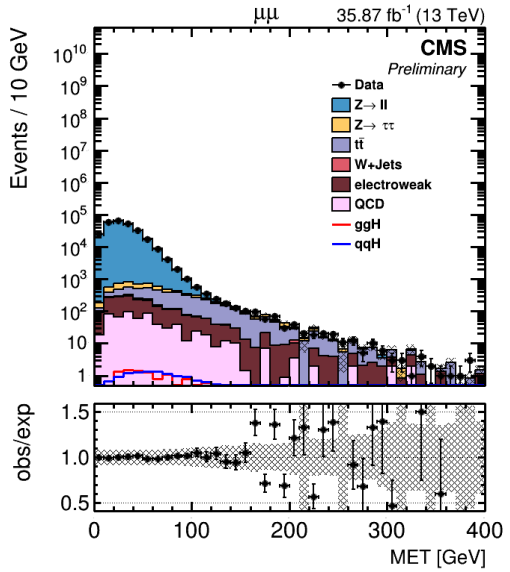

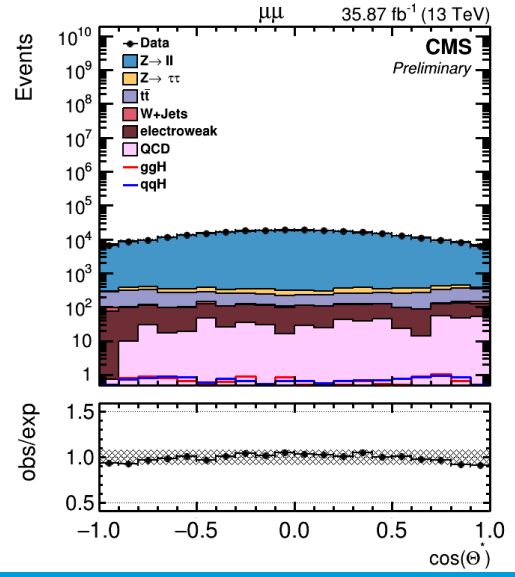

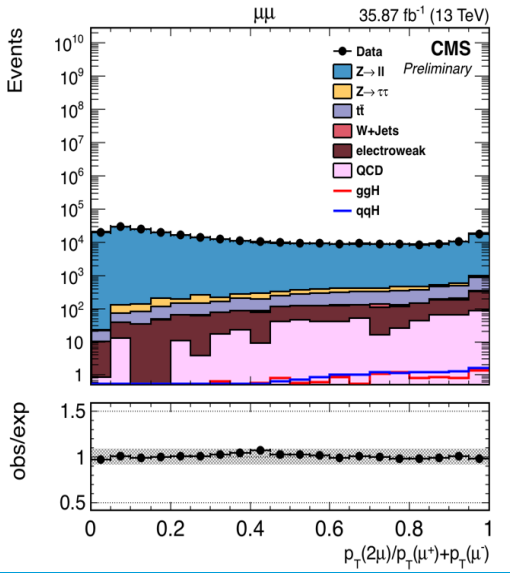

Boosted Decision Trees

Ending nodes are called leaves

For each branch will repeat the step and form further two branches

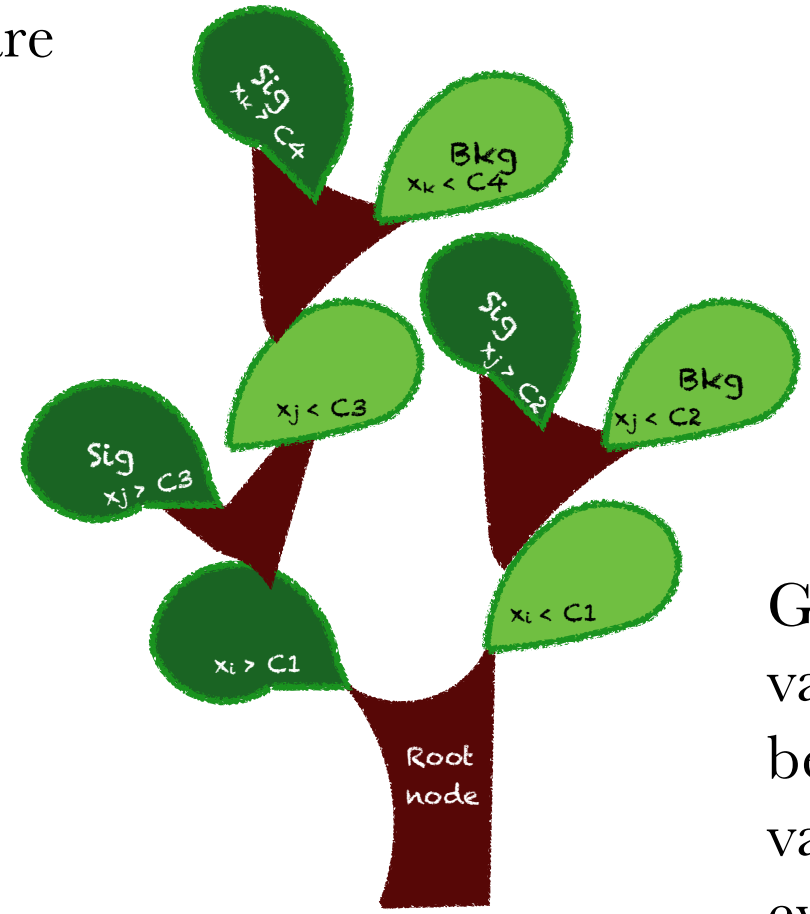

Tree is formed through this process

Go through all input variable and find the best variable and value to plot the event

Boosted Decision Trees (BDT)

- BDTs are trained and evaluated independently for each jet category using Higgs signal samples ggH (0-jets and boosted category), qqH (VBF category) and $Z \to \mu\mu$ and $Z \to \tau\tau$ background samples.
- The variables used in the BDT training are:
  - $\boldsymbol{\eta_{dimuon}}$ The pseudo-rapidity of the dimuon system.
  - $\boldsymbol{p_T(2\mu) / [p_T(\mu^+)+p_T(\mu^-)]}$ The ratio of the transverse momentum of the dimuon system to the scalar sum of the transverse momenta of the positive and the negative muon.
  - $\boldsymbol{E_T^{miss}}$ The missing transverse energy of the system.
  - $\boldsymbol{\Delta\Phi(\mu^+, p_T^{miss})}$ The azimuthal angle between the positive muon transverse momentum and the missing transverse momentum.
  - $\boldsymbol{\cos(\theta^*)}$ The polar angle of the μ^+ in the rest frame of the dimuon system

BDT continued ..

- $\mathbf{D_\zeta}$ is defined as the difference of the projection of the visible transverse momentum of the τ decay products plus missing transverse momentum and visible transverse momentum of the τ decay products on the ζ axis which is the center line between visible momenta.
- $\mathbf{p_T^{tot}}$ (only for boosted category) Total transverse momentum of the system.
- $\mathbf{m_{jj}}$ (only for VBF category) Di-jet mass

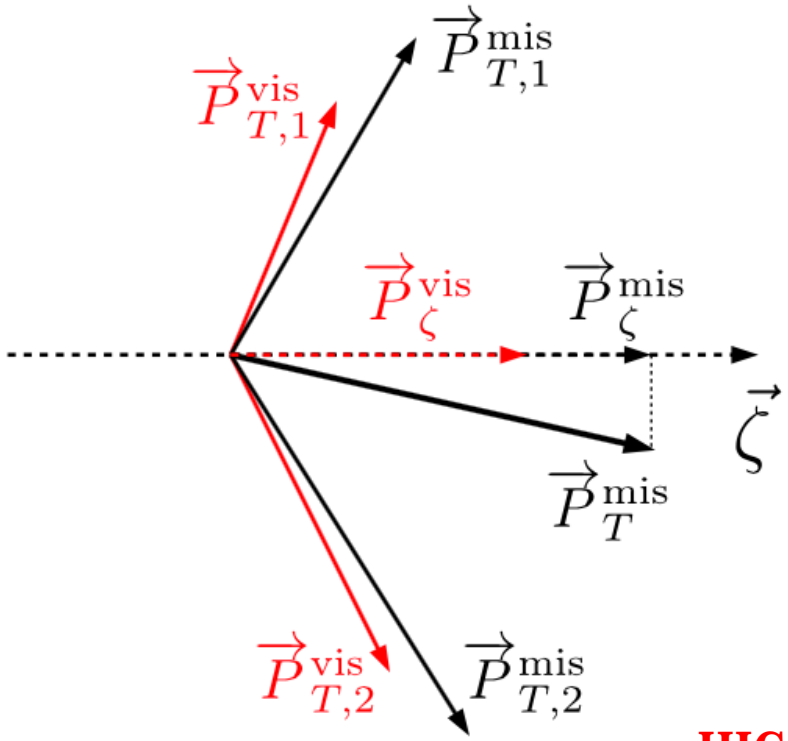

HIG-16-043

BDT Input Variables for 0-jet Category

Signal

Background

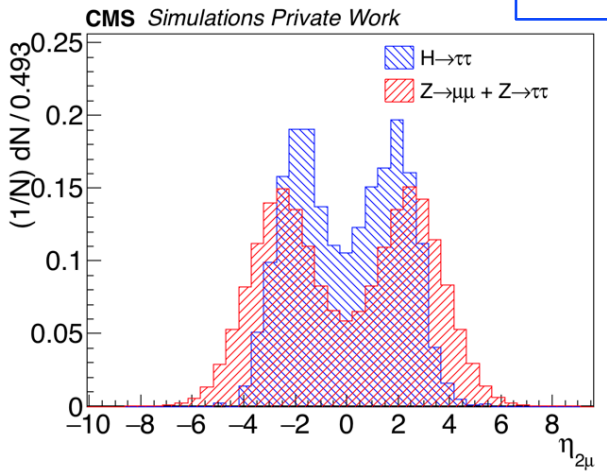

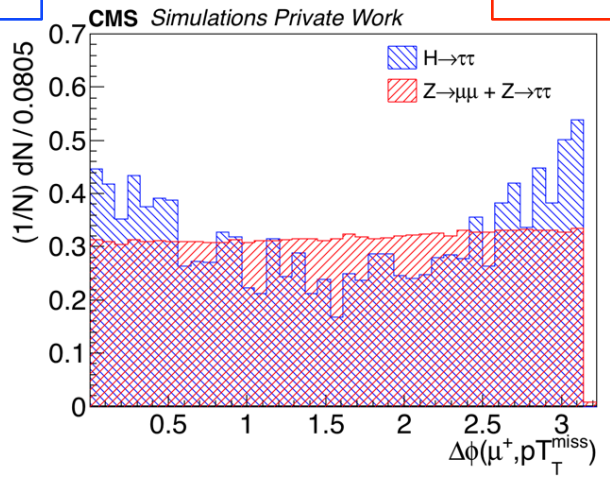

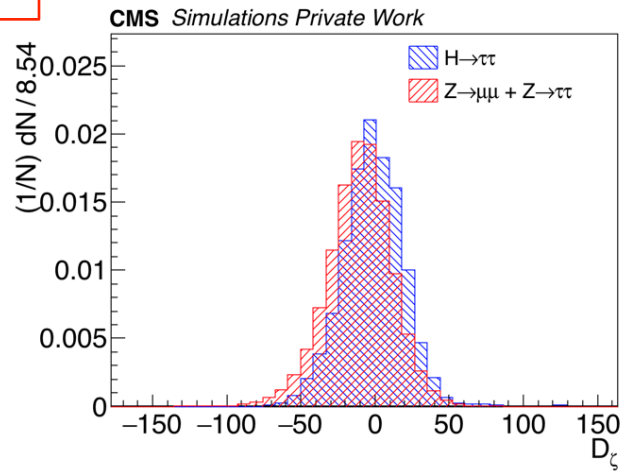

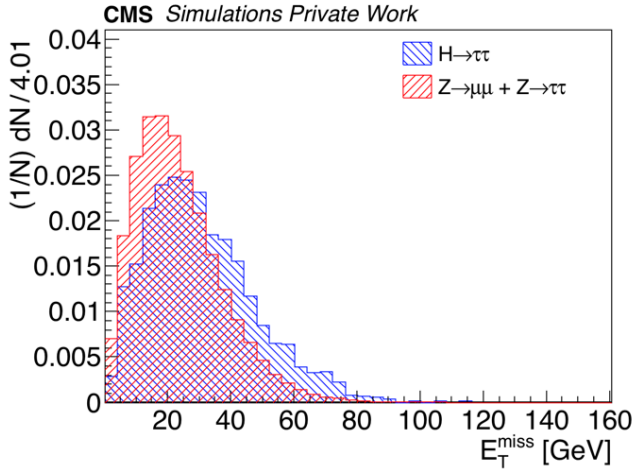

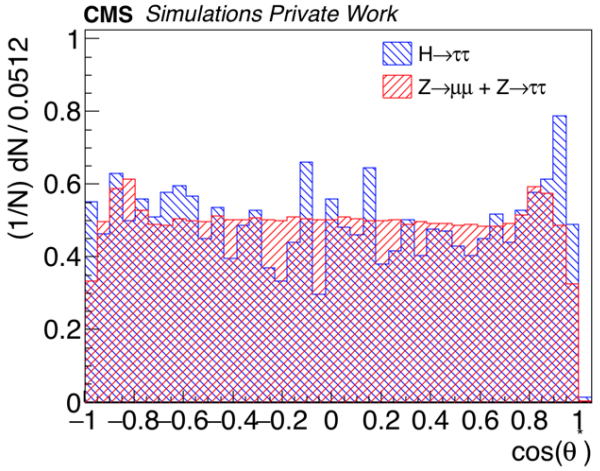

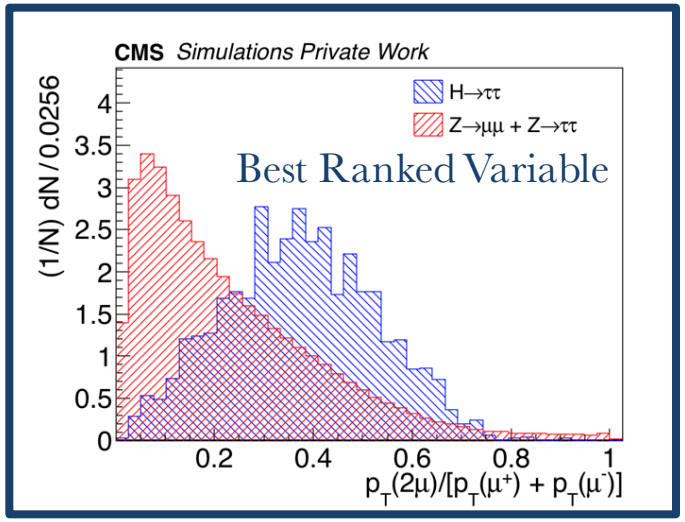

BDT Input Variables for Boosted Category

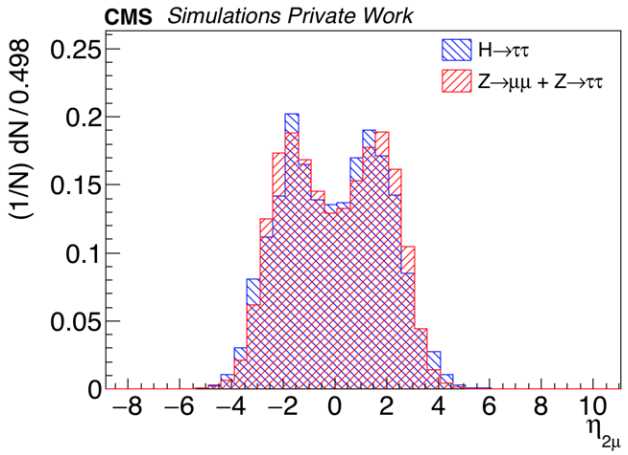

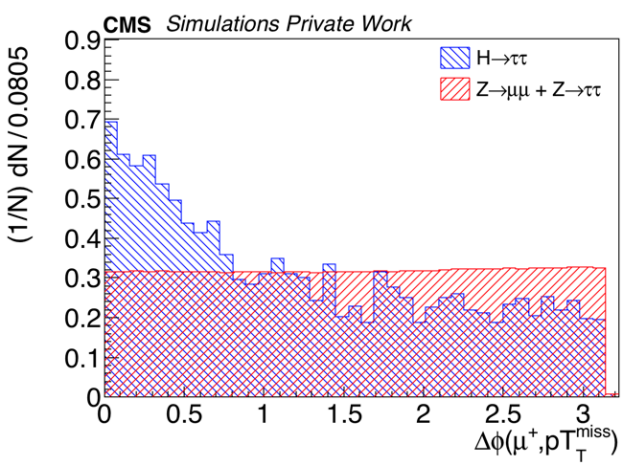

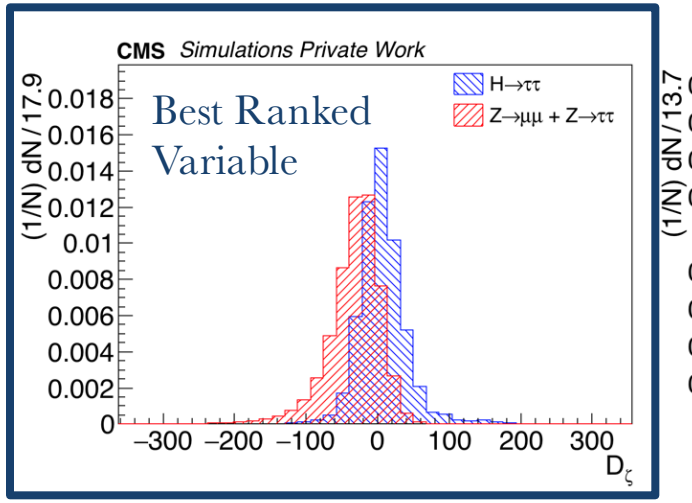

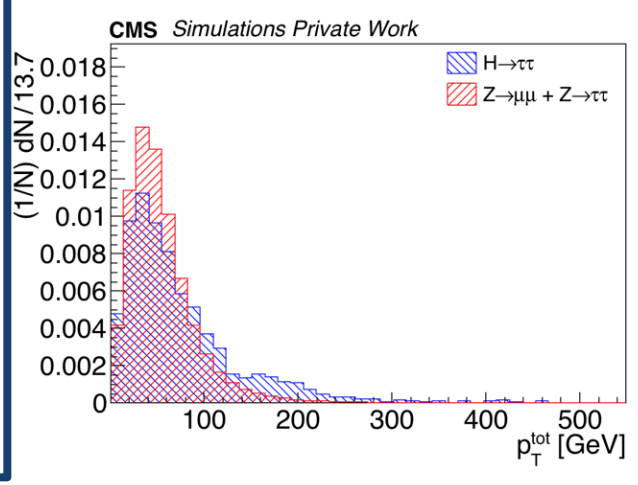

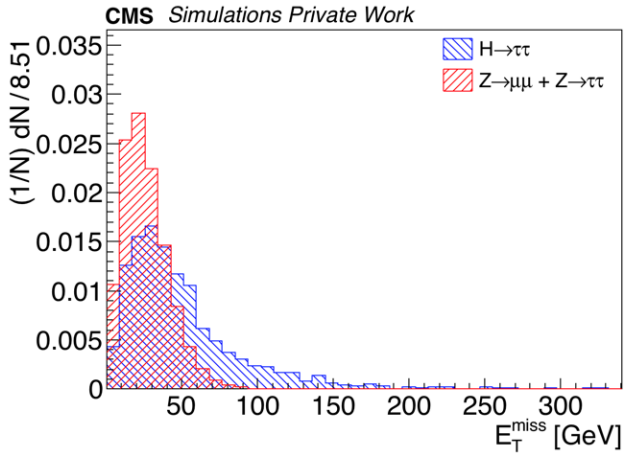

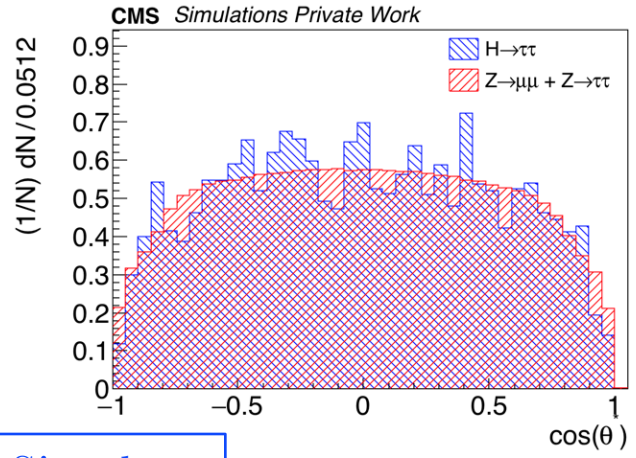

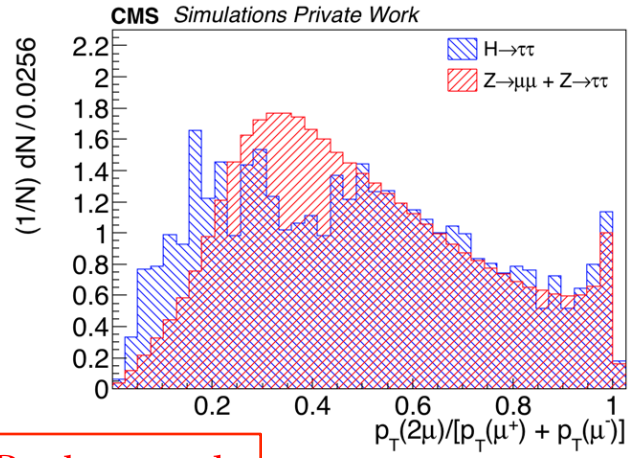

Signal

Background

BDT Input Variables for VBF Category

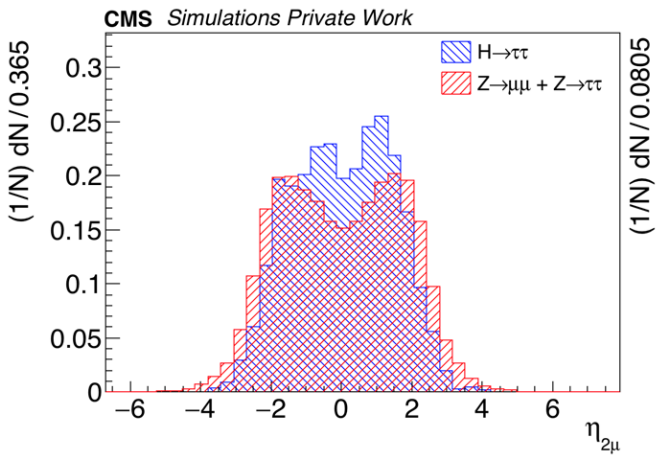

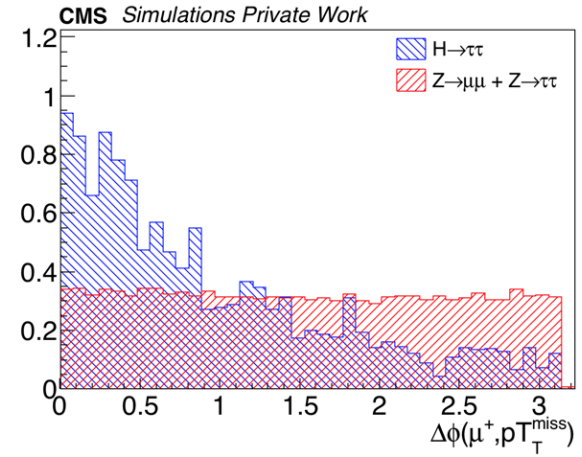

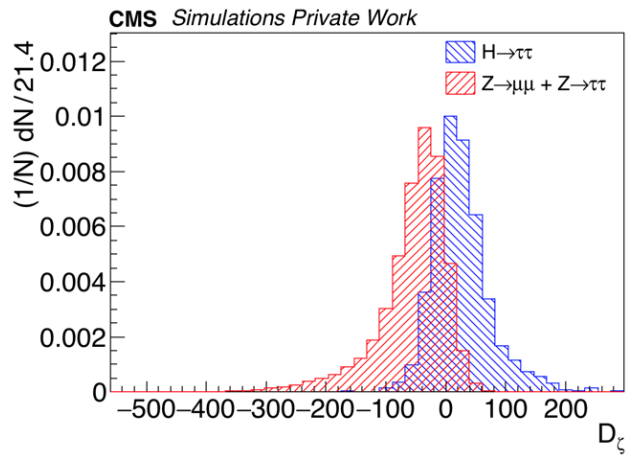

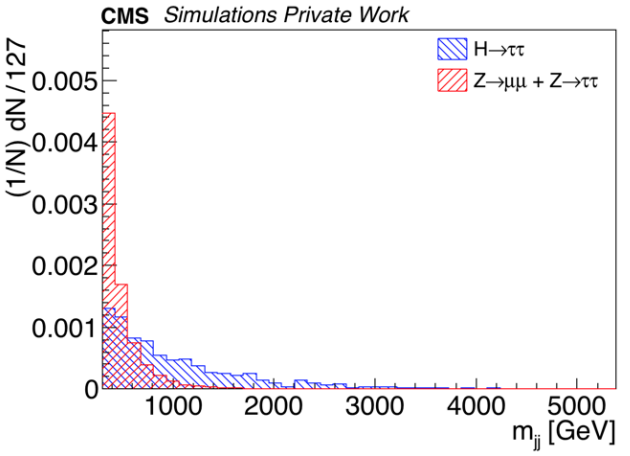

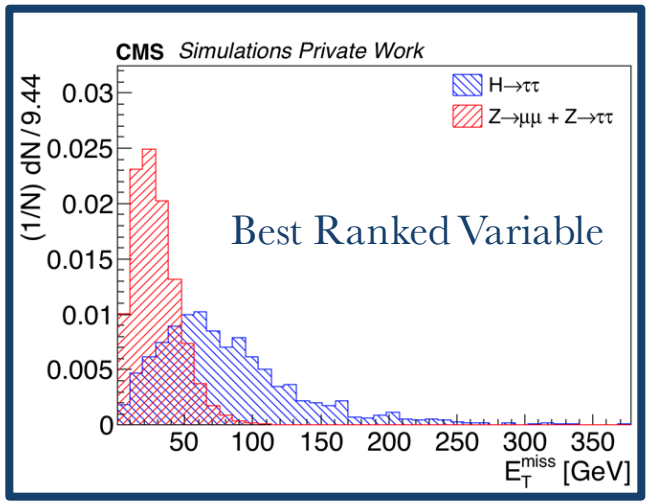

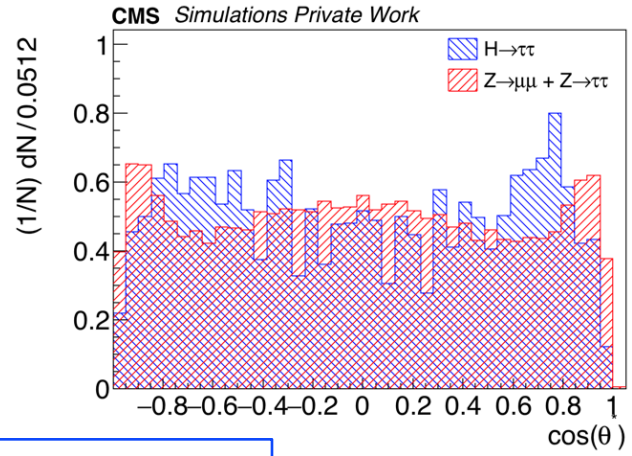

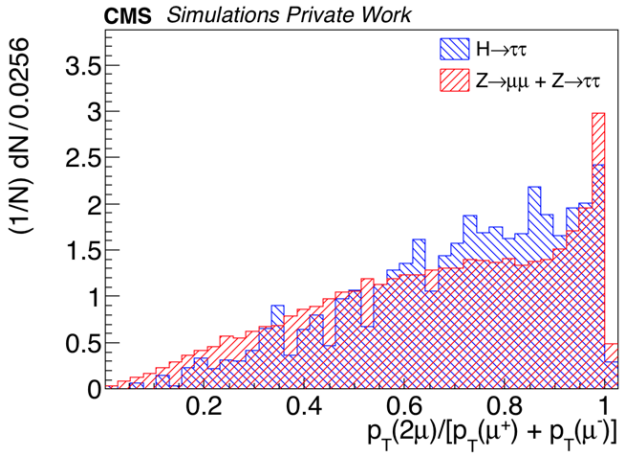

Signal

Background

BDT Response for Each Category (TMVA)

0-Jet

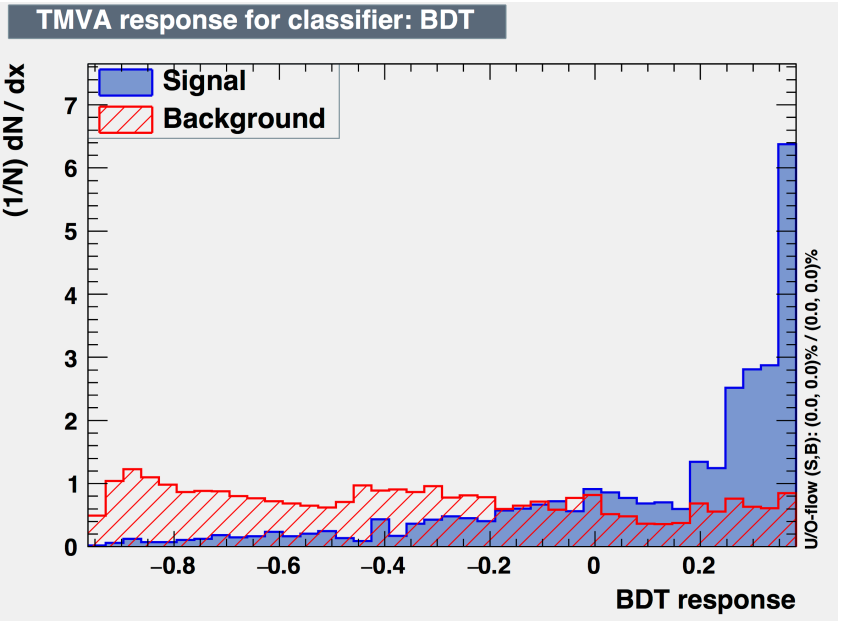

boosted

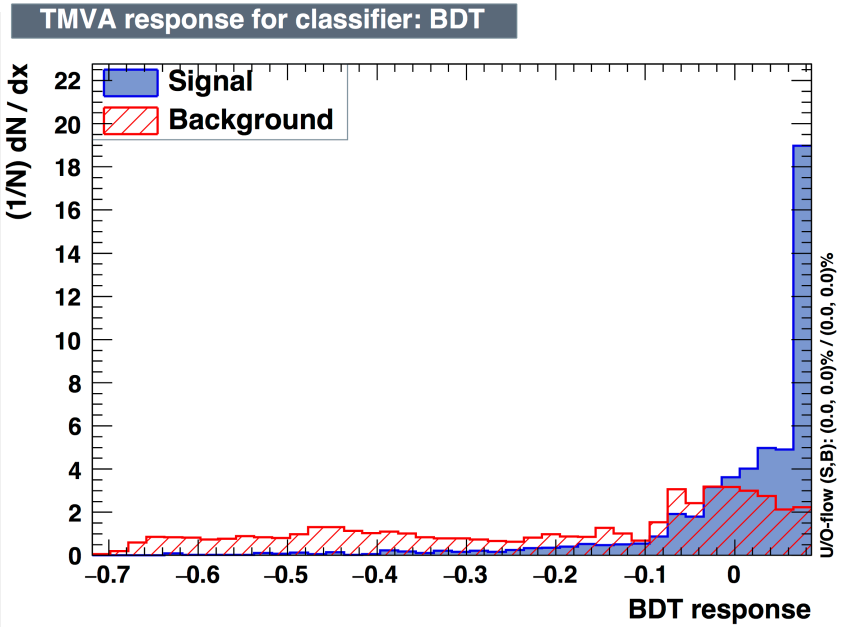

VBF

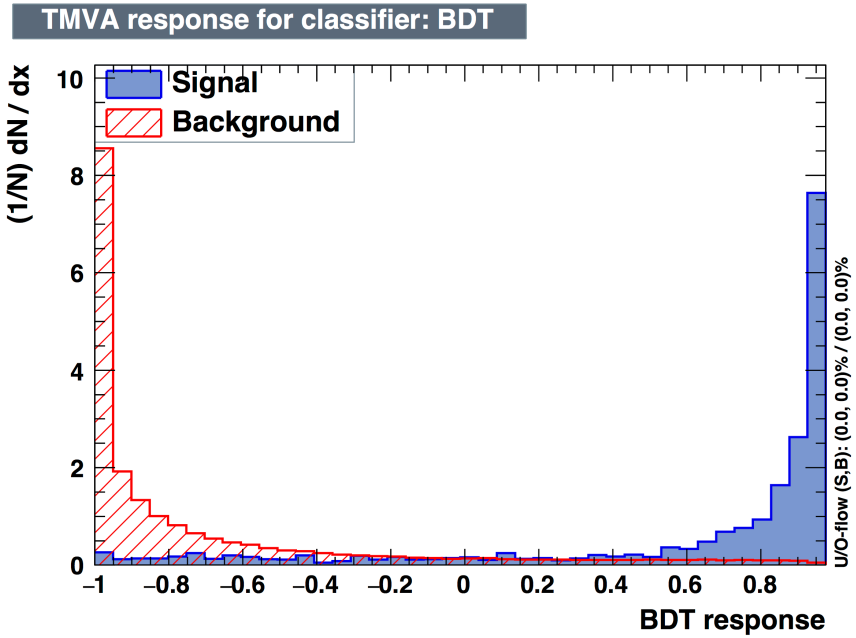

Background Estimation

- The dominating background for this channel is **DY** and this background is estimated using the simulated MC events after applying all required corrections.
- The **QCD multijet** background is estimated from the same-sign (SS) data events, and then normalized by applying the extrapolation factor derived from the ratio of the opposite-sign events to same-sign events .
- **Diboson, Single top, and W+jets** together are referred to as the **"Electroweak"** background. It is estimated directly from MC after applying all the necessary corrections and reweighting.
- $t\bar{t}$ background is estimated from the MC events after applying the top p_T reweighting
- Events yield for respective backgrounds are derived from the prefit plots.

BDT Response for Each Category

0-Jet

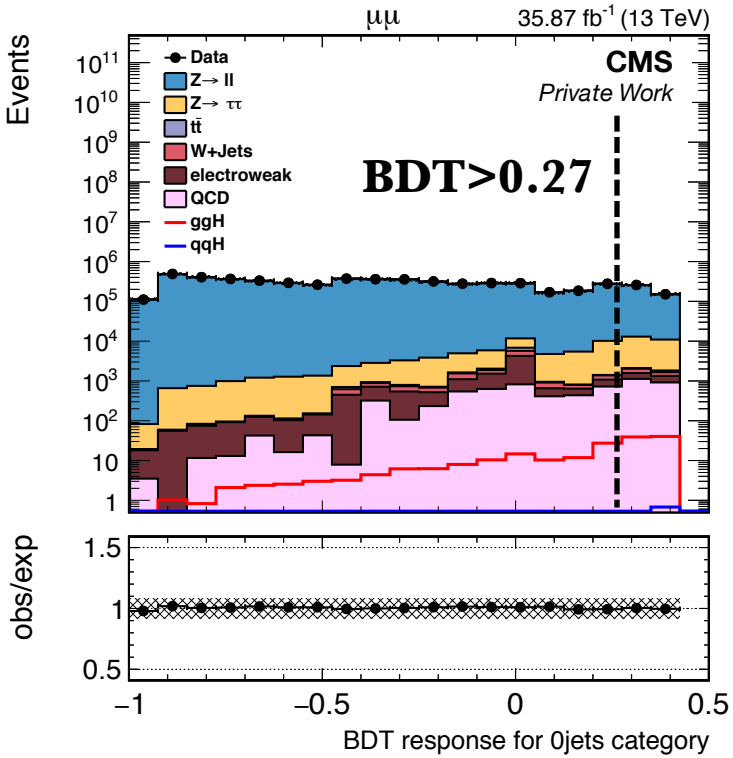

boosted

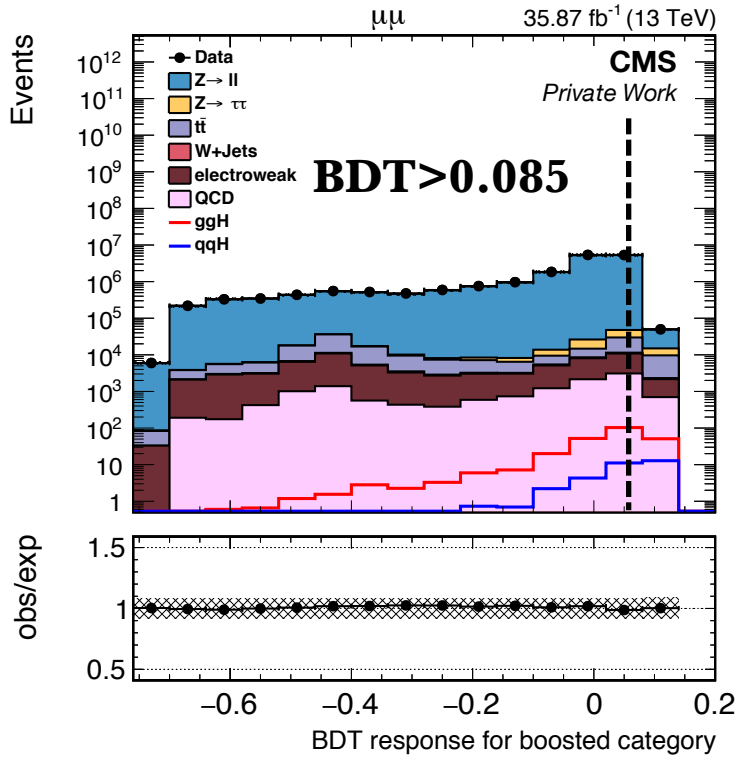

VBF

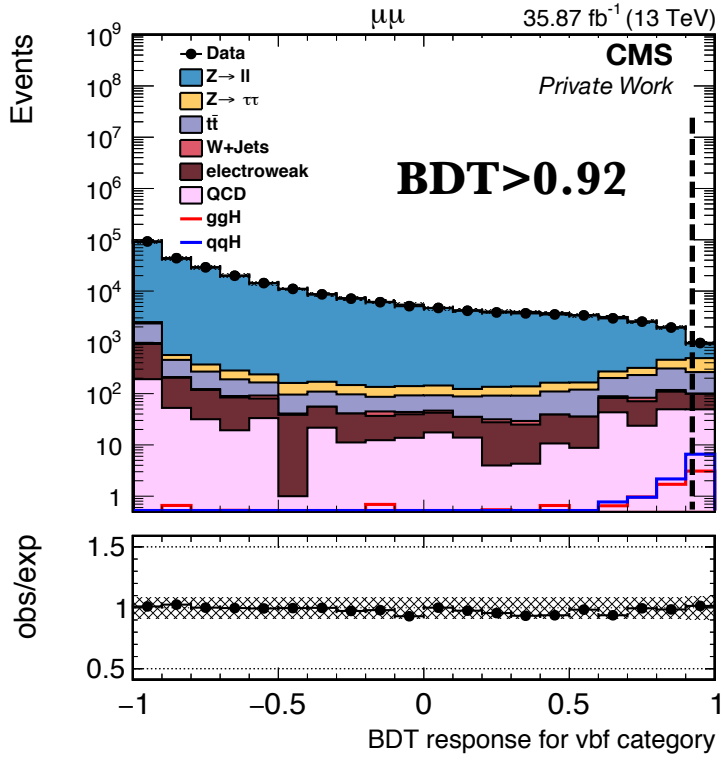

- BDT cuts are optimized by maximizing the sensitivity for signal and minimizing the upper limit on $\mu = \sigma/\sigma_{SM}$
- For SVFit calculation a loose cut on the BDT is applied

Signal Extraction Method

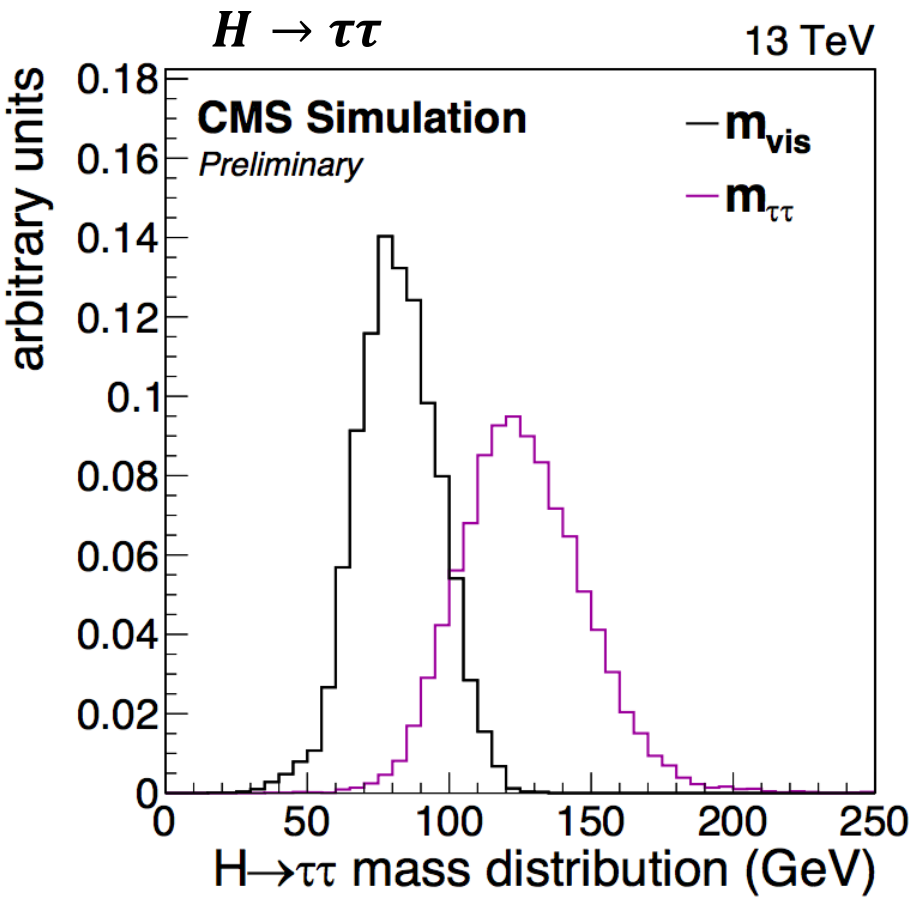

- Di-tau mass ($m_{\tau\tau}$) is reconstructed using **S**econdary **V**ertex **Fit** (SVFit)
  - It is a likelihood-based estimation of the parent boson mass
  - Inputs used for the calculations are: MET, MET uncertainties and four-vectors of the muon candidate
- Signal is extracted using 2-dimensional distribution in the plane of reconstructed SVFit mass $m_{\tau\tau}$ and visible mass $m_{\mu\mu}$

Mass Distributions – Visible mass ($m_{\mu\mu}$)

0-Jet

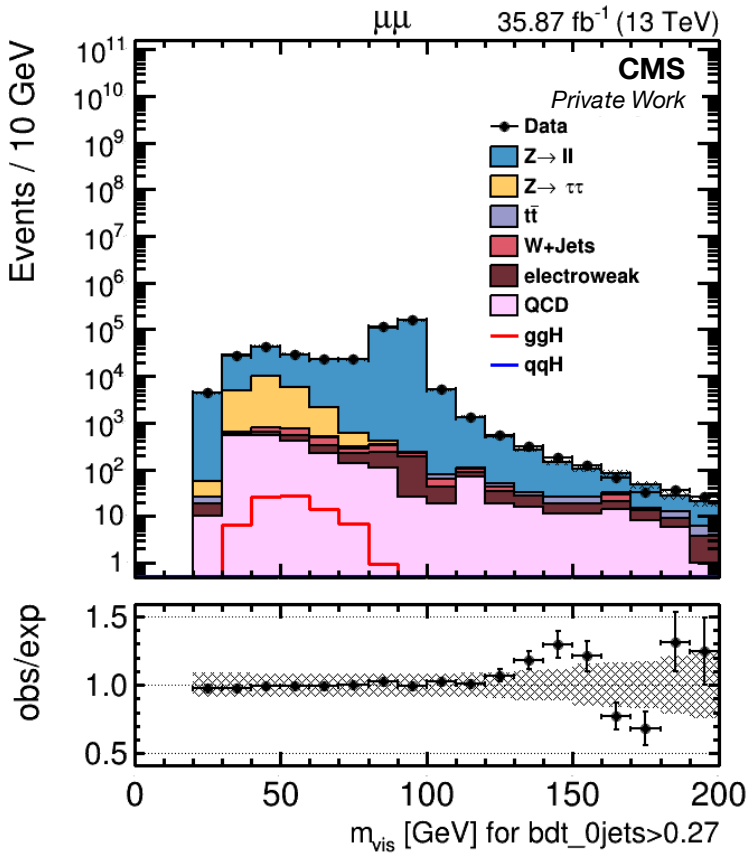

boosted

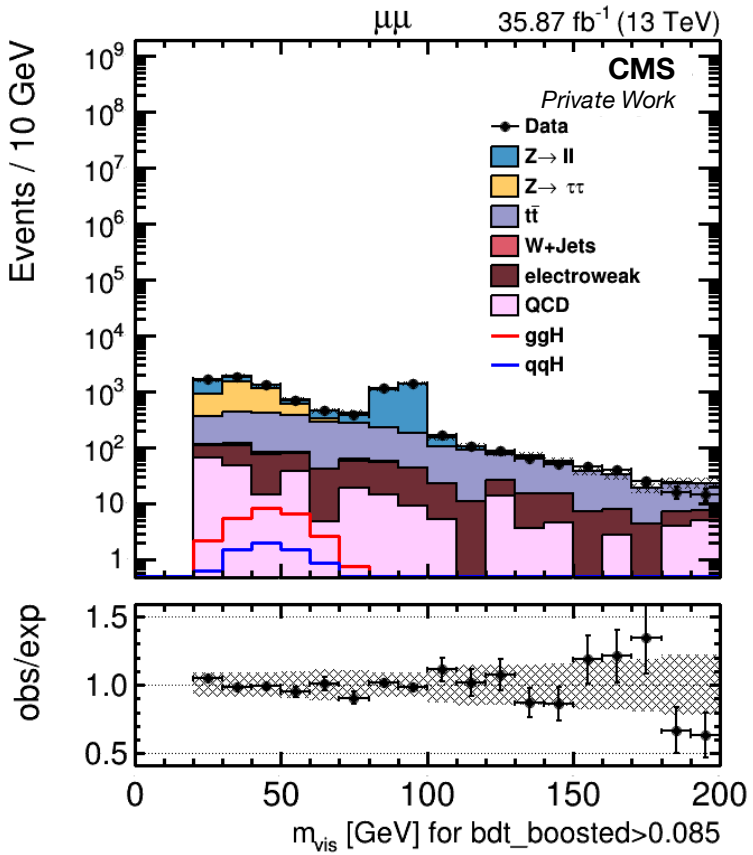

VBF

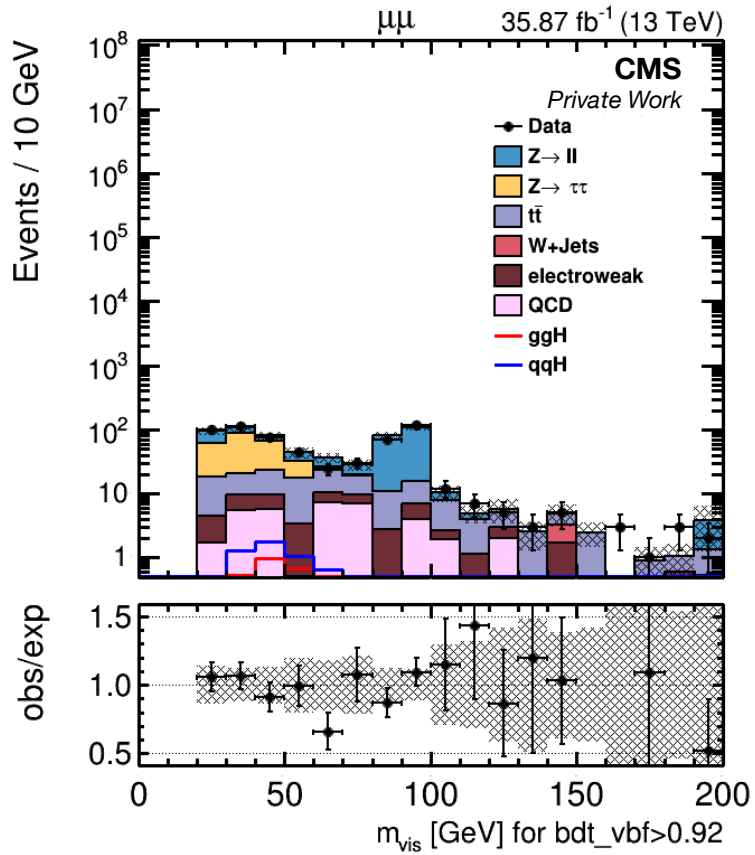

Mass Distributions - SVFit mass ($m_{\tau\tau}$)

0-Jet

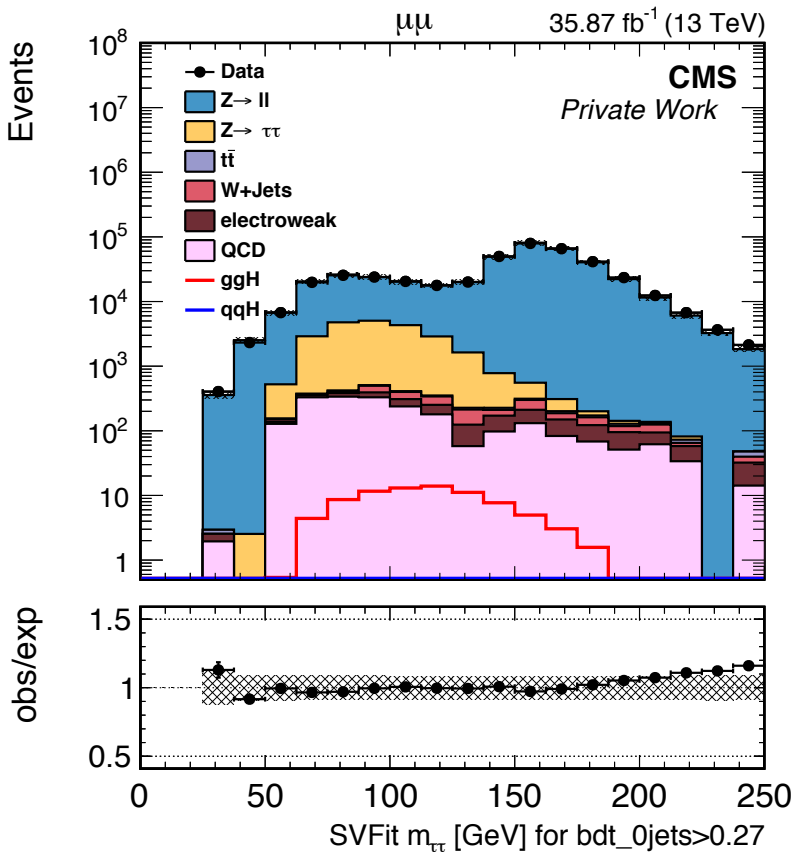

boosted

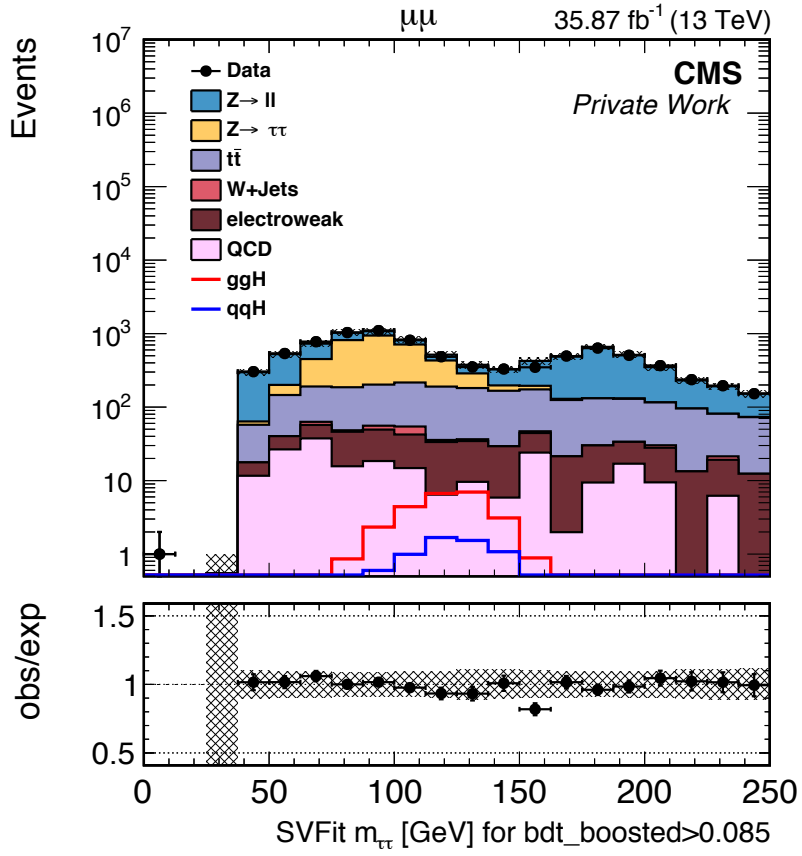

VBF

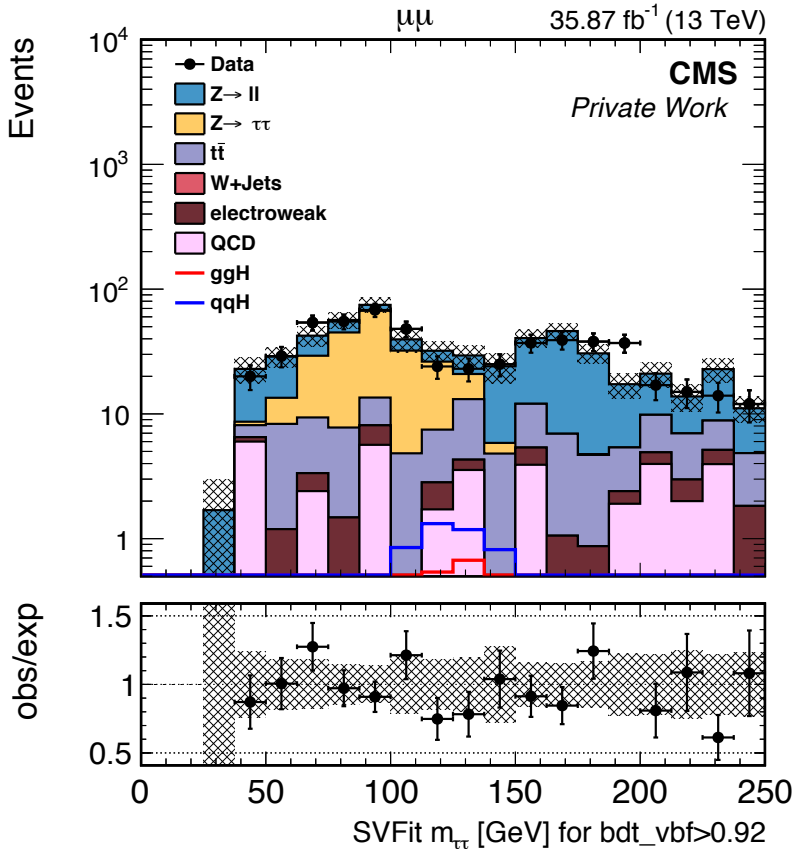

2-D Mass distribution (0-jet)

After applying all selections

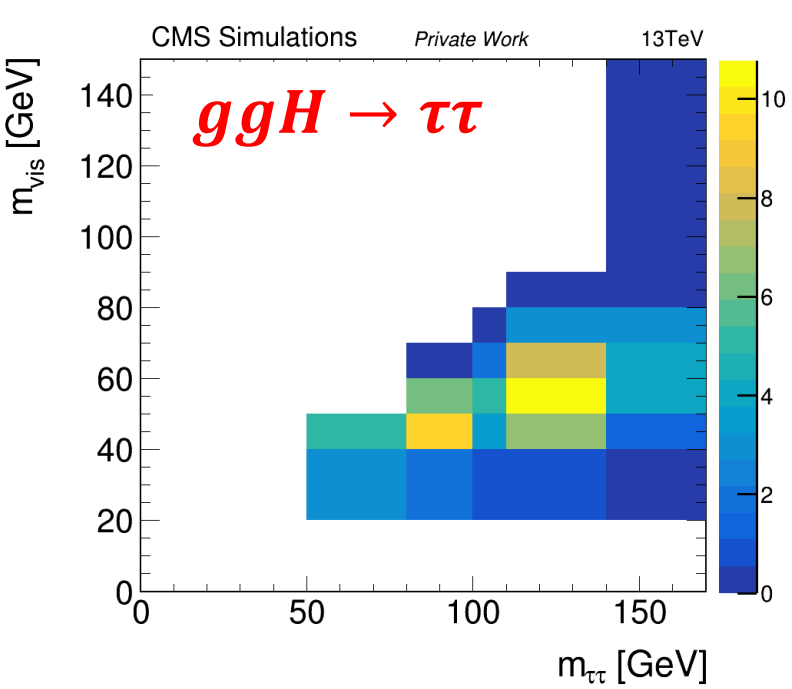

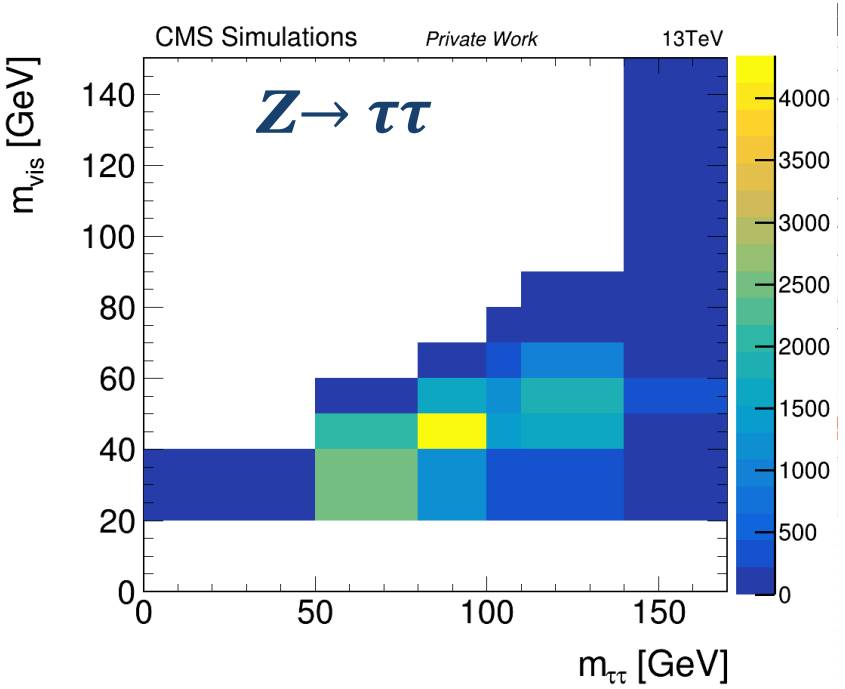

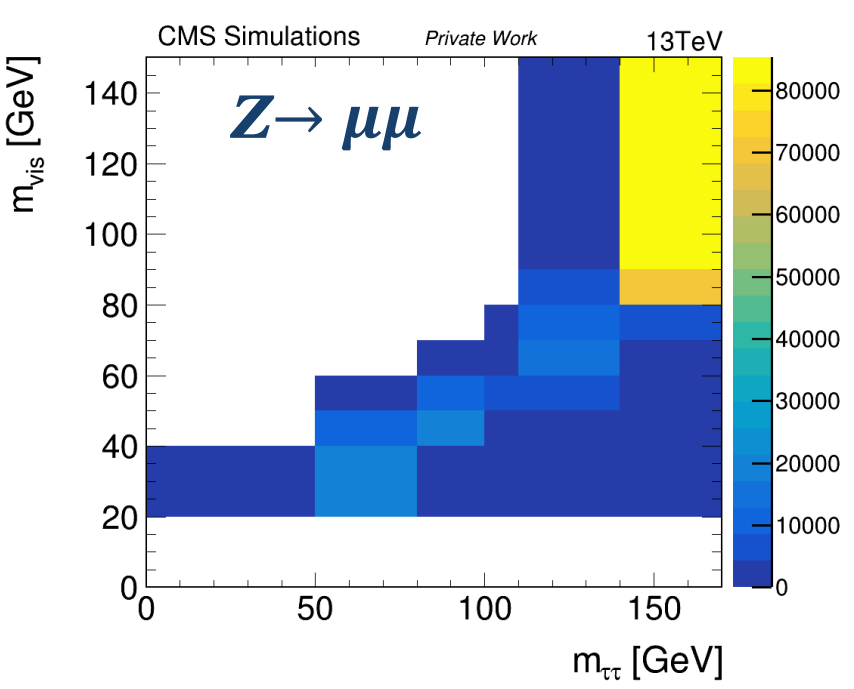

2-D Mass distribution (boosted)

After applying all selections

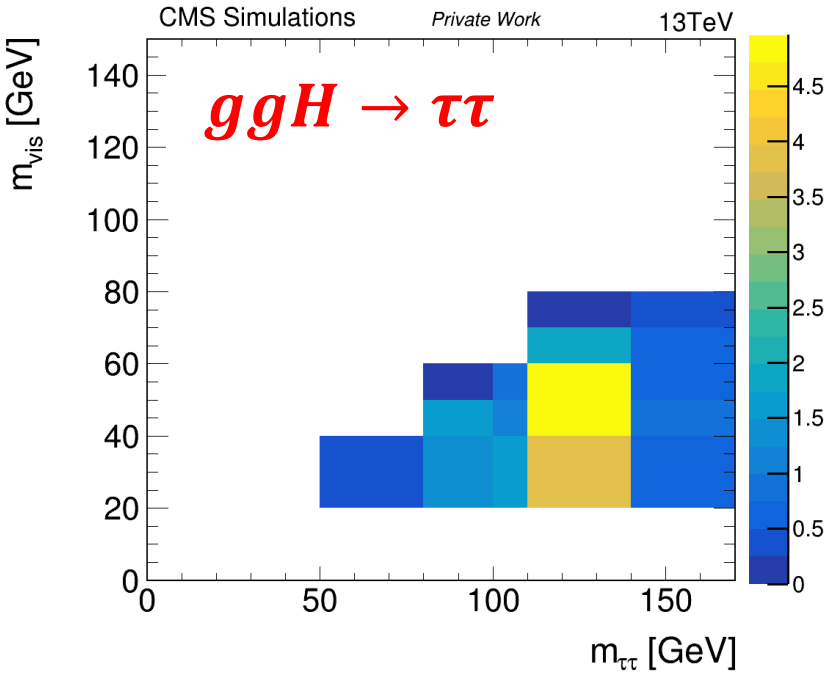

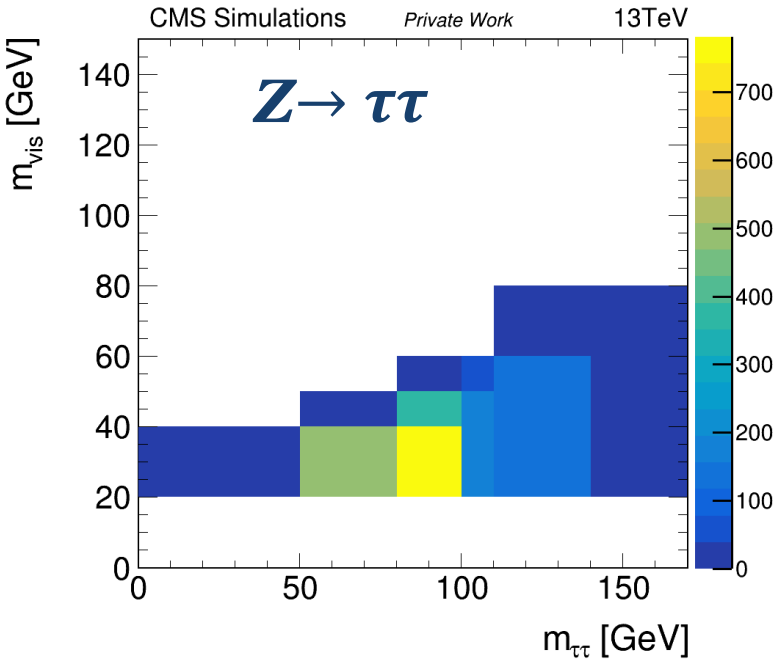

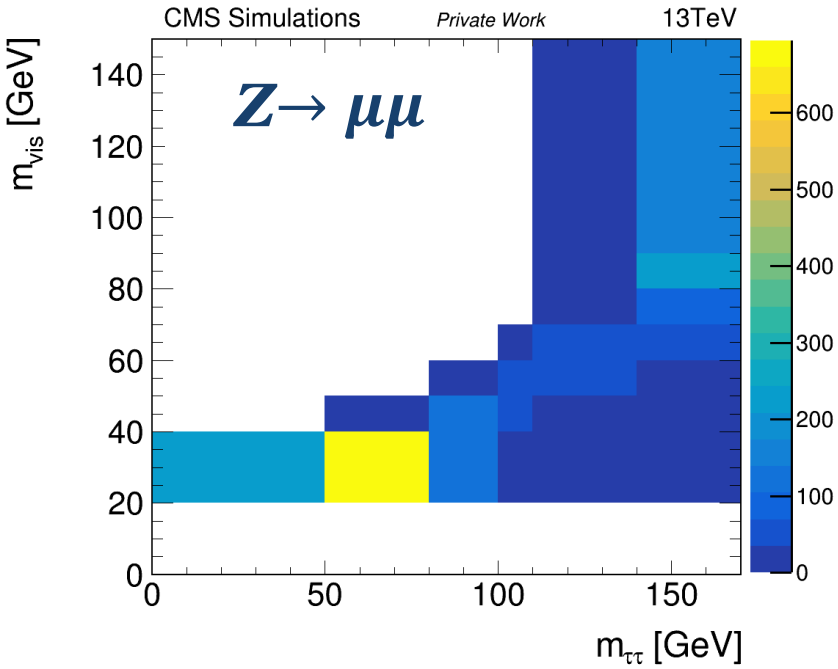

2-D Mass distribution (VBF)

After applying all selections

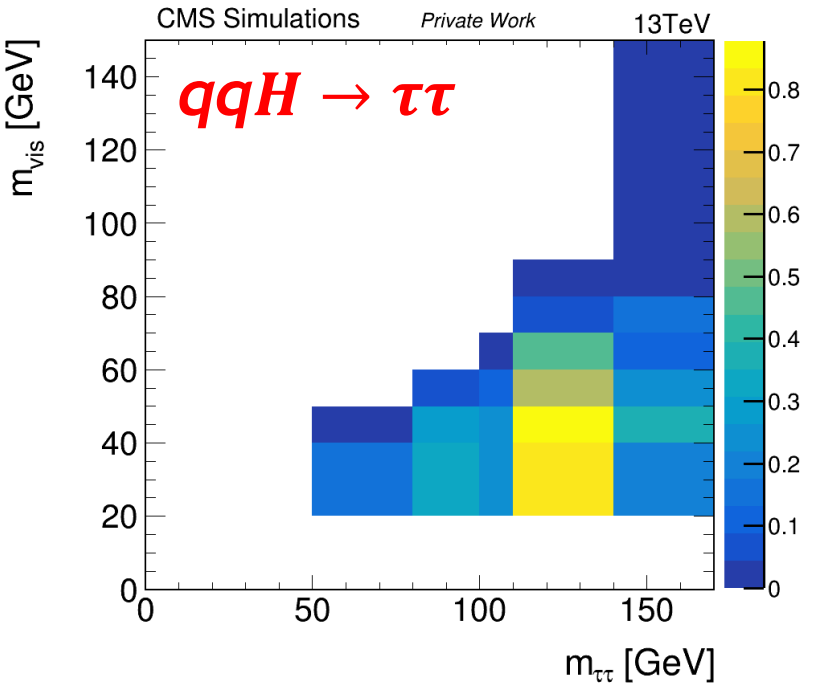

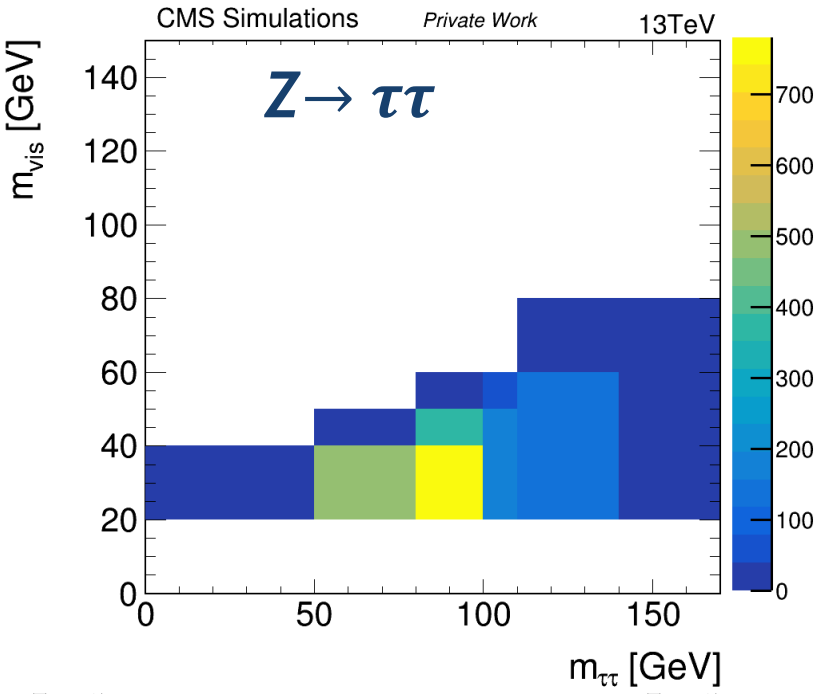

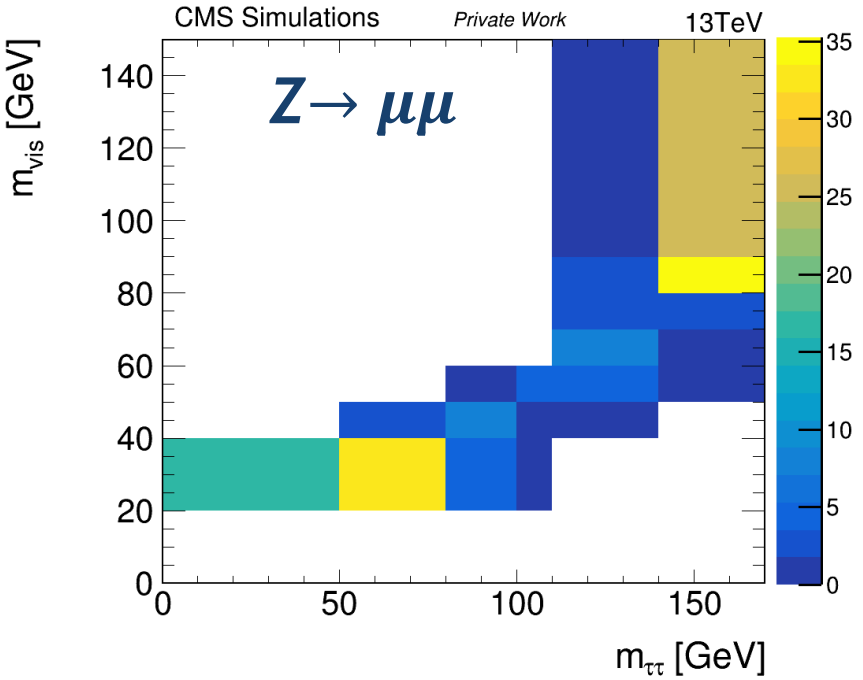

Uncertainty Model

Normalization Uncertainties

- Luminosity 2.6%
- Identification/Isolation Efficiencies 2% for each muon
- Background (Systematic uncertainties on the sideband)
  - QCD multijets 20%
  - $t\bar{t}$ 7%
  - Electroweak 15%

Shape Uncertainties

- Muon momentum scale 1% (conservative)
- Top p_T reweighting
- DY reweighting
- b-tag efficiency
- Jet Energy Scale (JES)
- Missing Transverse Energy response

These uncertainties are used as nuisance parameters in likelihood function. The expected and observed limits are extracted by maximizing the likelihood function for each bin of the unrolled mass.

Likelihood Function

$$\mathcal{L}(\vec{n}|\vec{b}) = \prod_{i=0}^{N} \frac{e^{-b_i} b_i^{n_i}}{n_i!} \prod_{j=0}^{L} p(\bar{\theta}_j|\theta_j)$$

- n is observed number of events, b is expected number of events
- N is total number of bins
- $p(\bar{\theta}_j|\theta_.)$ is PDF for nuisance parameter θ, where $\bar{\theta}_j$ is consider the default value of the parameter and reflects the degree of belief on what the real value of parameter θ

Goodness of Fit

Using 1000 toy runs

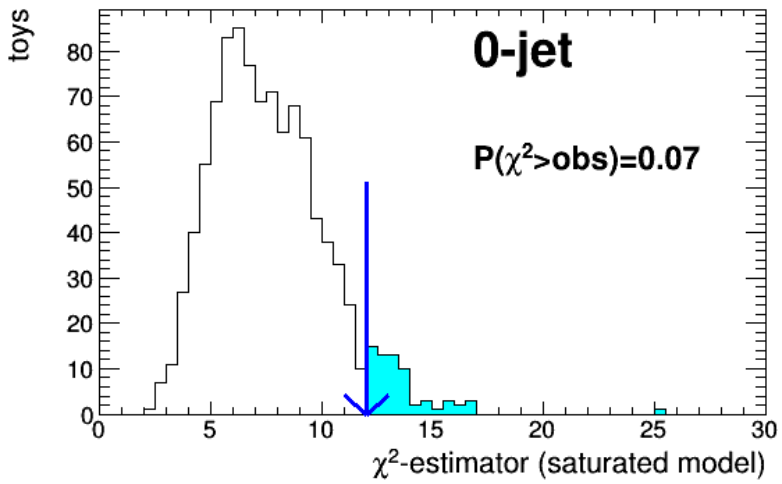

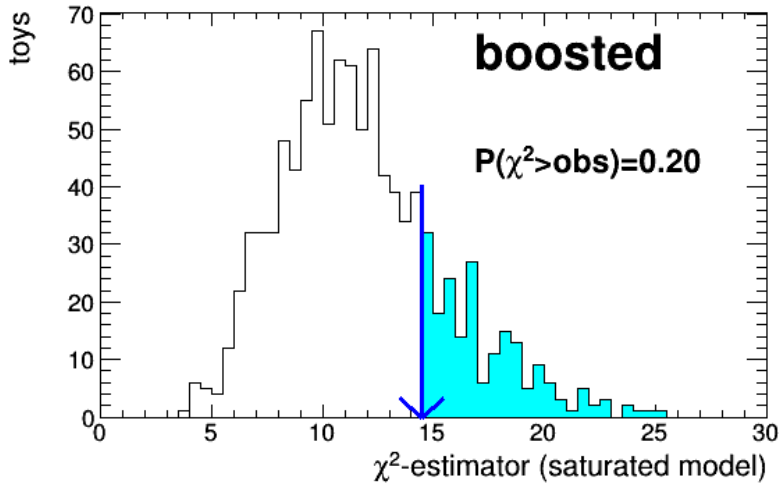

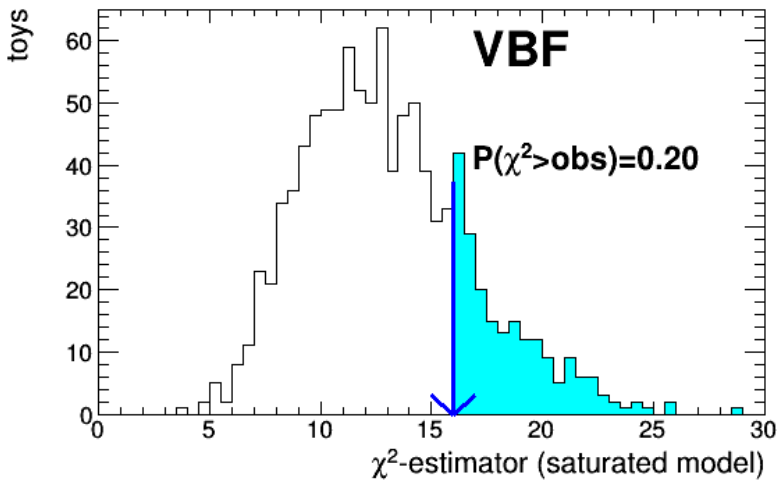

Prefit and Postfit Plots for 0-jet Category

Prefit

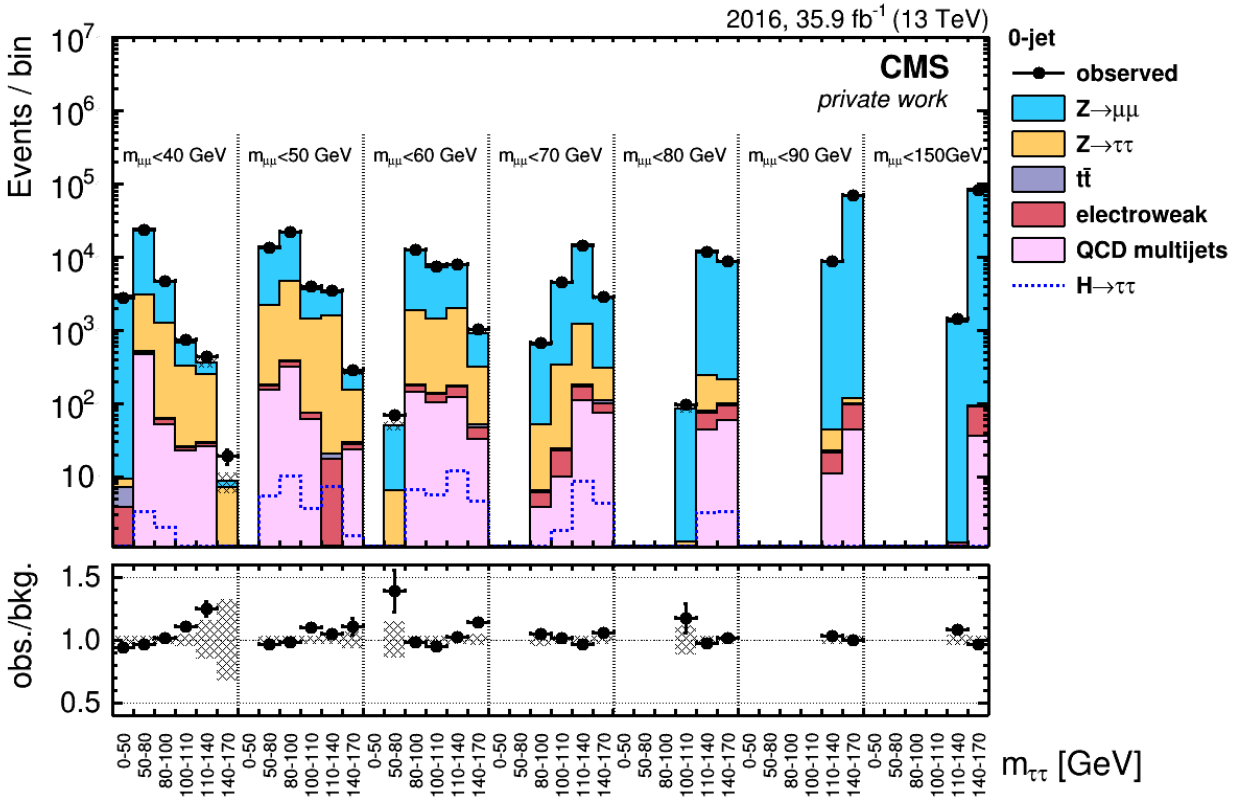

Postfit

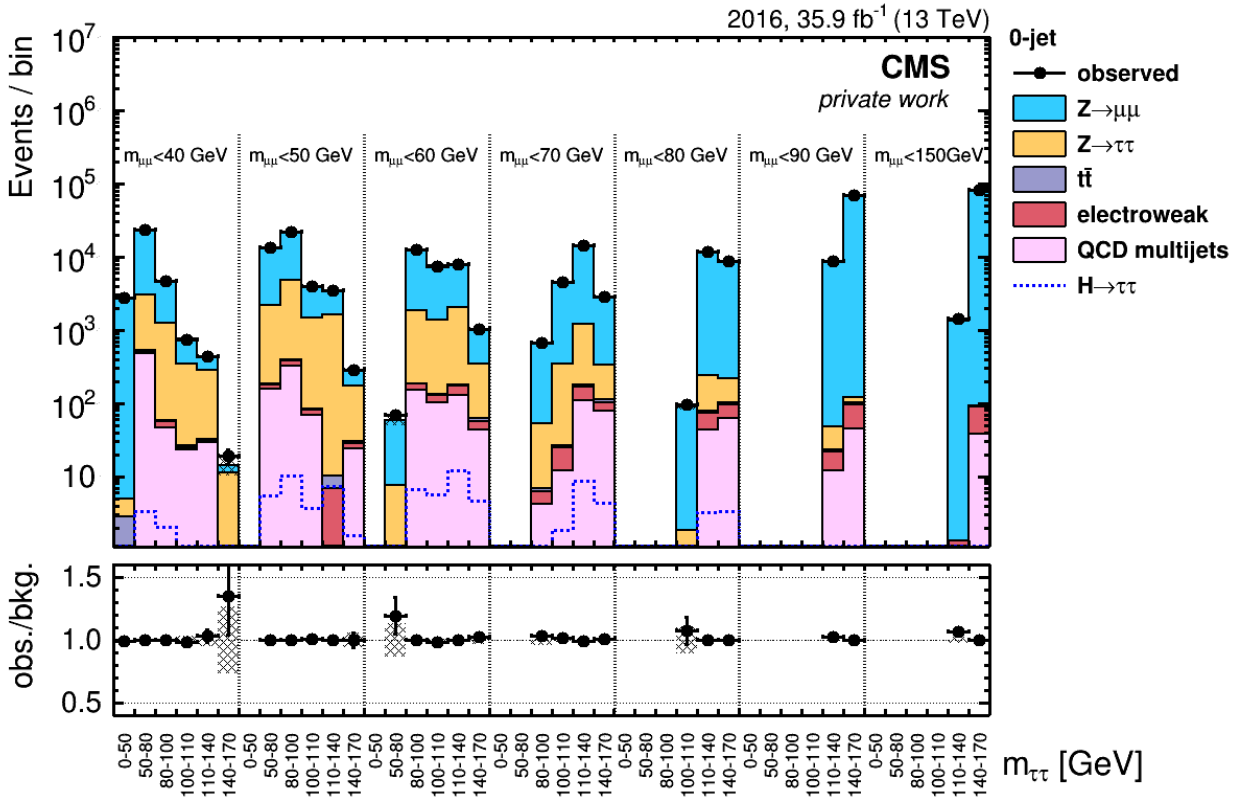

Prefit and Postfit Plots for Boosted Category

Prefit

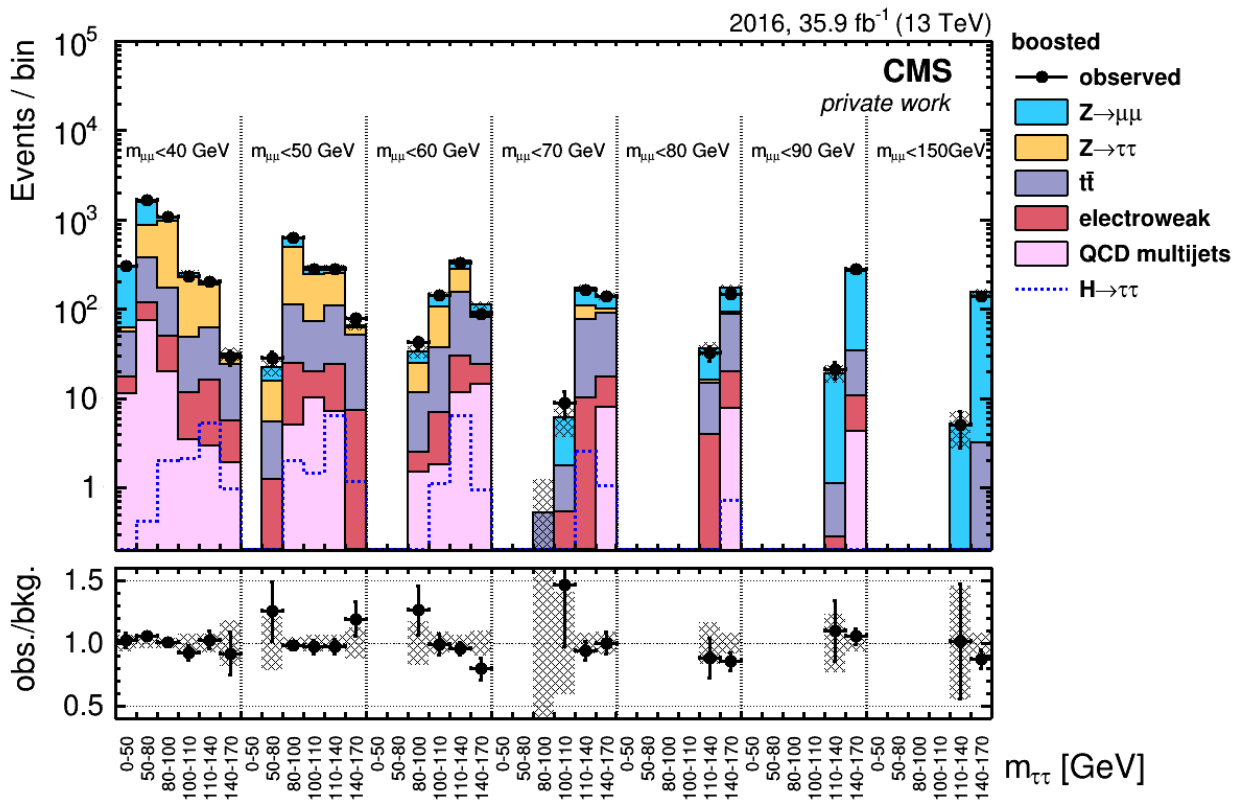

Postfit

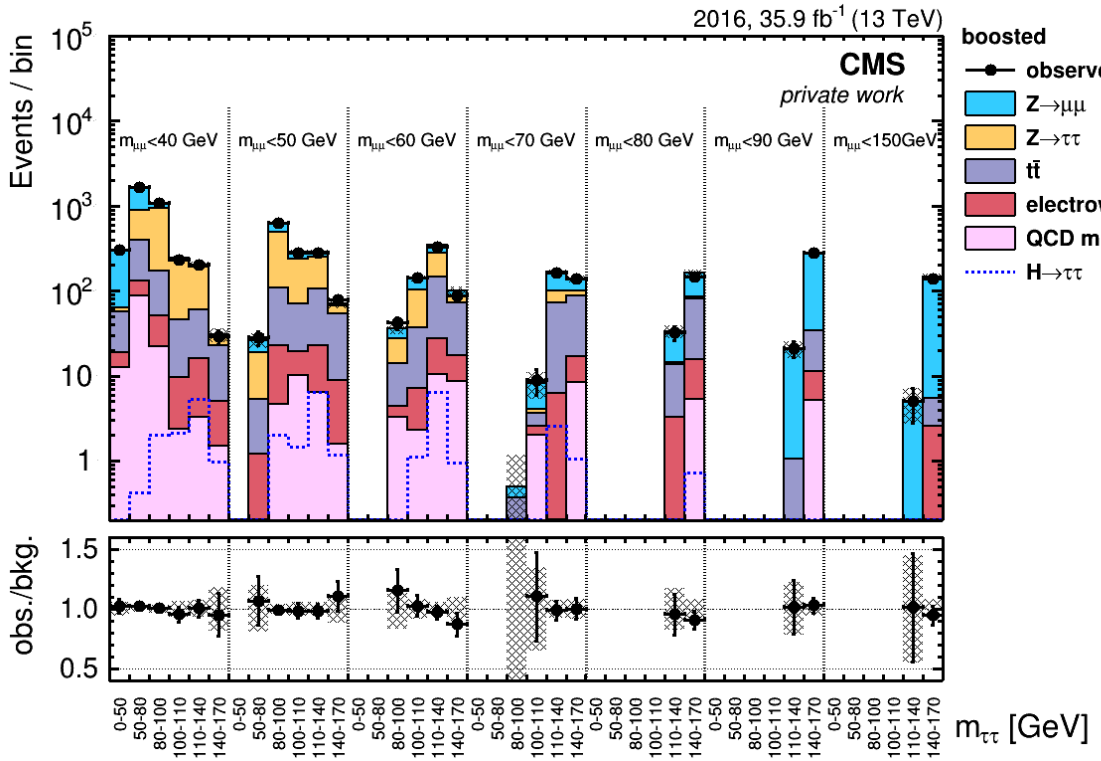

Prefit and Postfit Plots for VBF Category

VBF

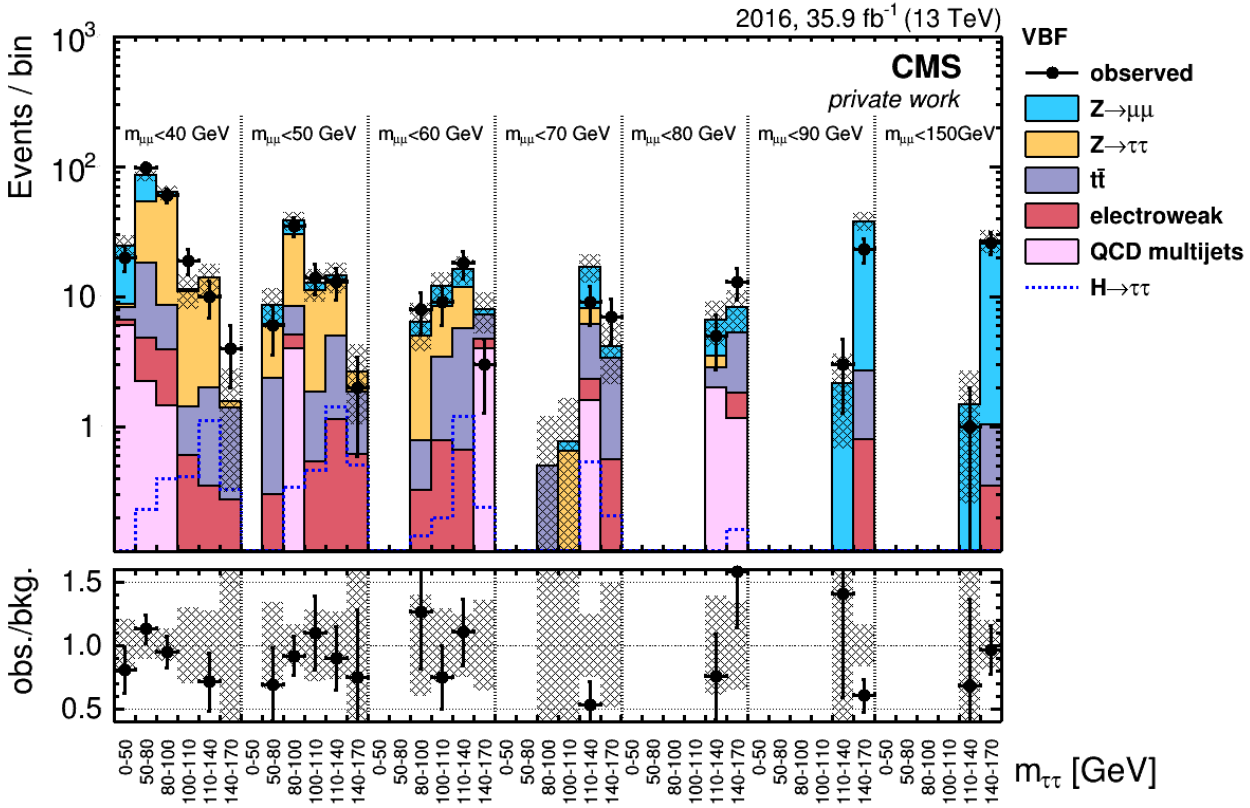

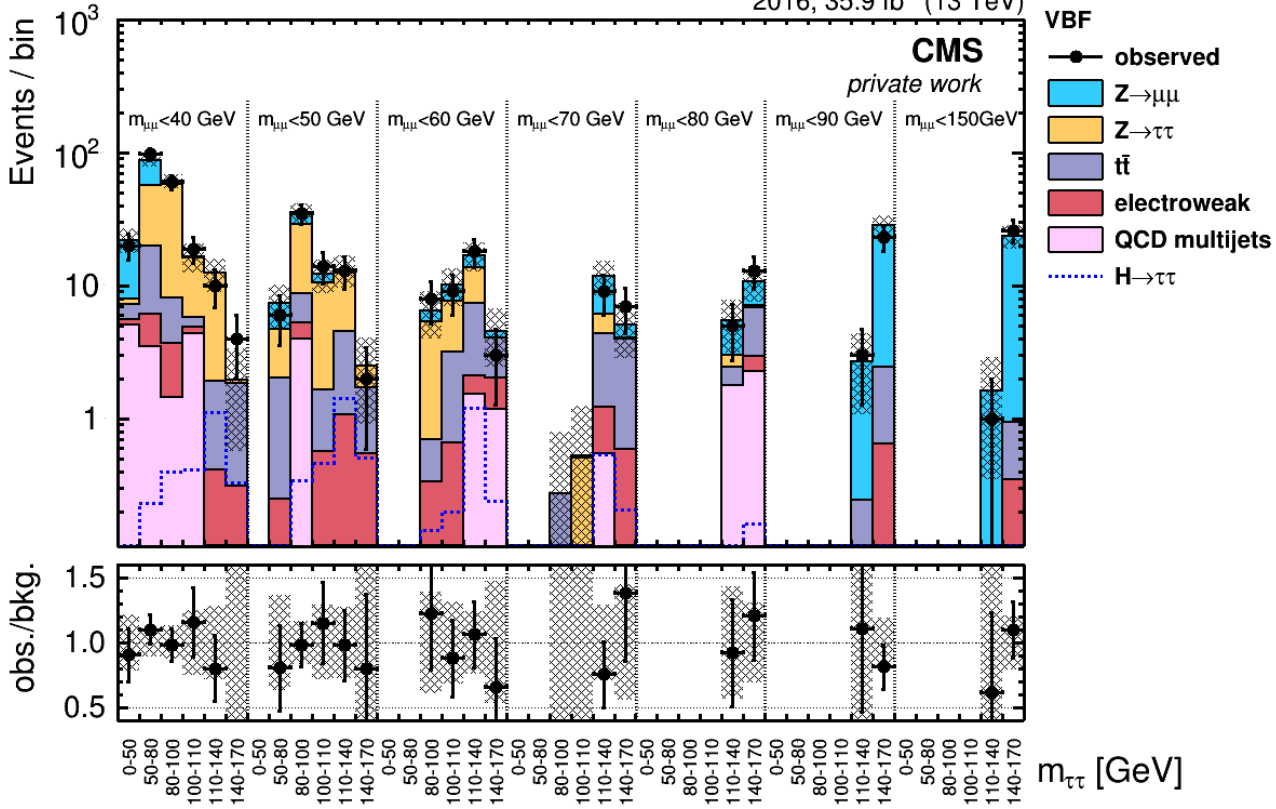

Postfit Plots

- The event yield in the $H \rightarrow \tau\tau$ signal and respective background events in this channel in the data corresponding to the integrated luminosity 35.9 fb^{-1}

Prefit

Process	0-jet	boosted	VBF
$Z \rightarrow \tau\tau$	20 502 ± 156	2 585 ± 37	171 ± 12
$Z \rightarrow \mu\mu$	288 856 ± 928	2 027 ± 37	155 ± 11
Multijet	1 900 ± 150	182 ± 36	22 ± 10
$t\bar{t}$	111 ± 7	1 266 ± 23	60 ± 5
Electroweak	560 ± 7	240 ± 7	16 ± 2
Total Expected Background	31 2495 ± 561	6 336 ± 80	425 ± 21
Signal $H \rightarrow \tau\tau$	86 ± 3	28 ± 2	6 ± 0
Data	308 013	6 342	405

Postfit

Process	0-jet	boosted	VBF
$Z \rightarrow \tau\tau$	20 851 ± 144	2 585 ± 51	167 ± 13
$Z \rightarrow \mu\mu$	283 967 ± 533	2 044 ± 45	134 ± 12
Multijet	1 973 ± 45	194 ± 14	26 ± 5
$t\bar{t}$	110 ± 11	1 248 ± 35	59 ± 8
Electroweak	550 ± 23	229 ± 15	16 ± 4
Total Background	308 032 ± 555	6332 ± 80	402 ± 20
Signal $H \rightarrow \tau\tau$	86 ± 3	28 ± 2	6 ± 0
Data	308 013	6 342	405

Fitted Signal Strength and Limits

Signal Strength relative to SM

Category	Best Fit	Post fit deviation from SM
0-jet	12.1±13.0	0.9σ ↑
boosted	-2.3±2.8	0.8σ ↓
VBF	0.4±1.9	0.2σ ↑
Combination	-1.0±1.7	0.6σ ↓

Upper 95% CL limits on the signal strength in mumu channel

Category	-2σ	-1σ	exp.	+1σ	+2σ	**obs.**
0-jet	12.7	17.0	23.8	33.6	45.8	**34.9**
boosted	2.8	3.8	5.3	7.4	10.0	**4.0**
VBF	2.1	2.8	4.0	5.7	8.0	**4.2**
Combination	1.7	2.3	3.2	4.6	6.2	**2.7**

Limit Plots

Run I ($\tau_\mu\tau_\mu$ Channel)

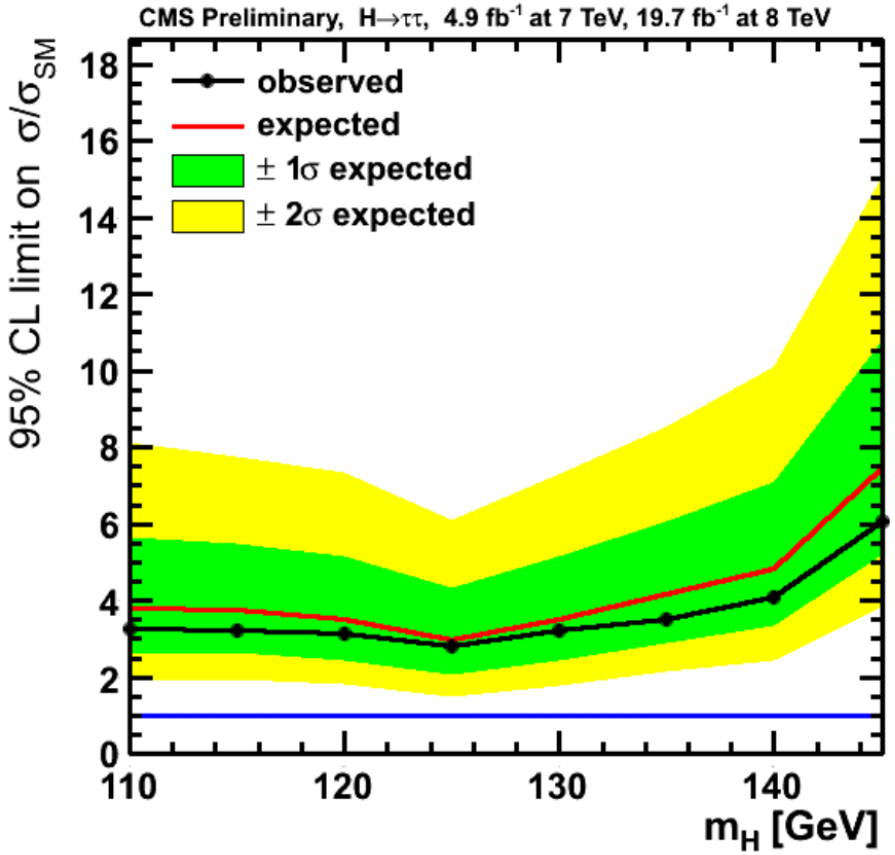

Run II ($\tau_\mu\tau_\mu$ Channel)

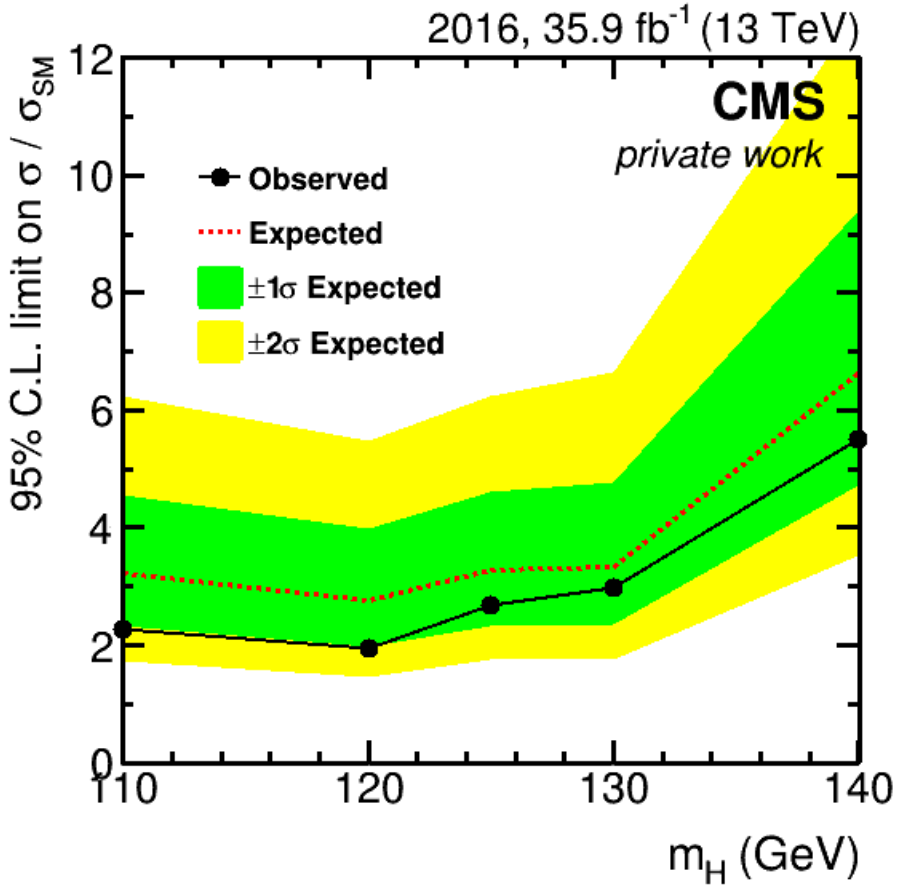

Summary

- Successfully implemented Single BDT method to suppress the DY dominating background in each event category.
- The signal strength in $H \rightarrow \tau\tau \rightarrow \mu\mu$ channel relative to SM is

$$\hat{\mu} = \sigma/\sigma_{SM} = -1.00 \pm 1.7 \text{ (Run II)}$$

- The expected and observed 95% CL limits on signal strength in the combination category are

3.2 (Exp.) and 2.7(Obs.)

Thanks!!!!

Publications

- Direct Contributions:
  - **CMS Collaboration, "Validation of analysis techniques relevant for studies of τ lepton production and application to measurement of the $Z/\gamma^* \rightarrow \tau\tau$ cross section in pp collisions at $\sqrt{S}$ = 13 TeV" CMS PAS HIG-15-007 (submitting soon to EPJC)**
  - **Bhopatkar, V., et al. "Measurement of the charge induced on the readout strips of a GE1/1 detector prototype for the CMS muon endcap GEM upgrade", CMS IN-2017/001, http://cms.cern.ch/iCMS/user/noteinfo?cmsnoteid=CMS%20IN-2017/001**
  - **CMS Collaboration, "CMS Technical Design Report for the Muon Endcap GEM Upgrade," CERN-LHCC-2015-012/CMS-TDR-013**
  - Zhang, A., et al. "Performance of a Large-Area GEM detector Read Out with Radial Zigzag Strips", Nuclear Instruments and Methods in Physics A, 811(2016) pp. 30-41 http://dx.doi.org/10.1016/j.nima.2015.11.157
  - **Bhopatkar, V., on behalf of CMS GEM collaboration, "Performance of a Large-Area GEM Detector Prototype for the Upgrade of the CMS Muon Endcap System", Proc. 2014 IEEE Nucl. Sci. Symposium, Seattle, WA IEEE, 8-15 Nov. 2014, http://dx.doi.org/10.1109/NSSMIC.2014.7431249**
- Indirect Contribution
  - Zhang, A., et al. "R&D on GEM Detectors for Forward Tracking at a Future Electron-Ion Collider", Proc. 2015 IEEE Nuclear Sci. Symposium, San Diego, CA, 31Oct-7Nov. 2015, http://dx.doi.org/10.1109/NSSMIC.2015.7581965
  - All other CMS publications

Conferences

Oral Presentations:

- *APS DPF meeting 2017, Fermilab, Batavia, IL, USA,* "Search for SM Higgs Boson in the H⟶tautau⟶mumu decay mode with the CMS experiment at 13TeV"
- *IEEE Nuclear Science Symposium and Medical Imaging Conference (NSS/MIC) 2014 IEEE, Seattle, WA, USA 8-15 Nov 2014,* "Performance of a large-area GEM detector prototype for the upgrade of the CMS muon endcap system"
- *April Meeting of the American Physical Society APS2014, Savannah, GA, USA 5-8 Apr 2014,* "Beam test of a large-area GEM detector prototype for the upgrade of the CMS muon endcap system"
- *78th Annual Meeting of Florida Academy of Sciences(FAS) at Indian River State College, FL, FAS2014,* "Construction and beam test of a full-size GE1/1 gas electron multiplier (GEM) prototype detector for the CMS muon detector upgrade"(Outstanding Graduate Student Oral Presentation)
- *77th Annual Meeting of Florida Academy of Sciences at Barry University, Miami, FL USA FAS2013,* "Gain Measurements of the triple gas electron multiplier (GEM) detector with zigzag readout strips" (Outstanding Graduate Student Oral Presentation)

Conferences

Poster Presentation:

- *38th International Conference on High Energy Physics 3-10 August 2016, Chicago, IL, USA* "Search for a neutral MSSM Higgs Boson decaying into a Pair of Tau Leptons at 13 TeV with the CMS Experiment" (received ICHEP 2016 travel grant award)
- *CMS Week Dec 2014, Miami, FL, USA,* "Performance of a GE1/1-III Prototype GEM Detector for the Upgrade of the CMS Muon Endcap System"
- *CMS Upgrade Week CMSUP2014, Karlsruhe, DE,* "Beam Test of a large-area GEM detector prototype for the upgrade of the CMS muon endcap system"

Acknowledgement

My sincere thanks to:

Dr. Marcus Hohlmann (Thesis and research advisor at Florida Tech)

Dissertation committee member:

Dr. Francisco Yumiceva

Dr. Ming Zhang

Dr. Debasis Mitra

Dr. Alexei Raspereza (co-research advisor at DESY)

Dr. Elisabetta Gallo (co-research advisor at DESY)

Florida Tech GEM + HEP group

DESY HTT group

CMS HTT group

Backup Slides

Compact Muon Solenoid (CMS) Experiment

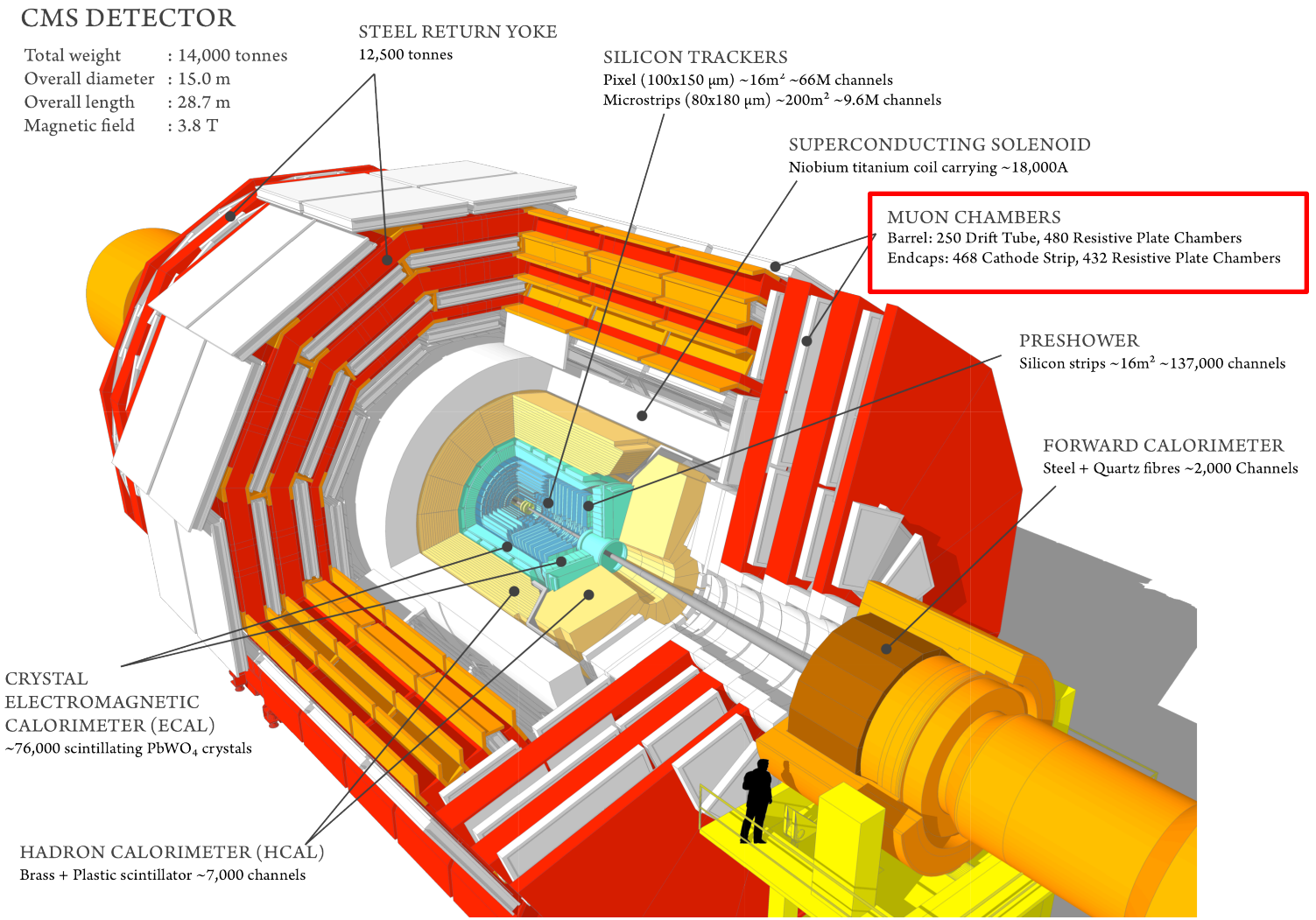

Compact Muon Solenoid (CMS) Experiment

CMS DETECTOR

Total weight 14,000 tonnes
Overall diameter 15m
Overall length 28.7 m
Magnetic field 3.8T

STEEL RETURN YOKE

125,000 tonnes

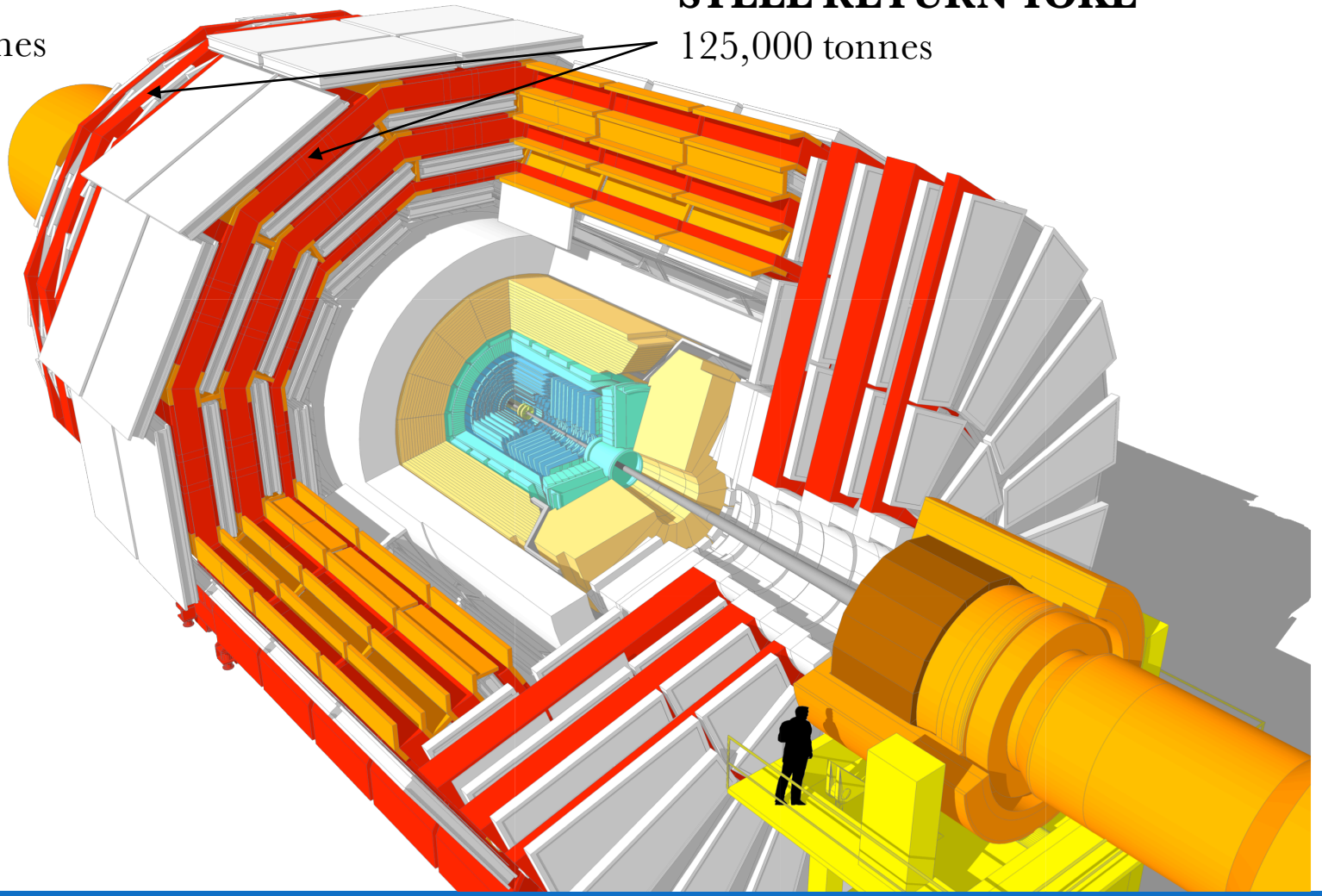

Efficiency Measurements

- Studied the hit distribution, charge distribution and cluster size for HV scan and Position scan
- Evaluates the efficiency from cluster multiplicity(CM)

$$Efficiency = \frac{N1}{(N - N2)}$$

Where, N1: No. of events with CM≥1 for given sector

N: Total no. of events

N2: sum of the no. of events with CM≥1 for other sectors

GE1/1 Tracking Analysis

- Tracking is done in three steps:
- Step I - Alignment: By iterating the shift parameters in X and Y, we center all detector residuals on zero and then with respect to the first reference tracker, we rotate the remaining three trackers until the residual widths are minimized
- Step II - Conversion from (x,y) to (r,ϕ) coordinate system: Since we are dealing with radial readout strips in the GE1/1, it is more appropriate to use (r,ϕ) coordinates for tracking.

$$r=\sqrt{x^2+y^2} \qquad \varphi=\text{atan}\,(y/x)$$

- Step III - Calculate final residuals (inclusive and exclusive)
- We measure both exclusive and inclusive residuals for GE1/1 detector and then calculated the resolution (Geometric mean of inclusive and exclusive residual) $\sigma=\sqrt{(\sigma\_inc\times\sigma\_exc}\ )$

Tracking results

Beam profiles with first tracker

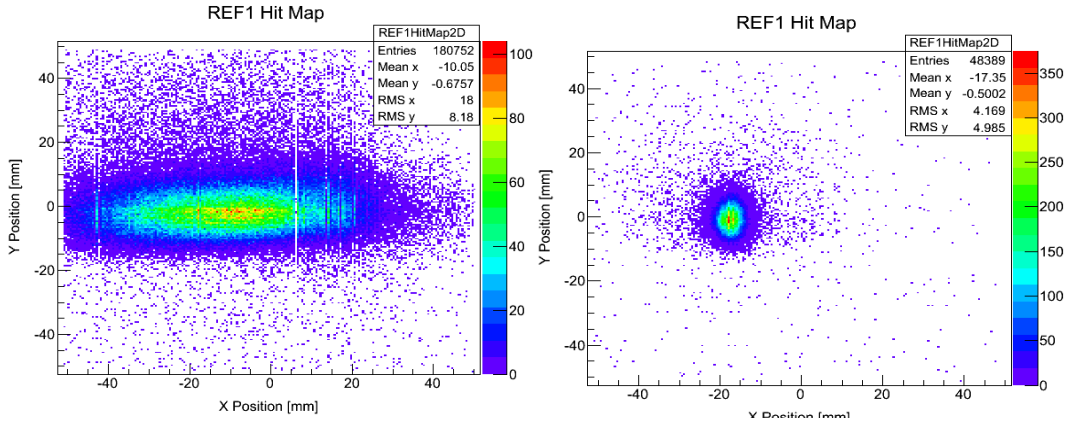

Correlation of GE1/1 detector hits with hits in first tracker detector:

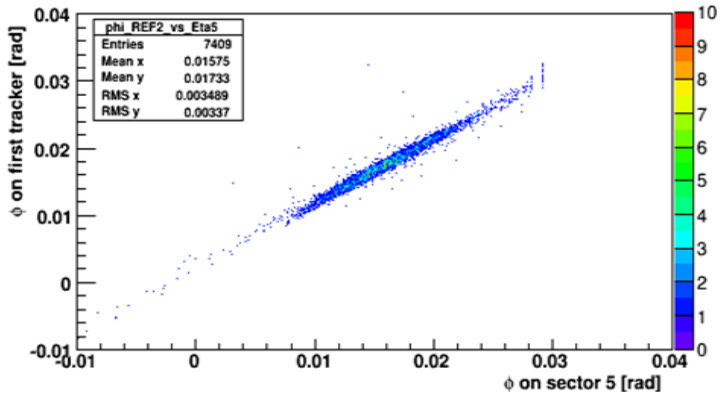

Residuals of Tracker 1 in φ

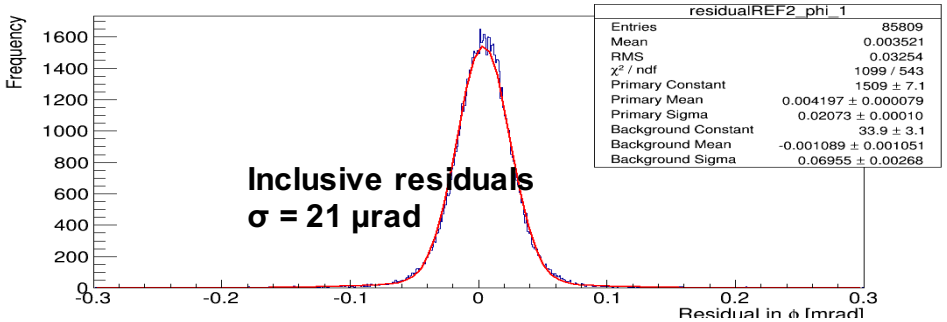

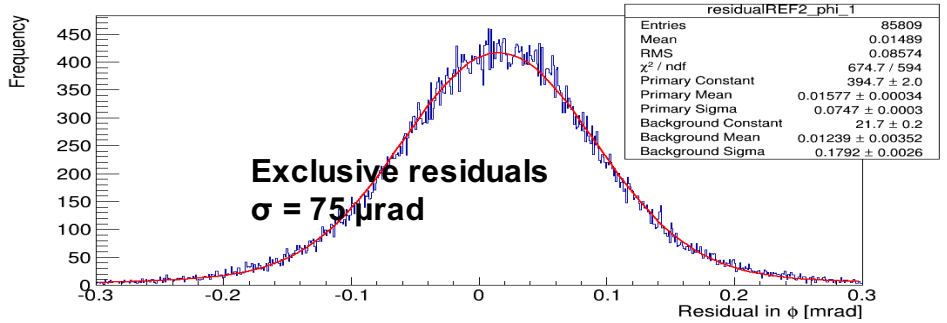

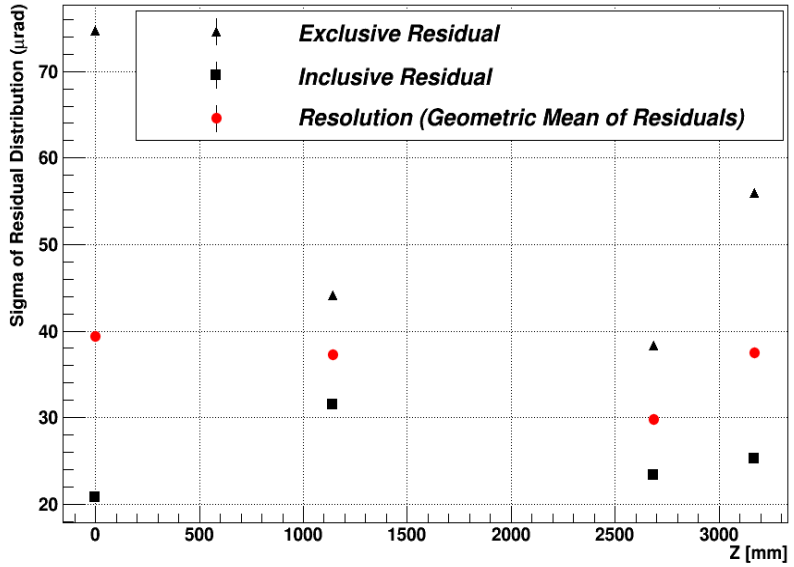

Non-Linear Strip Response Correction

- The resolution of the same detector with a zigzag-strip readout board can be improved by ~30%
- Hence, we implemented the same correction to find the corresponding improvement in the resolution of the standard GE1/1 detector discuss here
- Strip cluster position is reconstructed via cluster barycenter (centroid): $S_b = \sum_{i=1}^{n} \frac{q_i s_i}{q_{total}}$, where q_i is charge of the ith strip, s_i is strip number, and q_{total} is total cluster charge
- For cluster size N > 1, we define $\eta_N = s_b - s_{max}$, where s_{max} is the strip with maximum charge value. Then we plot exclusive residuals against η_N for N = 2 and N = 3
- Corrected resolution is obtained by subtracting the exclusive residual means as function of η_N from the original residuals

Scatter Plots of Exclusive Residual vs. η_N using combined HV scan data

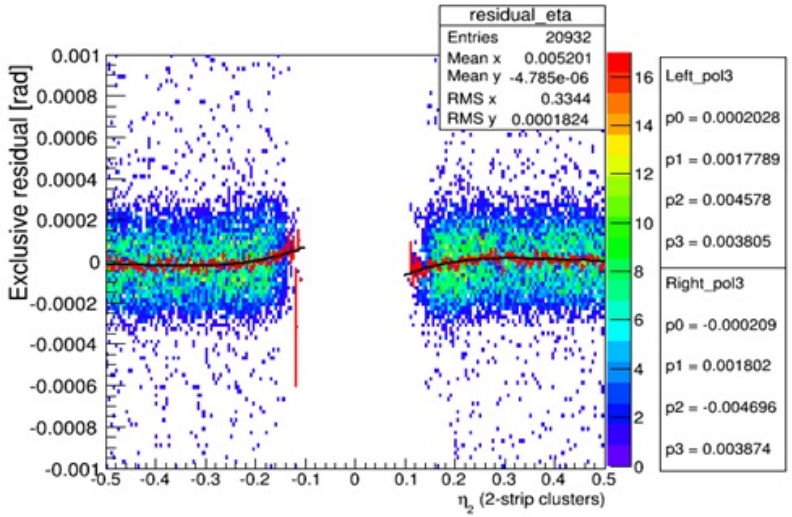

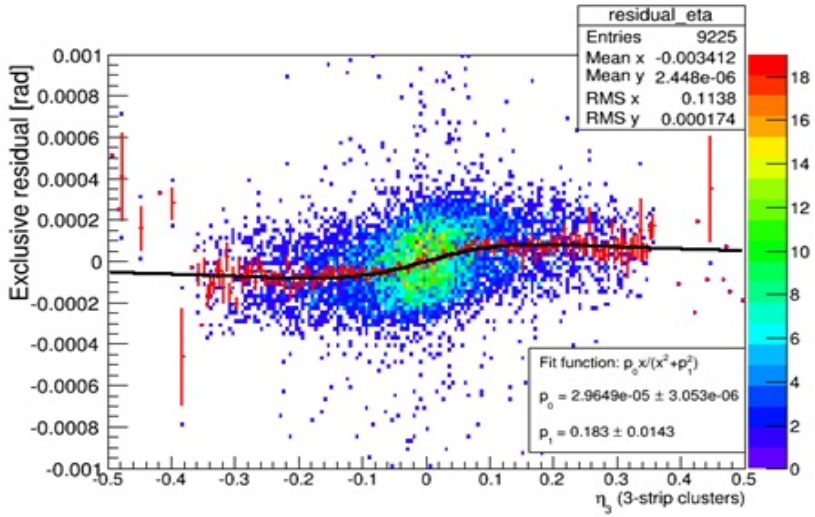

Non-Linear Strip Response Correction

For N= 2 and N =3

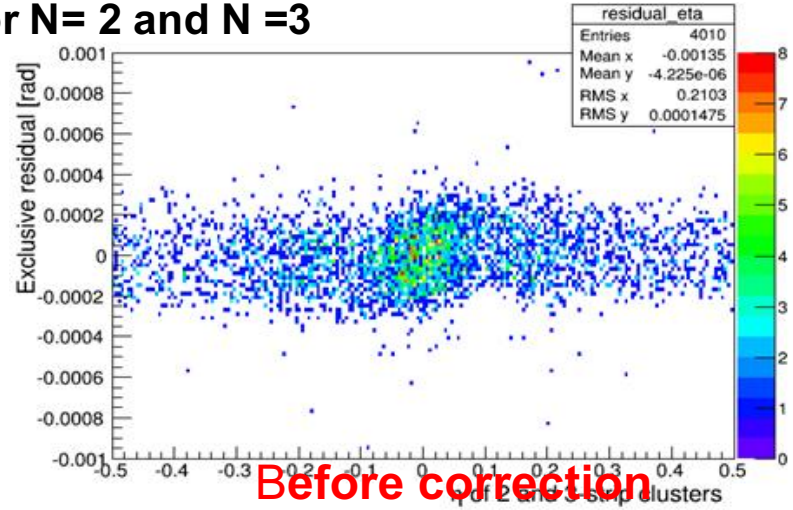

Before correction

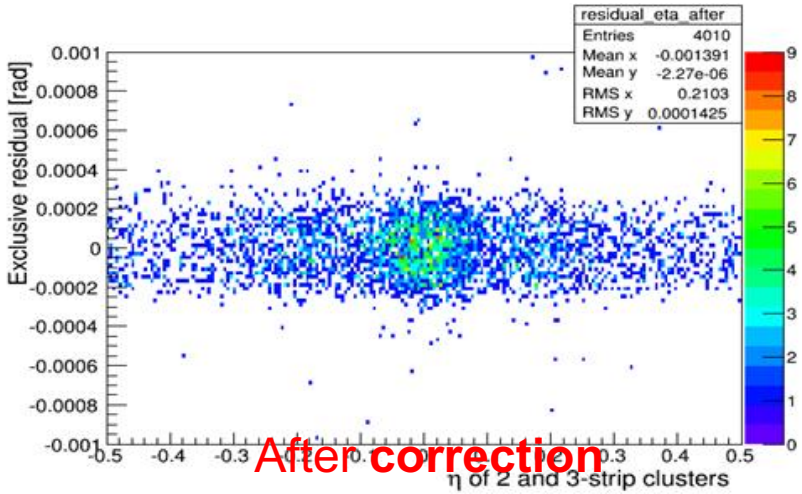

After correction

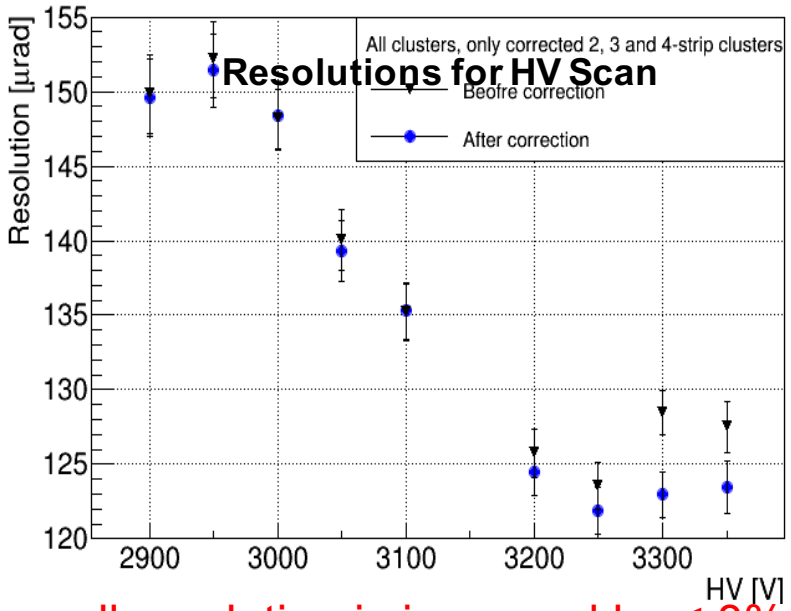

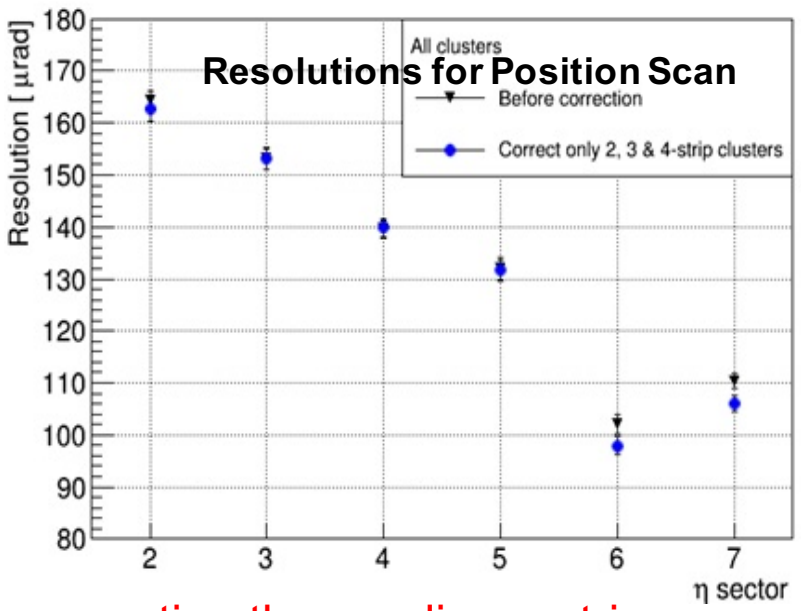

Overall resolution is improved by ≤ 8% after correcting the non-linear strip response

BDT Input Variable for Z Cross Section Measurements

$Z/\gamma^* \rightarrow \tau\tau \rightarrow \tau_\mu \tau_\mu$

$Z/\gamma^* \rightarrow \mu\mu$

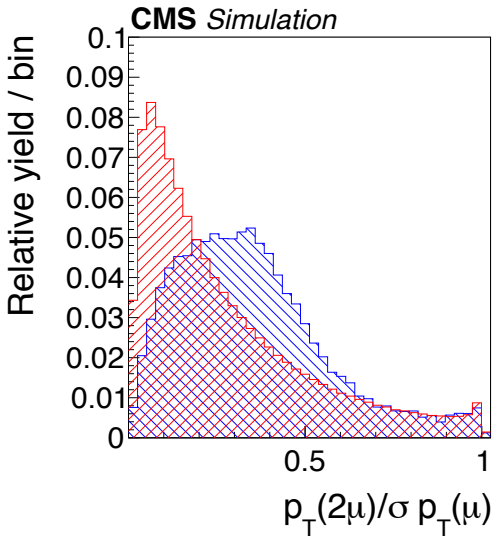

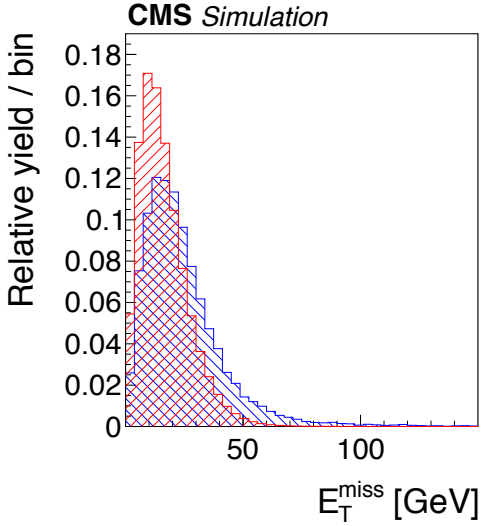

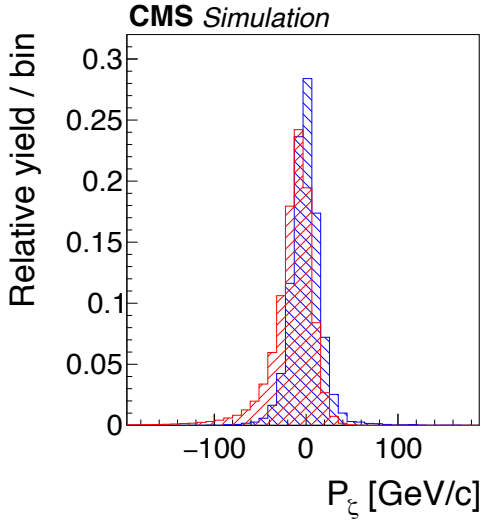

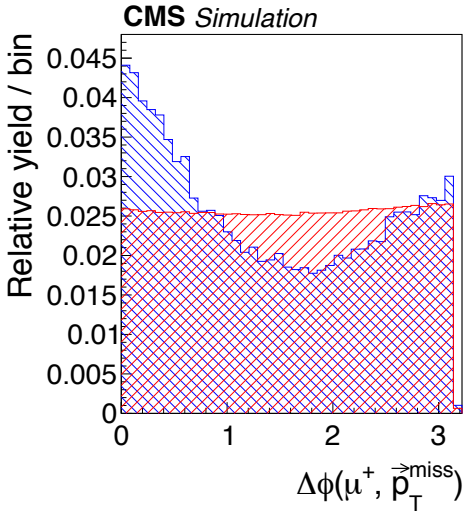

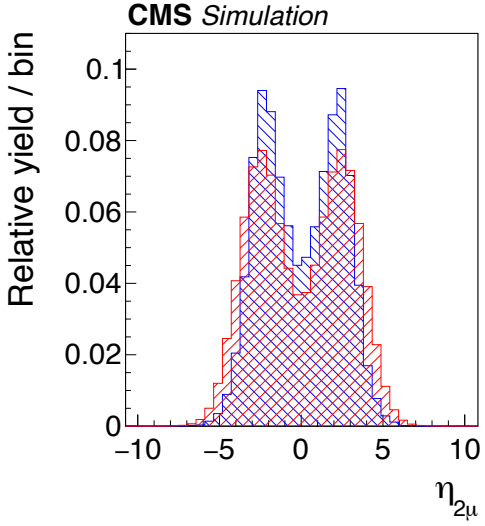

BDT Distribution for Z Cross Section Measurements

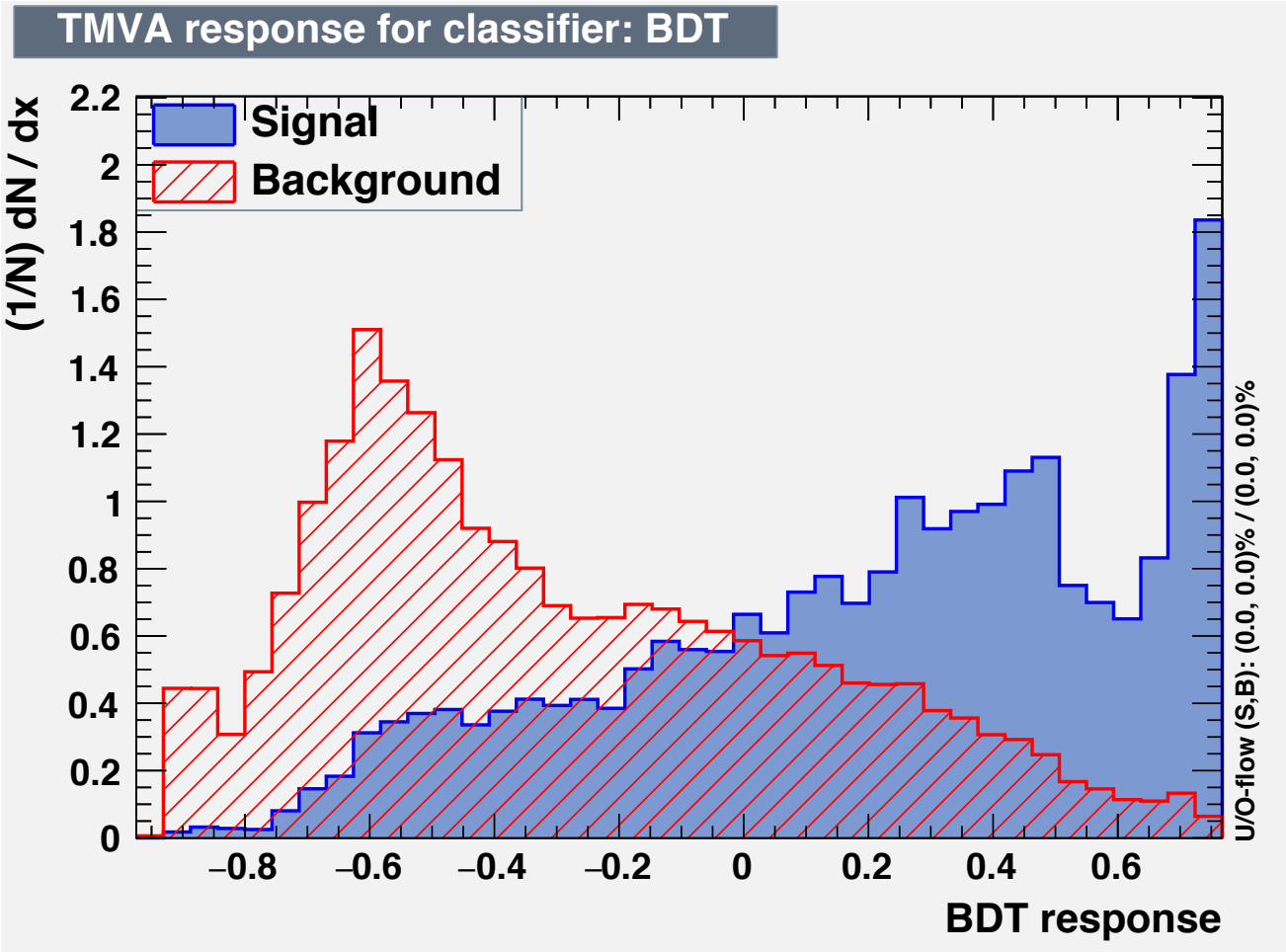

Impact Parameter Plots for VBF Category

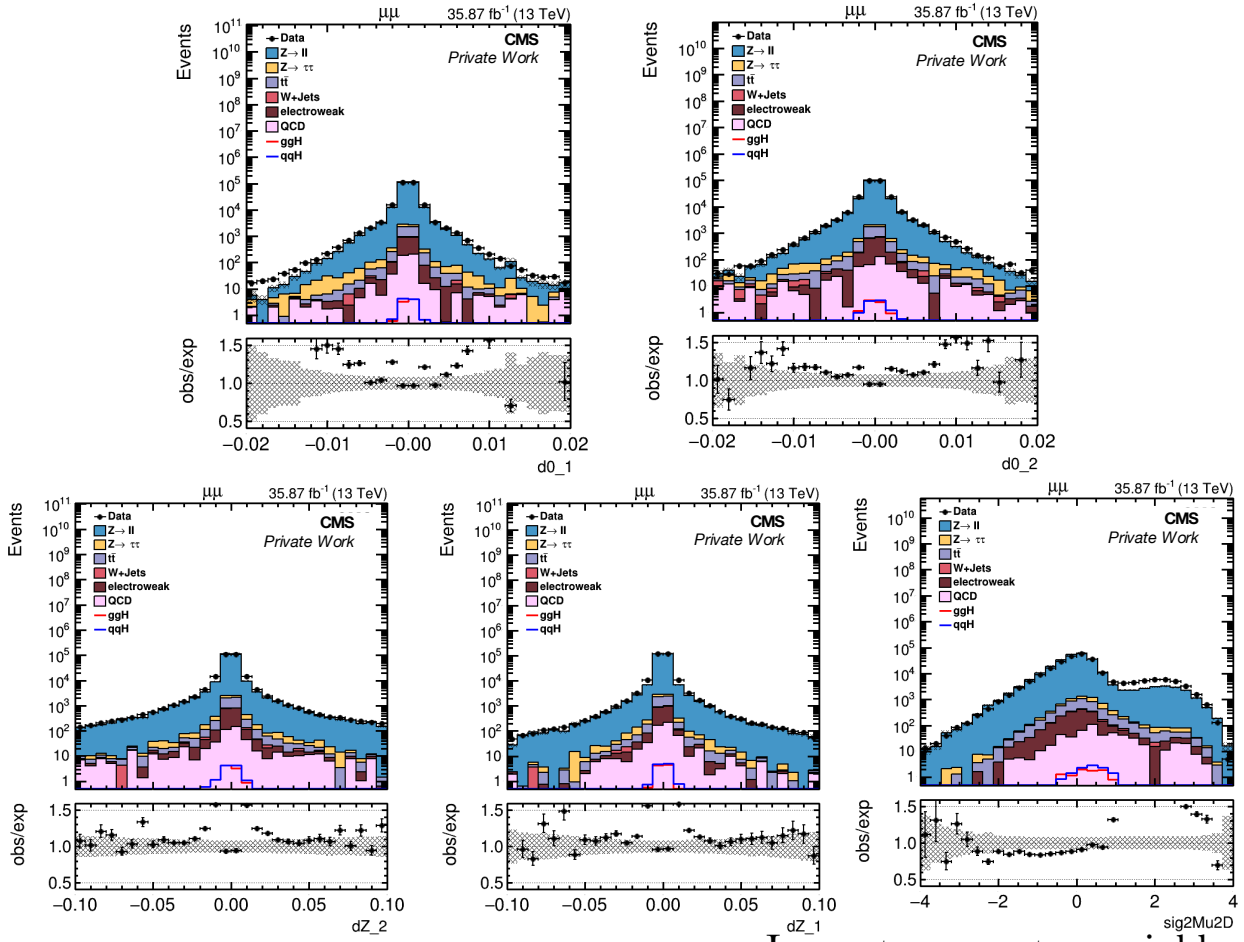

Impact parameter variables are excluded from BDT due to the discrepancy coming from misalignment of the trackers

Kinematic and Impact Parameter Plots for 0-jet Category

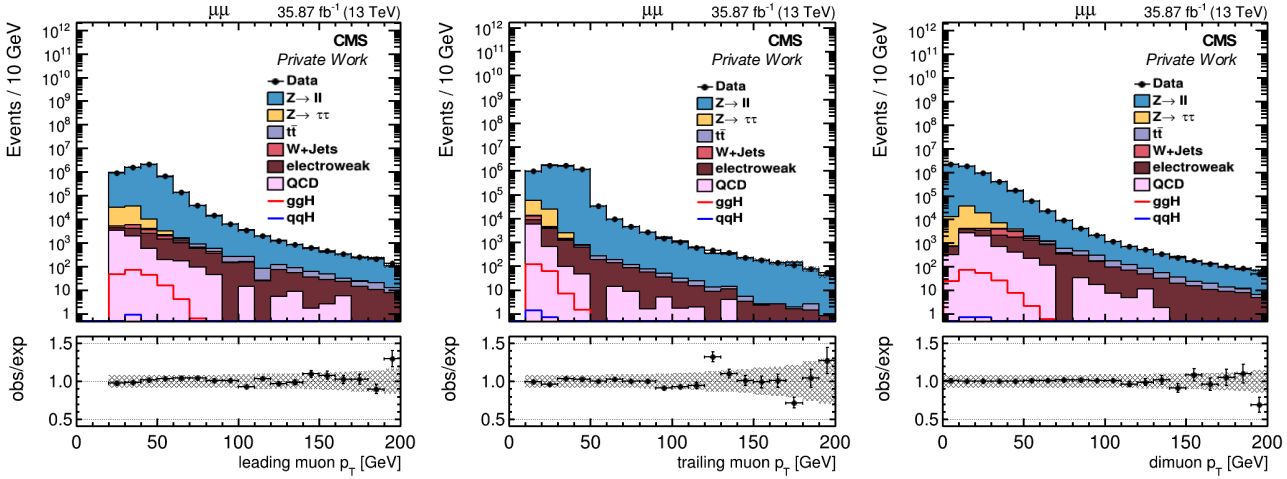

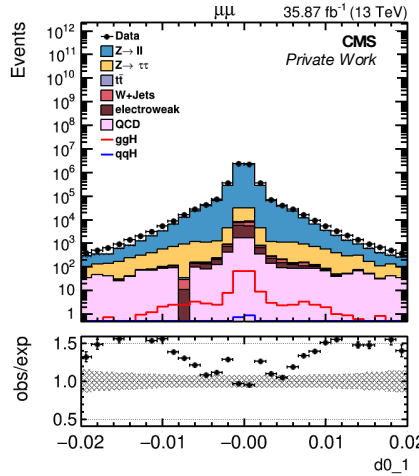

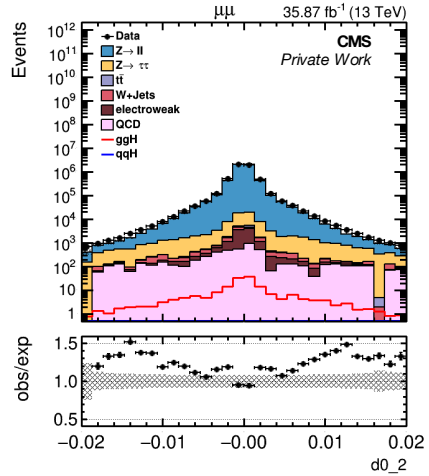

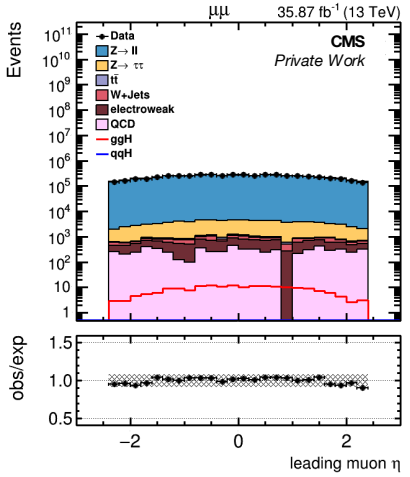

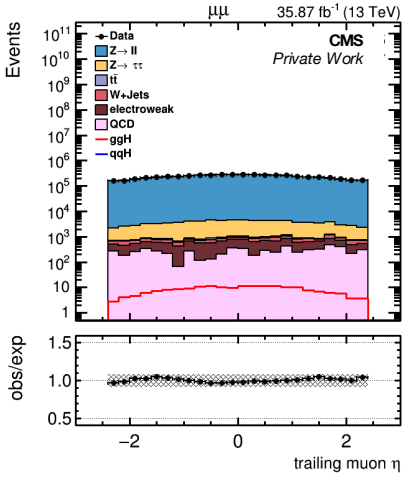

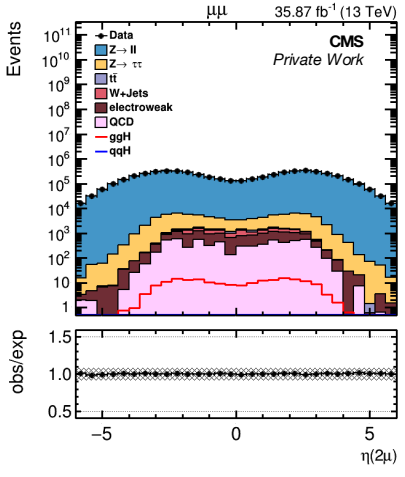

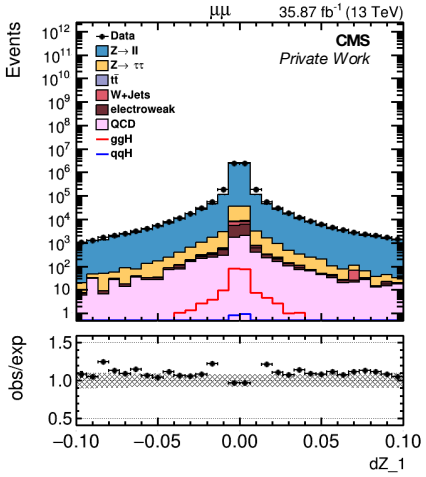

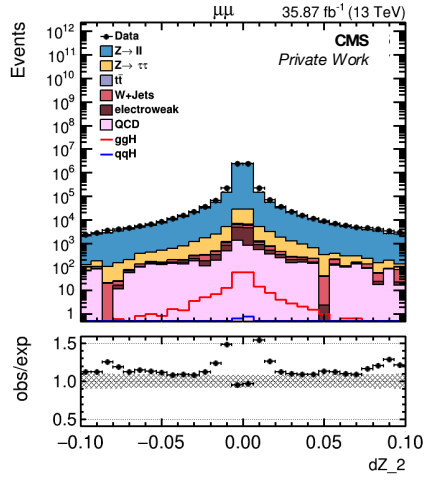

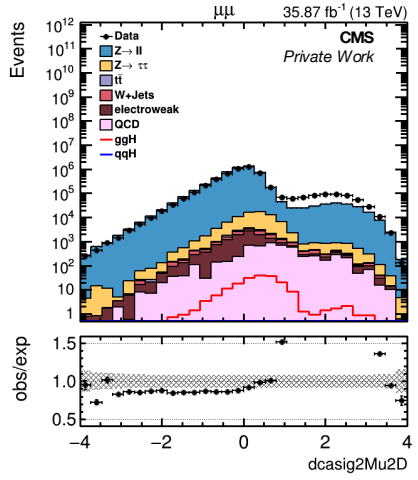

Discriminating Variable Plots for 0-jet Category

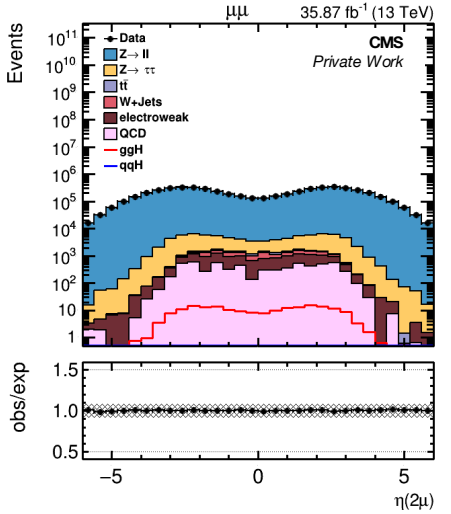

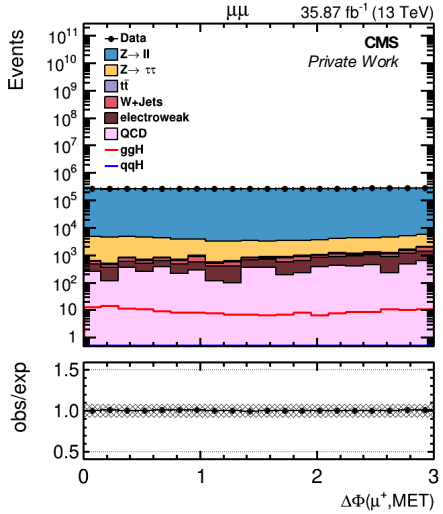

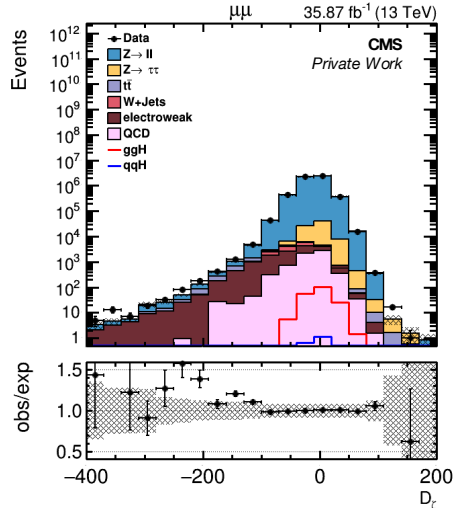

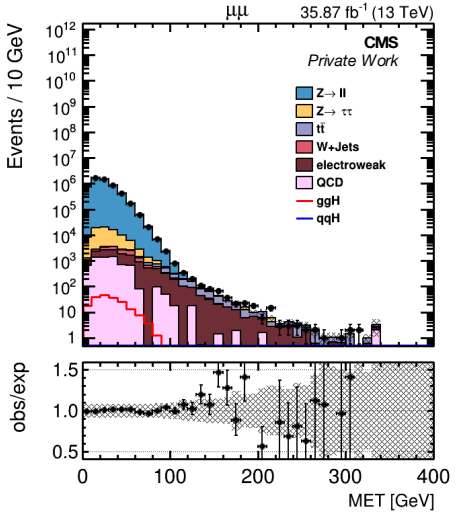

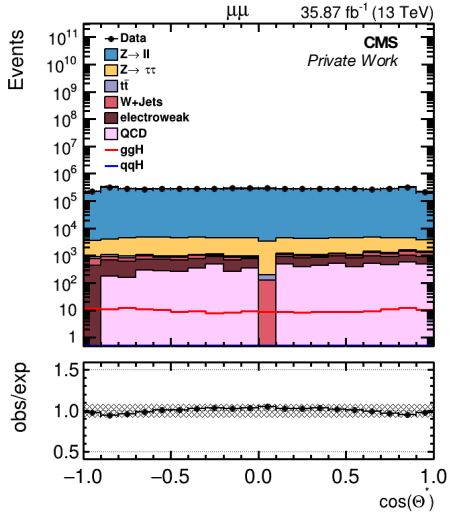

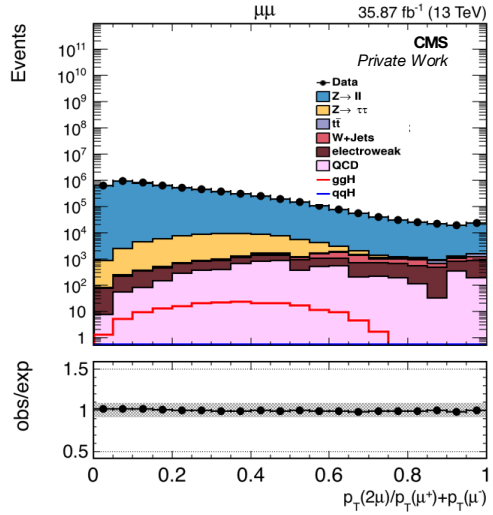

Kinematic and Impact Parameter Plots for Boosted Category

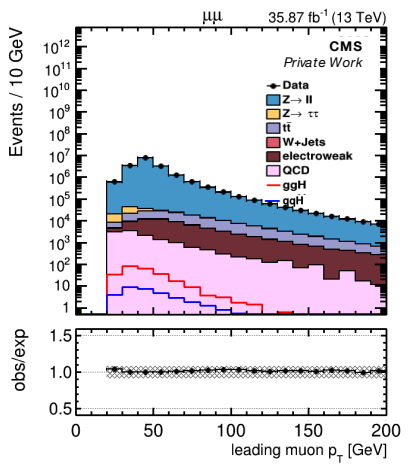

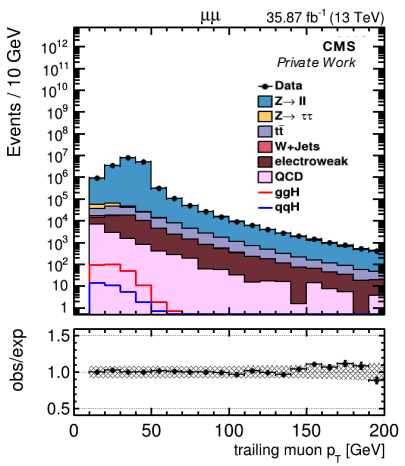

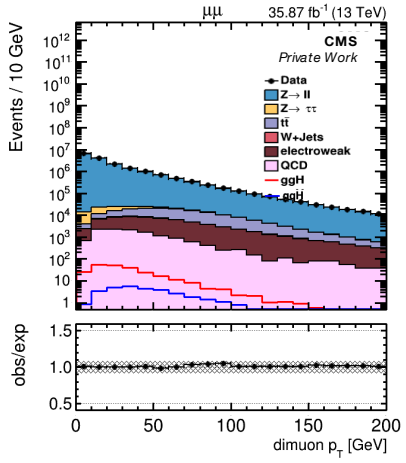

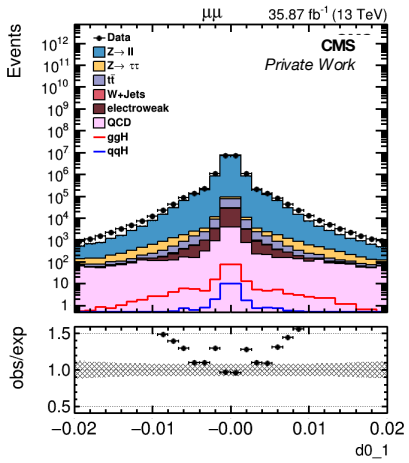

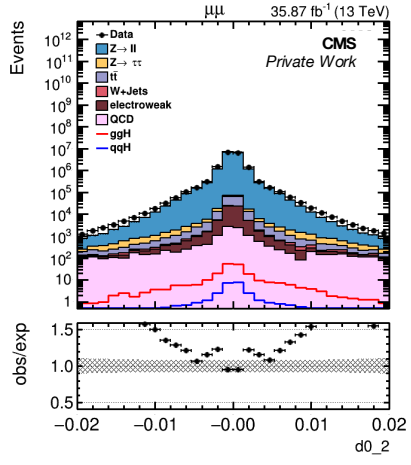

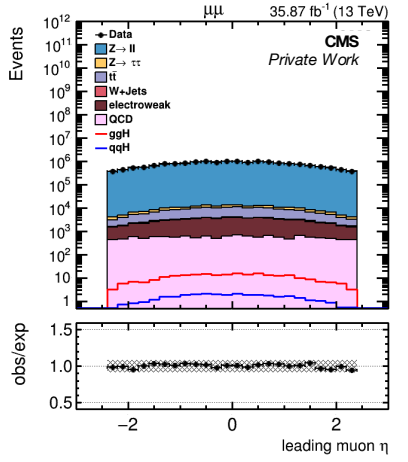

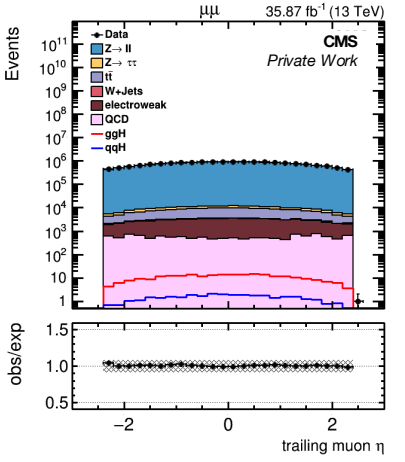

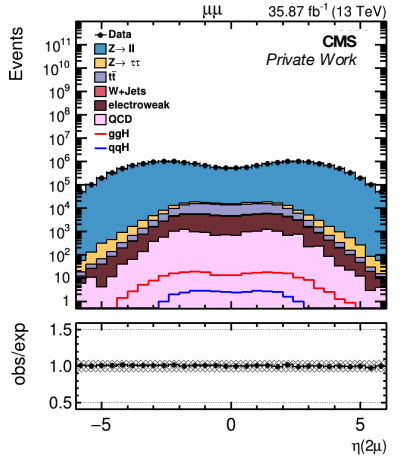

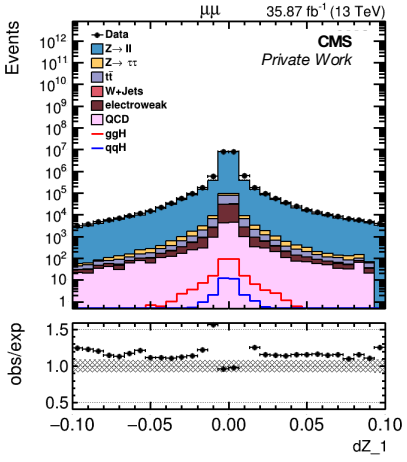

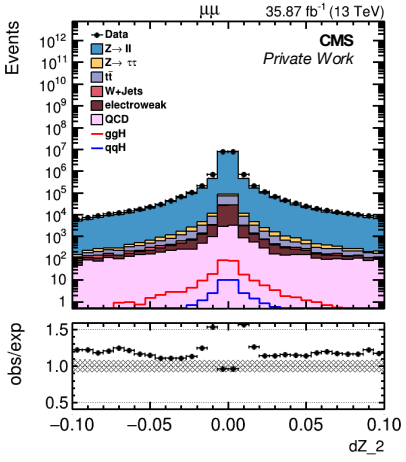

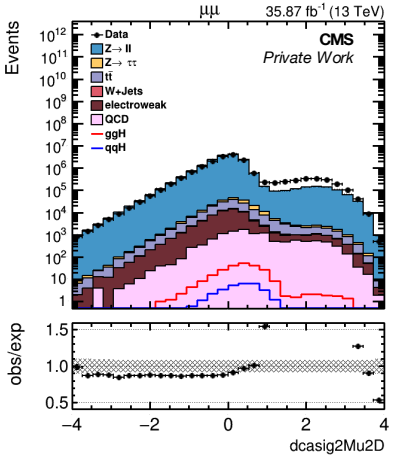

Discriminating Variable Plots for Boosted Category

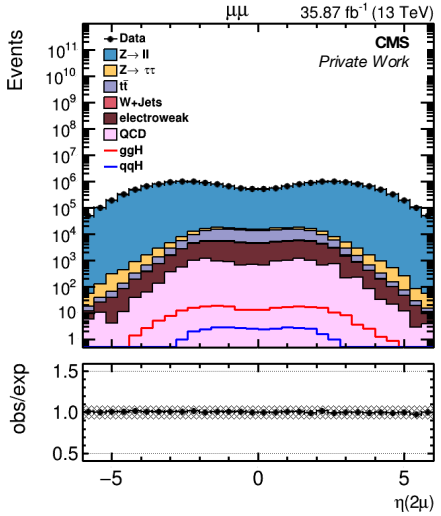

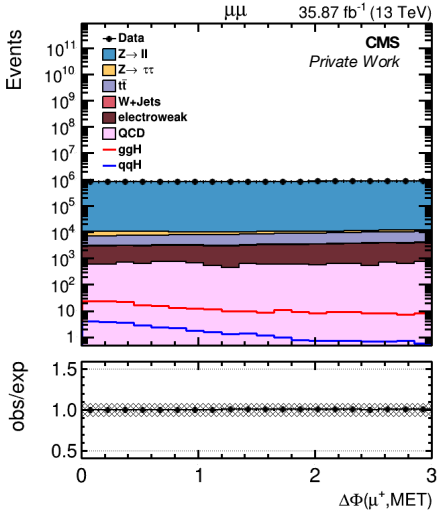

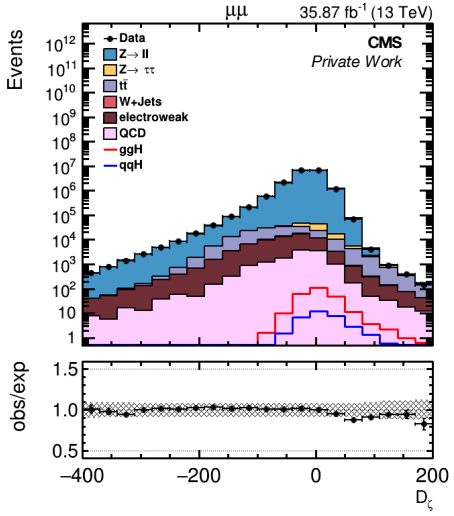

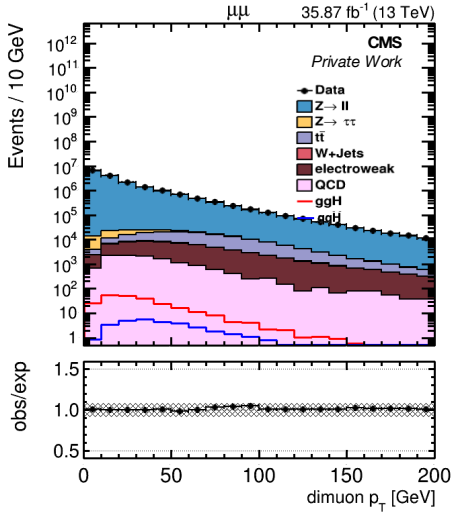

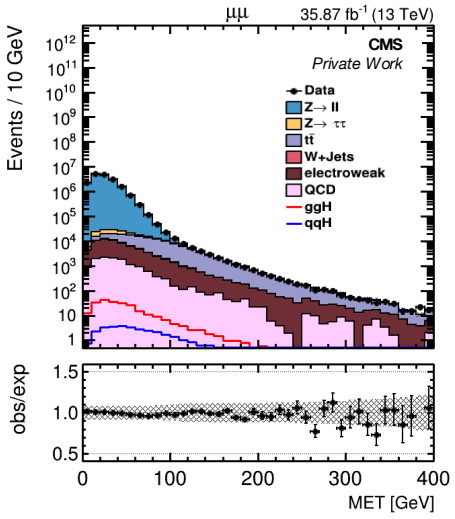

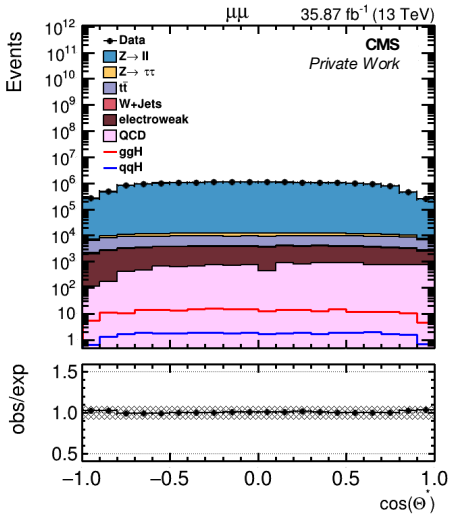

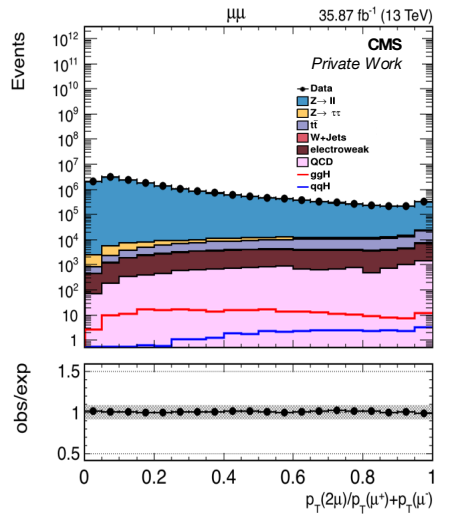

Overtraining check

0-Jet

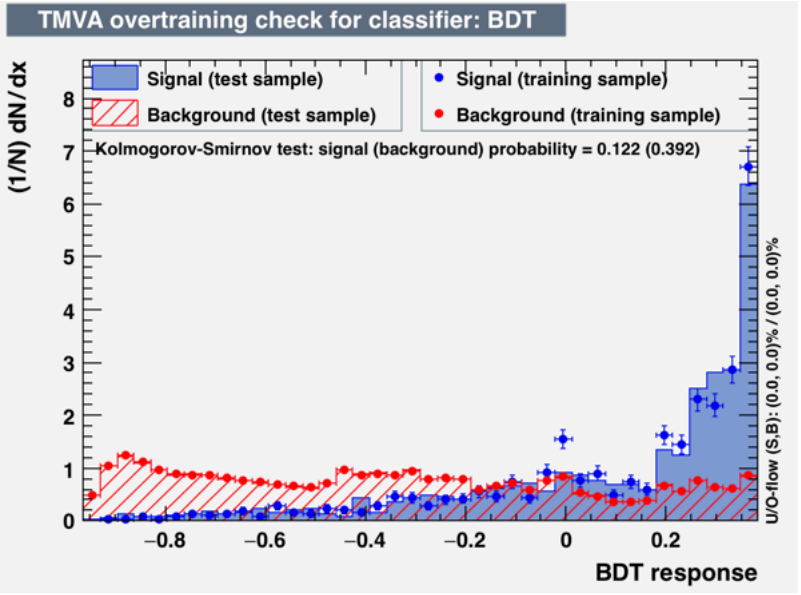

boosted

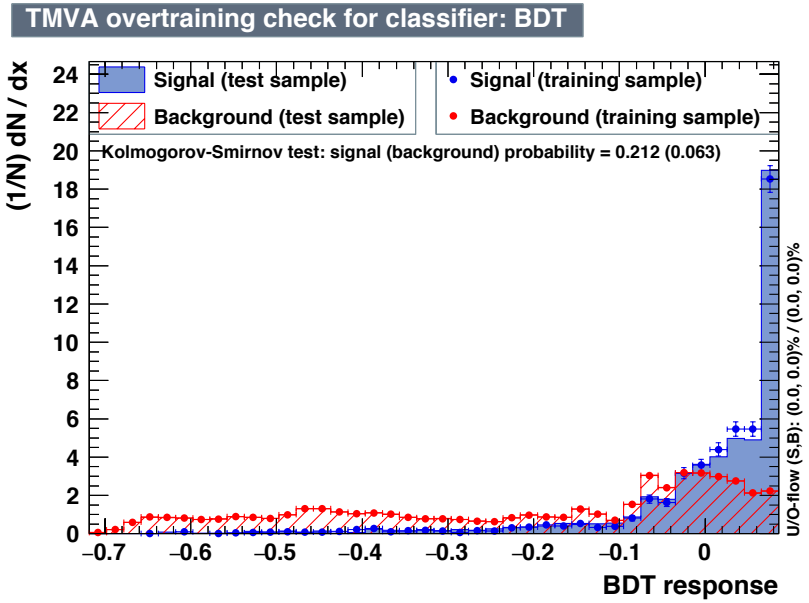

VBF

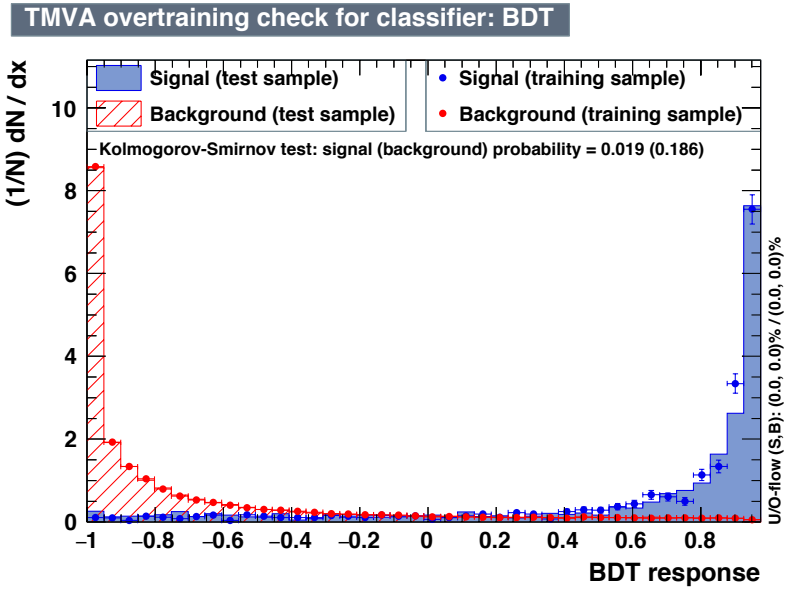

ROC Curve

0-Jet

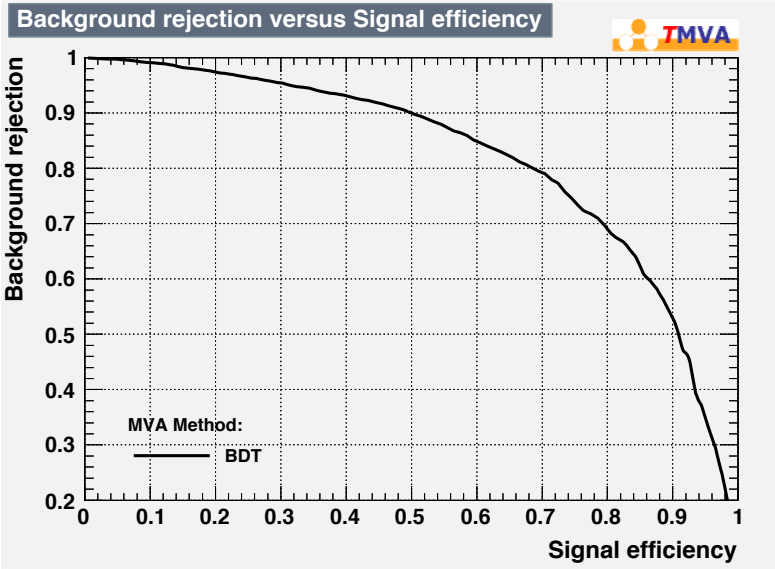

boosted

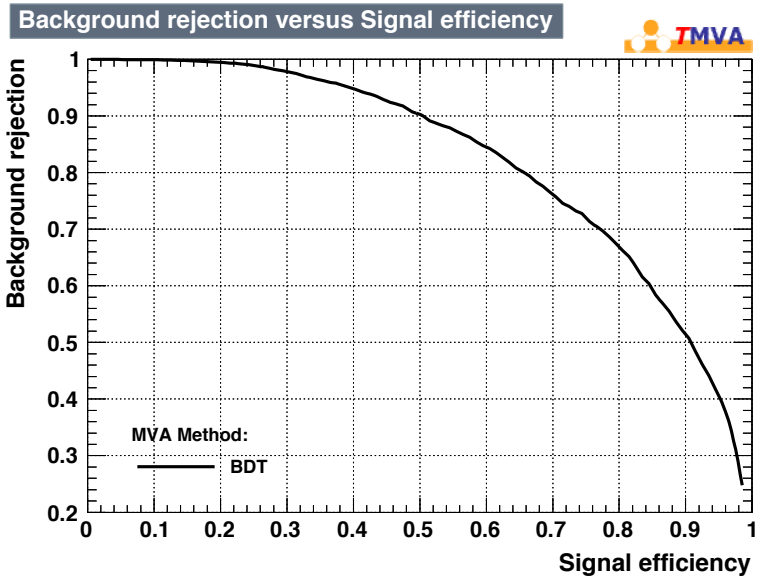

VBF

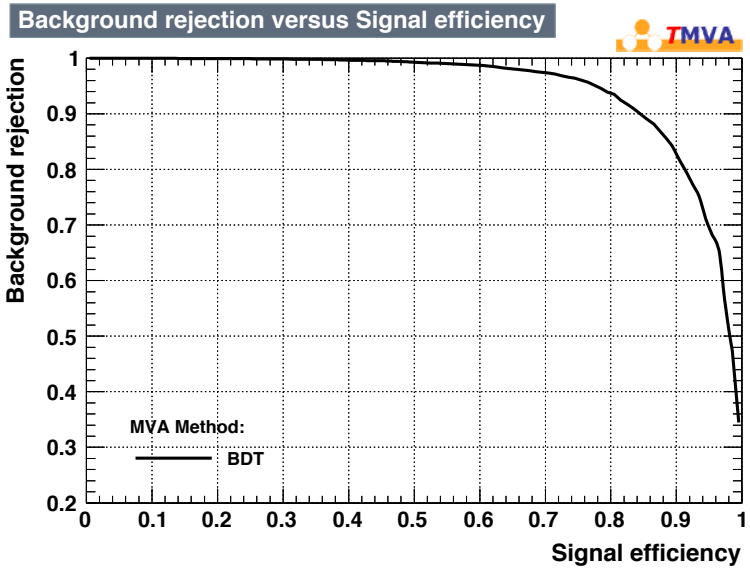

Pulls and Impact (combine) Page1

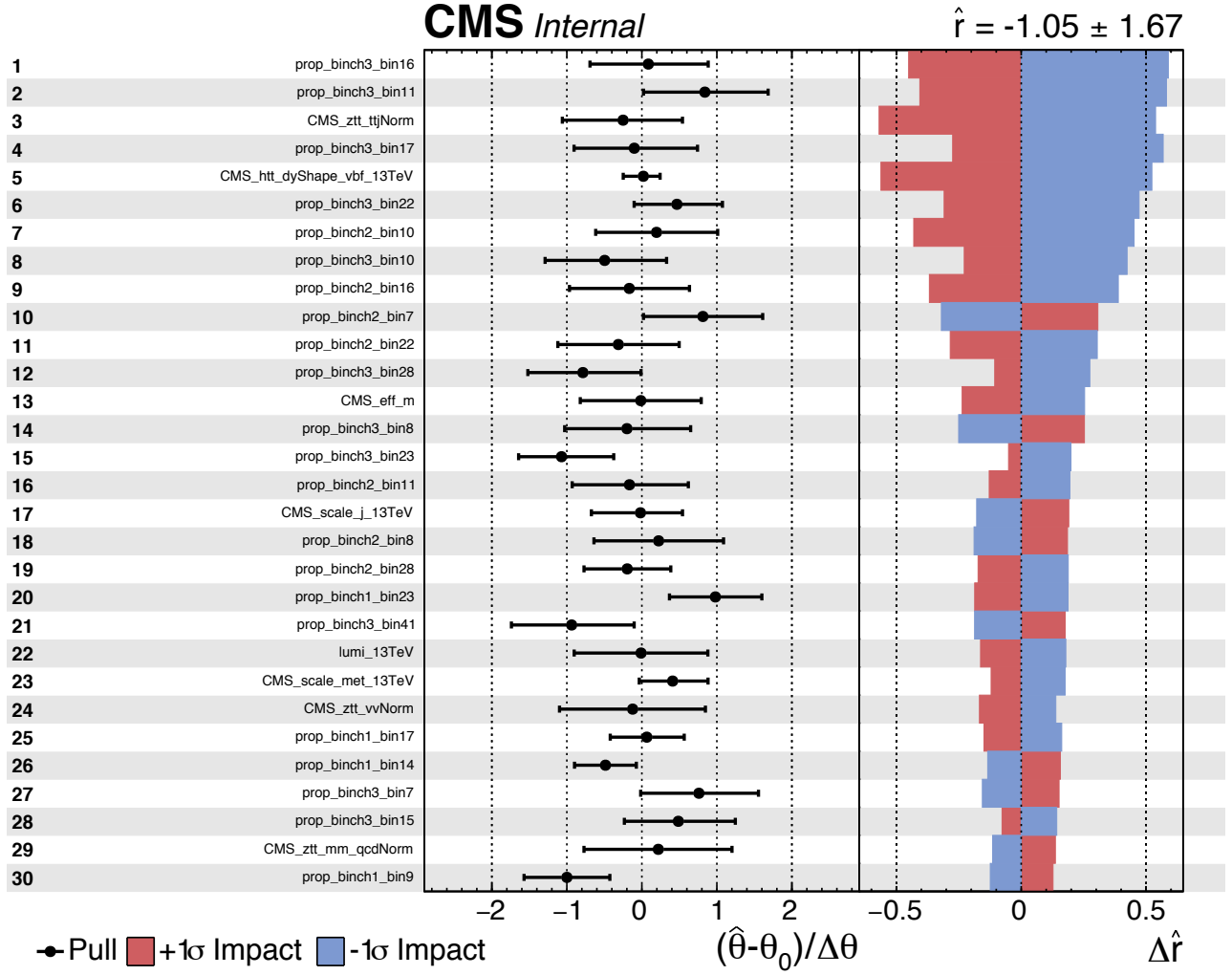

Pulls and Impact (combine) Page 2

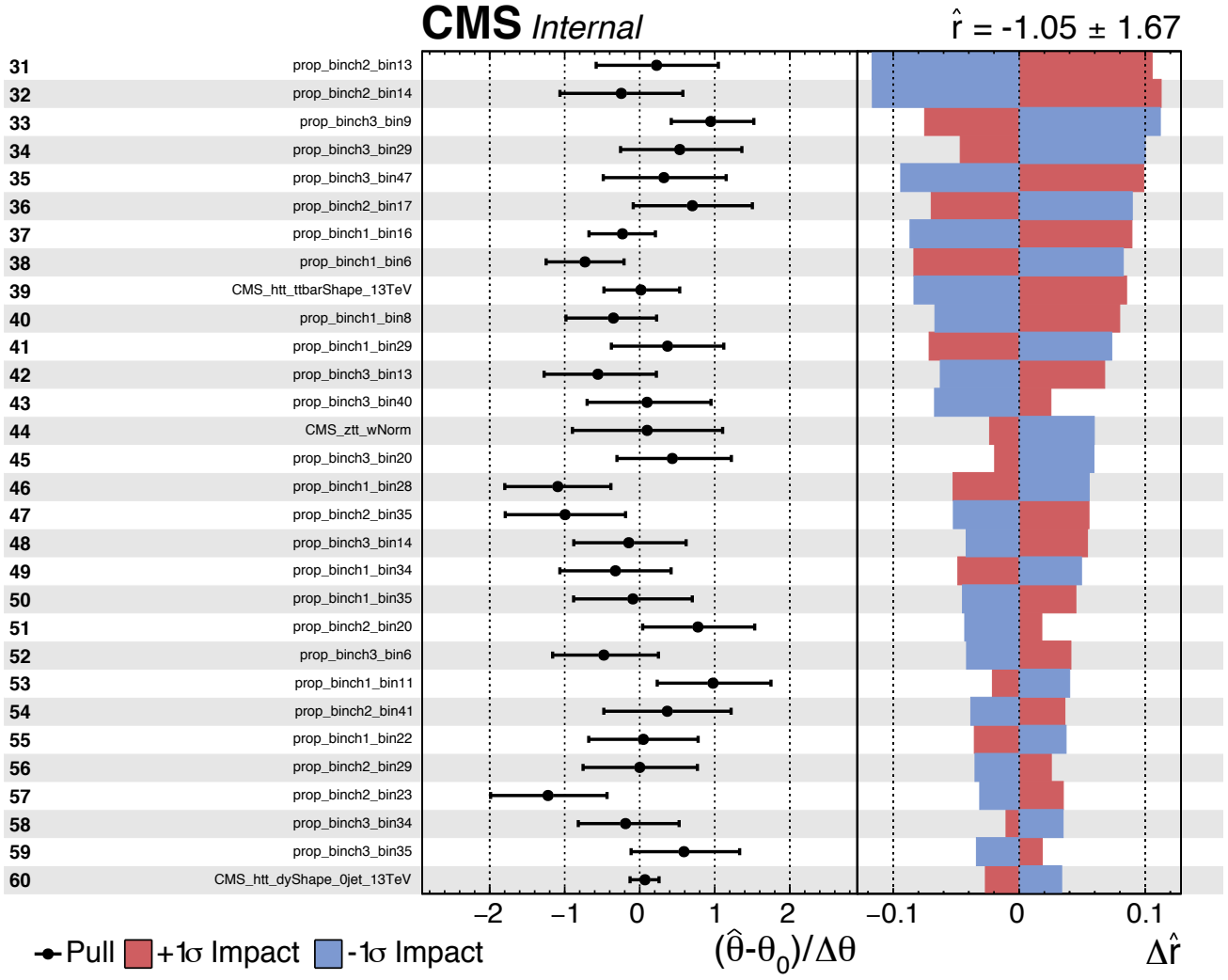

Pulls and Impact (combine) Page 3